DEVELOPMENT OF A CROSSLINKABLE BIOMIMETIC COLLAGEN FOR MIMICRY OF MOLECULAR ARCHITECTURE, BIOLOGICAL ACTIVITY AND APPLICATIONS

KHEW SHIH TAK

(*B.Eng. (Hons), UNIVERSITI TEKNOLOGI MALAYSIA*)

A THESIS SUBMITTED FOR

THE DEGREE OF DOCTOR OF PHILOSOPHY

DEPARTMENT OF CHEMICAL AND BIOMOLECULAR ENGINEERING

NATIONAL UNIVERSITY OF SINGAPORE

2008

To my dearest parents, brother and sisters

To my beloved, Renpian

ACKNOWLEDGEMENTS

Earning the degree would have been unattainable without the love and support of several persons. I would foremost like to offer my heartfelt thanks to my thesis advisor, Professor Tong Yen Wah, for giving me not only many opportunities to learn and grow but also freedom to try and err. He is always a good friend and true mentor of mine. I appreciate his trust in me and his care and friendship. I am grateful to his insight and advice not only in scientific but also in personal and professional matters, such as job seeking and future planning.

I am also thankful to Professor Michael Raghunath for his unreserved support and guidance. It is a pleasure and a privilege to work with him. His insightful comments and suggestions are essential for the completion of this thesis. I am also indebted to his research staff and students, Dr. Dimitrios Zevgolis, Pradeep Paul Panengad, and Clarice Chen Zhen Cheng, for their kind assistance and support. I thank Professor Wang Shu and Dr. Frank Alexis for their invaluable help and for allowing me to use their laboratory facilities.

I would like to extend my earnest thanks to all the members of the research group and past colleagues, especially Jeremy Daniel Lease, Zhu Xinhao, Tan Chao Jin, Nikken Wiradharma, Zhong Shaoping, Qin Weijie, and Zhao Haizheng, for their unconditional help and the mutual encouragement. I also thank all the lab mates, Shalom Wangrangsimakul, Chen Wenhui, Loh Shin Shion, Niranjani Sankarakumar, Tan Weiling, Duong Hoang Hanh Phuoc, and Deny Hartono, for providing not only support but also a pleasant working environment. I always enjoy the great experience of being a part of them and working together with them. I would also like to thank the laboratory officers, Li Xiang, Li Fengmei, Han Guangjun, Teo Ai Ping, and Qin Zhen, for their invaluable technical help.

I am forever indebted to my parents and siblings, Seow Chin, Seow Wei, and Sze Zien, for their everlasting love and support. They have been the constant source of support and comfort to me, no matter where I go and in what I do. I am eternally grateful to my best companion, Renpian, for her care, love, selfless support and companionship.

Finally, I would like to acknowledge again all those who have contributed to this thesis. This work was funded by the National University of Singapore under Grant Number R279000168112.

TABLE OF CONTENTS

ABSTRACT

This thesis focuses on establishing a molecular strategy to engineer a functional collagen-like biomaterial, namely a biomimetic collagen that exhibits stable collagen-like triple-helical conformation, cell binding activity, and substrate specificity for tissue transglutaminase (TGase). The central hypothesis of this work is that the complexation of multiple functional domains, such as cell binding motifs, structural domains and non-collagenous enzyme crosslinking substrate sequences, may be of significant contribution to creating artificial collagens that not only structurally but also functionally resemble their natural counterpart.

Collagen-mimetic peptide (CMP) supplemented with a specific cell binding sequence spanning residues 502-507 of collagen α_1(I) (GFOGER) was used to support Hep3B liver cell adhesion and growth. The triple-helical CMP showed excellent performance when being used as a tissue support matrix to promote cell adhesion and proliferation and maintain cellular function. A template-assembly system, wherein no complex strategies are used, was developed. A template characterized by its fully amino acid based constitution and collagen-like primary structure composed of GFGEEG sequence was devised and used to covalently assemble CMPs in a

staggered array thus promoting the assembly of the triple-helical conformation. The template-assembled $(Pro\text{-}Hyp\text{-}Gly)_3$ and $(Pro\text{-}Hyp\text{-}Gly)_5$ displayed significantly enhanced stability. Conversely, non-templated counterparts showed no evidence of assembly of triple-helical structure. It was shown that the template-assembled CMPs supplemented with the cell binding motif of collagen (GFOGER) promoted adhesion of both Hep3B and L929 cells considerably. However, it was also demonstrated that different cell types may recognize the GFOGER sequence at different levels, probably because of the difference in their expression of the specific integrins for GFOGER. L929 cells were shown to have higher affinity for the triple-helical GFOGER. Cell recognition of the CMPs supplemented with the GFOGER sequence appeared to be both conformation- and sequence-specific, the absence of which resulted in a marked loss of cell recognition.

Furthermore, a specific sequence spanning residues 2800-2807 of human fibrillin-1 (EDGFFKI) was identified and characterized as an amine donor substrate for tissue TGase, using a previously characterized APQ^3Q^4EA, derived from human osteonectin as an amine acceptor probe. EDGFFKI patterned on the C-terminal propeptide of fibrillin-1 exhibited good substrate reactivity toward tissue TGase and it bound specifically to Q^3 of the acceptor probe. CMPs supplemented with the identified EDGFFKI and APQQEA substrate sequences were conjugated onto a generation 1.5 poly(amidoamine) dendrimer, resulting in crosslinkable collagen-mimetic dendrimers, denoted as CMD-K and CMD-Q, respectively. Tissue

TGase-mediated crosslinking between CMD-K and CMD-Q resulted in supramolecular structure that exhibited stable collagen-like triple-helical conformation and improved cellular recognition. The result showed that the triple helix structure is important in preserving the GFOGER cell binding site and the tissue TGase-mediated protein crosslinking may be also a crucial recognition mark for cell surface integrin-receptors. The molecular strategy developed in this thesis could be a promising approach for engineering biomimetic collagen of biological function and characteristic a little, if not significant, closer to that of the natural collagen. This research may contribute to taking us one step further toward realizing an artificial collagen.

LIST OF TABLES

LIST OF FIGURES

NOMENCLATURE

Notations

T_m	Melting point temperature
U	Activity unit of pig liver tissue transglutaminase

Abbreviations

BSA	Bovine serum albumin
CD	Circular dichroism
CHCA	α-cyano-4-hydroxy-cinnamic acid
CLSM	Confocal laser scanning microscope
CMD	Collagen-mimetic dendrimer
CMP	Collagen-mimetic peptide
DAPI	4’,6-diamidino-2-phenylindole
DMEM	Dulbecco’s modified Eagle’s medium
DMF	Dimethylformamide
DNA	Deoxyribonucleic acid
DTAF	Streptavidin-dichlorotriazinylaminofluorescein
ECM	Extracellular matrix

EDC	*N*-ethyl-*N*'-(3-dimethylaminopropyl)carbodiimide
EDTA	Ethylenediaminetetraacetic acid
EGTA	Ethylene glycol tetraacetic acid
ELISA	Enzyme-linked immunosorbent assay
EROD	Ethoxyresorufin-O-deethylase
FBS	Fetal bovine serum
FITC	Fluorescein isothiocyanate
Fmoc	Fluorenyl-methoxy-carbonyl
HBSS	Hank's balanced salt
HBTU	2-(1H-Benzotriazole-1-yl)-1,1,3,3-tetramethyluronium hexafluorophosphate
HOBt	N-Hydroxybenzotriazole
HPLC	High performance liquid chromatography
MALDI-TOF	Matrix-assisted laser desorption/ionization time of flight
MDC	Monodansylcadaverine
MS	Mass spectroscopy
MWCO	Molecular weight cut off point
MTT	3-(4,5-dimethylthiazol-2-yl)-2,5-diphenyltetrazolium bromide
NHS	*N*-Hydroxysulfosuccinimide
NMM	N-methylmorpholine
NMP	1-methyl-2-pyrrolidone
NMR	Nuclear magnetic resonance

KTA	Kemp triacid
PAMAM	Poly(amidoamine)
PBS	Phosphate buffered saline
PHBV	Poly(3-hydroxybutyrate-*co*-3-hydroxyvalerate)
PT	Peptide template
PVA	Poly(vinyl alcohol)
Rpn	Ratio of positive peak to negative peak intensity (in the circular dichroism spectra)
SD	Standard deviation
SEM	Scanning electron microscope
TBO	Toluidine blue O
TFA	Trifluoroacetic acid
TGase	Transglutaminase
TRITC	Tetramethylrhodamine isothiocyanate
UPLC	Ultra performance liquid chromatography
UV	Ultraviolet

CHAPTER 1

INTRODUCTION

1.1 Background

Biomaterials research has evolved significantly since the last 20 years. Today, scientists are moving toward a new era of biomaterials research in which they strive to establish a molecular strategy to engineer functional or “biomimetic” materials that can reproduce and exhibit specific biological functions of the target molecule. Undoubtedly, nature offers a great model for imitation, copying and learning, and also inspiration for new biomaterials. Thus, “biomimetic” represents a new field of material science that studies how nature designs, processes and assembles molecular building blocks, such as protein and peptide molecules, and applies these designs and processes to engineer native-like biomaterials with desirable characteristics.

One of the hallmarks of biological systems is the intricate network of the extracellular matrix (ECM) comprising multifunctional macromolecules that modulate cell behavior through interaction with specific receptors as well as through

nonspecific mechanisms. Several approaches, such as protein, peptide, nucleic acid, and enzyme modifications of materials, are being explored to realize the vision of mimicking such *in vivo* systems. Of these approaches, the use of peptides to establish biomolecular engagement between the material and cell integrin-receptors has gained broad acceptance and appears to have great potential to mimic the many roles of natural proteins (Massia and Stark, 2001; Hanks and Atkinson, 2004; Yang et al., 2004; Thorwarth et al., 2005; Guler et al., 2006). The synthesis of mimetic peptides to mimic a small domain of ECM proteins (Graf et al., 1987; Ruoslahti and Pierschbacher, 1987; Massia and Hubbell, 1991; Massia et al., 1993; Boateng et al., 2005), thereby recapitulating the potent and targeted biological activities of the whole protein without the ancillary drawbacks of animal-derived protein application, offers an exciting range of avenues for engineering a new generation of biomaterials.

Most cells *in vivo* adhere to the ECM to survive, either directly to the components of the collagen-rich interstitial matrix or to the basement membrane, which comprises a variety of adhesive proteins, including collagen, fibronectin, and laminin (Gumbiner, 1996). Among the ECMs, type I collagen can directly promote the adhesion and migration of numerous cell types, including hepatocytes, fibroblasts, melanoma, keratinocytes and neural crest cells (Rubin et al., 1981; Faassen et al., 1992; Grzesiak et al., 1992; Scharffetter-Kochanek et al., 1992; Perris et al., 1993). Collagen functions as an important structural component in tissues and is also intimately associated with cell proliferation, cell-cell and cell-ECM communications,

migration and differentiation (Grab et al., 1996; Koide, 2005). It is thus mainly thought of as the primary source of materials for many biological applications (Lee et al., 2001). However, it remains an unresolved challenge to assure adequate supplies of collagen from safe biological sources. The intrinsic problems, such as poor reproducibility, difficulties in purification, possible induction of systemic immune response and potential risk of disease transmission (Sakaguchi et al., 1999; Lynn et al., 2004), associated with the use of animal-derived collagen necessitate engineering of a biological substitute for natural collagen, namely a biomimetic collagen to address the drawbacks in the collagen based applications.

Although works toward realizing collagen-like peptide supramolecules, especially in forming higher order molecular architectures, has been satisfactorily achieved with various self-assembling and template-assembled collagen-like peptides, the biological properties of these collagen mimics are still some distances away from those of the native collagen. The lack of a cell binding sequence or an important functional domain may cause these synthetic triple helices to exhibit minimal functions and cellular recognition thus limiting their application as a substrate for supporting cell adhesion. The complexation of multiple functional domains, such as cell-binding motifs, structural domains and non-collagenous enzyme crosslinking substrate sequences, may be of significant contribution to creating artificial collagens that not only structurally but also functionally resemble their natural counterpart.

1.2 Hypothesis

It is hypothesized that the integration of collagen-like structural domain and biologically relevant epitopes, such as cell binding motif and enzyme-specific crosslinking domain, into the molecular design of collagen-mimetic biomolecule may result in a biomimetic collagen that exhibits stable triple-helical conformation, cell binding activity, and substrate specificity for enzyme-mediated crossliking.

1.3 Research objectives

Interactions between cells and biomaterials are a complex phenomenon. Cell adhesion to the ECM proteins controls morphology, gene expression, and survival of adherent cells (Hynes, 1992; Ruoslahti and Reed, 1994). However, cell adhesion, function, and proliferation *in vitro* can be relatively distinct from those in the physiological environment *in vivo*. The true challenge to material scientists is thus closely associated with the duplication of the functional events of the ECM proteins in their biomolecular design.

The objective of this thesis is to develop an enzymatically crosslinkable collagen-like biomaterial, namely a biomimetic collagen that resembles the native molecular architecture and cell binding activity of collagen. The specific aims of this

research include:

1) **Synthesize collagen-mimetic peptides (CMPs) that resemble both collagen-like molecular architecture and cell binding activity.**

   A series of CMPs supplemented with a specific cell binding sequence spanning residues 502-507 of collagen α_1(I) (Gly-Phe-Hyp-Gly-Glu-Arg; GFOGER) will be synthesized and characterized for their ability to self-assemble into collagen-like triple-helical conformation. The CMPs will also be assessed for their cell binding activity and potential applications as a tissue support matrix for tissue engineering. (Chapter 3)

2) **Establish a template-assembly system to tether CMPs in close proximity thus reinforcing the intra-molecular folding and stabilizing the collagen-like triple-helical conformations.**

   A fully amino acid based peptide template (PT) characterized by its collagen-like primary structure with three C-terminal free carboxyl groups is to be synthesized to covalently knot three CMPs in a staggered array. The conformational characteristic of the PT-assembled structures will be assessed by a series of biophysical studies. (Chapter 4)

3) Study the specific recognition of a cell binding sequence of type I collagen by different cell types.

The affinity of two different cell types, human carcinoma Hep3B liver cells and mouse carcinoma L929 fibroblast cells, toward a specific cell binding sequence of type I collagen (GFOGER) using the template-assembled CMPs as a model for natural collagen will be investigated. (Chapter 5)

4) Characterize an amine donor substrate peptide for tissue transglutaminase (TGase), an ubiquitously expressed crosslinking enzyme.

A novel amine donor substrate for tissue TGase is to be identified from a natural protein through a series of biochemistry assays, using a previously characterized APQQEA (Hohenadl et al., 1995), derived from human osteonectin as an amine acceptor probe. (Chapter 6)

5) Engineer collagen-mimetic dendrimers that exhibit enhanced triple-helical stability, cell binding activity, and substrate specificity for tissue TGase-mediated crossliking.

Collagen-mimetic dendrimers (CMDs) based on a generation 1.5 poly(amidoamine) (G2-PAMAM) dendrimer core is to be synthesized. CMPs supplemented with the cell binding sequence (GFOGER) and the identified EDGFFKI and APQQEA substrate sequences are to be conjugated onto the

dendrimer, thereby result in an enzymatically crosslinakble biomimetic collagen that exhibits both collagen-like structure and cell-binding activity. (Chapter 7)

Collagens are a diverse family of the ECM, found generally crosslinked *in vivo*. The integration of structural domain and biologically relevant epitopes, such as cell binding motif and enzyme-specific crosslinking domain, into the molecular design of a biomimetic collagen appears to be promising for making its biological function and characteristic a little, if not significant, closer to that of the natural collagen. This research may contribute to taking us one step further toward realizing an artificial collagen.

CHAPTER 2

LITERATURE REVIEW

2.1 Cell adhesion to extracellular matrices (ECM) and ECM mimetics

The extracellular matrix (ECM), due to its diverse nature and composition, serves many functions *in vivo*, such as providing support for cell adhesion and regulating intercellular communication. Cell-ECM interactions has been shown to control many cellular activities, including embryogenesis, homeostasis, and tissue remodeling and healing (Hynes, 1992; Ruoslahti and Reed, 1994). Cells *in vivo* adhere to the ECM, either directly to components of the collagen-rich interstitial matrix or to the basement membrane which comprises a variety of adhesive proteins, including collagens, fibronectin, laminin, proteoglycans, and elastin (Gumbiner, 1996). Similarly, anchorage-dependent cells *in vitro* must adhere to a substrate to survive and proliferate. Because of the fundamental importance of cell adhesion for subsequent function and survival, the ability to mimic microenvironment *in vivo* that supports cell adhesion and differentiation is of significant biomedical value. However, most synthetic materials offer little or no control over cell behavior and tissue response.

Cell adhesion to synthetic materials is mainly via interactions between the cell membrane proteins and surface functional chemical groups of the polymer (Bačáková et al., 2000a and 2000b). In contrast to the integrin-mediated cell adhesion, this type of cell-material contact cannot ensure adequate signal transmission from the extracellular environment to the cells thus survival of the anchorage-dependent cells (Huang et al., 1998; García et al., 1999; Groth et al., 1999; Moiseeva, 2001). Therefore, direct mimicry of natural ECM proteins for cell adhesion is crucial to ensure proper cell growth and to achieve successful tissue regeneration and it represents an important strategy in modern biomaterials. Understanding the natural system and knowing what is happening *in vivo* are fundamental for successful mimicry of such biological system in the context of synthetic materials.

Integrin-mediated cell adhesion

Cell adhesion to the ECM is primarily mediated by integrin receptors, a large family of heterodimeric transmembrane proteins with different α and β subunits (Hynes, 1992). Focal adhesions are sites where integrin-mediated adhesion links to the actin cytoskeleton (Wozniak et al., 2004). Multimeric ECM proteins bind to the integrins and thereby stimulate receptor clustering, namely focal adhesions, dynamic protein complexes that contain cytoplasmic structural proteins, such as vinculin, talin, and α-actinin, through which the actin cytoskeleton of a cell links to the ECM (Burridge et al., 1997). The focal adhesion plays an important role in the organization of actin cytoskeleton (LeBaron et al., 1988) and in triggering transmembrane signaling

pathways that direct cell growth and differentiation (Woods and Couchman, 1992; Longhurst and Jennings, 1998). The ability to mimic these ligand-receptor interactions is a key to the rational development of protein mimics. Focal adhesions found in anchorage-dependent cells are known to result from integrin recognition of ECM proteins. For many such ECM macromolecules it is now clear that integrins bind to specific domains within the macromolecules of a few amino acids in length, such as RGD (Pierschbacher et al., 1983; Pierschbacher and Ruoslahti, 1984) and YIGSR (Graf et al., 1987a and 1987b).

The need for ECM-mimetic peptides

ECM proteins have been widely employed to achieve specific cell surface interaction *in vitro*. However, the use of animal-derived proteins, especially for implantation, is often restricted due the potential risk of disease transmission, low purity, and poor reproducibility (Sakaguchi et al., 1999; Hersel et al., 2003). Furthermore, long term application of these proteins would be impossible, mainly because of the enzymatic attack or proteolytic degradation which can be even accelerated by inflammation and infection (Hersel et al., 2003). Additionally, proteins tend to fold randomly on a surface thus causing the specific binding sites not always sterically available.

Conversely, the use of protein-mimetic peptides is attractive for several reasons (Hersel et al., 2003; Shin et al., 2003). Firstly, they are relatively more stable than the natural protein and the cellular recognition sites are easily accessible for their

smaller size and higher density on the surfaces. In addition to the potential to mimic cell attachment activity of parental molecules, mimetic peptides can be produced synthetically, hence safe, pathogen-free, and reproducible, thus allowing precise control of their chemical composition and selective targeting of specific cell adhesion receptors.

Mimetic peptides for cell adhesion

Various peptides derived from a diversity of ECM molecules are now recognized as potential cell adhesion motifs, as summarized in Table 2.1. The most commonly used peptide for promoting cell adhesion is RGD (Pierschbacher et al., 1983; Pierschbacher and Ruoslahti, 1984), the cell recognition domain found in fibronectin, laminin, and collagen. Apart from RGD many other important cell adhesion motifs have been identified, such as YIGSR (Graf et al., 1987), DGEA (Staatz et al., 1991), and REDV (Humphries et al., 1986; Huebsch et al., 1995). Generally, the ability to support cell adhesion and proliferation is a prerequisite for any synthetic materials to serve as a substrate. There is increasing recognition of the role of integrin-mediated interactions between the cell membrane receptors and the specific ligands on regulating cellular behavior. In *in vitro* environment, such interactions could be acquired through the cell binding peptide sequences derived from the ECM proteins, such as RGD, YIGSR, GTPGPQGIAGQRGW (P-15), and REDV (Qian and Bhatnagar, 1996; Massia and Stark, 2001; Mann and West, 2002; Dhoot et al., 2004; Hanks and Atkinson, 2004; Boateng et al., 2005; Guler et al., 2006).

The molecular size of various ECM proteins is often several thousand amino acids long. Although the binding domains of the ECM proteins for cellular attachment are only several amino acids long, the exact role of the remaining domains of these macromolecules is largely unknown. In many instances, the small binding domain alone does not provide sufficient affinity for cell adhesion (Mardilovich et al., 2006). Presentation of short cell binding epitopes, such as RGD and GFOGER (Knight et al., 1998; Knight et al., 2000), may result in the loss of full biological activity because of the absence of supplementary functional domains, such as synergy sites and structural domain that present in the natural proteins (Aota et al., 1994; Danen et al., 1995; Emsley et al., 2000). Thus, many more studies are essential to design and develop ECM-mimetic peptides of improved biomolecular recognition that can better, if not fully, mimic the ECM integrin-mediated adhesion for therapeutic and medicinal applications.

Table 2.1. Cell recognition motifs derived from the ECM proteins for integrin-mediated cell adhesion.

Peptide sequences*	Origin	References
RGD	Fibronectin, Collagen, Laminin	(Pierschbacher et al., 1983; Pierschbacher and Ruoslahti, 1984)
YIGSR	Laminin	(Graf et al., 1987)
GTPGPQGIAGQRGW (P-15)	Collagen	(Qian and Bhatnagar, 1996)
IKVAV	Laminin	(Nomizu et al., 1995)
REDV	Fibronectin	(Humphries et al., 1986)
DGEA	Collagen	(Staatz et al., 1991)

* Standard one letter code is used to express amino acid sequences.

2.2 Collagen and collagen mimics

ECM proteins come in a wide variety of sizes, structures, and functions. One protein that is of wide interest to many scientists is collagen, which is the principal constituent of the ECM in the body. It can be distinguished from other proteins by its unique triple-helical structure composed of three left-handed poly(proline-II)-like chains, staggered by one residue from each other, intertwined into a right-handed triple helix (Engel and Prockop, 1991; Bella et al., 1994; Brodsky and Ramshaw,

1997). This assembly is a direct consequence of its unique primary structure composed of repetitive Gly-Xxx-Yyy triplets, where X and Y amino acid residues are frequently Pro and Hyp, respectively.

Collagen constitutes approximately one-third of human proteome. Its high natural abundance hints the important intrinsic roles that collagen plays in biological system. Thus far, 27 types of collagen have been identified (Boot-Handford et al., 2003). Among the various collagens, type I collagen, in which each strand consists of approximately 300 Gly-Xxx-Yyy triplets, is the most abundant and expressed ubiquitously in the human body. Although the primary, secondary, and tertiary structures of collagen have been known for about 40 years, it has only become clear that collagen is also important in directly supporting cell adhesion one or two decades ago (McCarthy et al., 1996). It has been found that type I collagen can directly promote the adhesion and migration of numerous cell types, including hepatocytes, fibroblasts, melanoma, keratinocytes and neural crest cells (Rubin et al., 1981; Faassen et al., 1992; Grzesiak et al., 1992; Scharffetter-Kochanek et al., 1992; Perris et al., 1993).

The diversity of collagen families makes development of a comprehensive, single model system challenging. A system capable of emulating specific variables, such as the structure and biological activity, of this protein is thus desirable, especially for the studies on collagen structure, folding process, interactions with other

collagen-binding molecules, as well as receptor-mediated cell attachment. Such a system could serve as a starting point for the development of a novel biomimetic collagen: creation of peptide-based supramolecules that mimic collagen structure and functions.

Self-assembling open-chain collagen-mimetic peptides

The folding into a well-defined structure is fundamental for any natural protein to implement its biological function. Mimicry of collagen molecular architecture thus represents the prerequisite in the preparation of novel collagen-like biomaterials. Synthetic peptides consisting of Gly-Xxx-Yyy repeating sequences possess an intrinsic propensity to fold into collagen-like triple-helical structures. Therefore, the use of self-assembling open-chain collagen-like peptides could be the simplest way to achieve triple-helical peptides as collagen mimics. However, to create stable collagen-like triple-helical peptides that can be used for biophysical and physiological studies, the peptide sequences must be carefully and appropriately designed. The stability of the synthetic triple helices often depends on the length and the amino acid sequence of the peptide chain (Goodman et al., 1998).

One of the pioneering works on collagen-like peptide was reported in 1960s by Sakakibara and co-workers (Sakakibara et al., 1968). Since then, many polypeptides composed of Pro-Pro-Gly or Pro-Hyp-Gly repeat units have also been synthesized chemically to mimic collagen-like triple-helical conformations

(Kobayashi et al., 1970; Sakakibara et al., 1973; Engel et al., 1977; Inouye et al., 1982). The primary sequence of peptides can significantly affect the folding and conformational stability of the collagen-like peptides, as studied by Brodsky, Raines and Goodman (Long et al., 1993; Holmgren et al., 1998 and 1999; Jefferson et al., 1998; Kwak et al., 1999). Many other collagen-like peptides containing unnatural residues have also been synthesized, including repeating Gly-Nleu-Pro, Gly-Pro-Nleu, and Gly-Pro-FPro (where Nleu = N-isobutylglycine, FPro = *trans*-4-fluoroproline) (Feng et al., 1996 and 1997; Holmgren et al., 1999). Among the various collagen analogs, the Gly-Pro-Pro or Gly-Pro-Hyp sequence-based peptides are known to have primary structure most similar to the structural domain of natural collagen and certainly self-assemble into collagen-like triple-helical conformation when the chain length is sufficiently extended (Inouye et al., 1982; Feng et al., 1996).

Template-assembled collagen-mimetic peptides

Another approach to create synthetic triple helices is to biophysically inter-bridge the collagen-like peptides in close proximity. Mutter et. al. introduced the template-assembled synthetic proteins approach for construction of stable artificial tertiary structure of globular protein, four α-helical bundle (Mutter et al., 1992). Similarly, the idea of a template-assembled synthetic protein can also be used for the engineering of collagen-like triple helices. The use of a template to covalently hold the collagen-mimetic peptides in a staggered array can reinforce and direct intramolecular folding thus stabilizing the triple-helical structures (Goodman et al.,

1998 and 2003).

The triple helix structure of collagen has been mimicked in synthetic model peptides with various C- and N-terminal templates (Figure 2.1). Branching side chains of amino acid residues have been utilized to covalently hold three collagen-mimetic peptides in proper registration. Among them, the C-terminal lysine dimer is frequently used for tethering collagen-mimetic peptides. Heidemann et. al. (Roth and Heidemann, 1976; Thakur et al., 1986; Germann and Heidemann, 1988) and Fields et. al. used two consecutively connected lysine residues with three functional groups to covalently link three collagen-mimetic peptides at the C-termini (Fields, 1991; Fields et al., 1993a and 1993b). Similarly, Tanaka and co-workers extended the use of dilysine template to tether three collagen-mimetic peptides at both C- and N-terminals resulted in enhanced thermal stability of the triple helix (Tanaka et al., 1993 and 1998). Undoubtedly, the C-terminal dilysine template-assembly system is feasible for standard solid phase peptide synthesis in which three collagen-mimetic peptides can be covalently knotted on a branching dilysine unit that is pre-constructed on a solid support. However, this template-assembly approach requires a complex and carefully planned protocol of orthogonal protection and deprotection strategies to ensure proper coupling and parallel growth of several peptide chains onto a single template (Fields et al., 1993a).

On the other hand, glutamate dimer (Hojo et al., 1997) and a built-in cysteine-knot (Ottl et al., 1996; Ottl and Moroder, 1999) have been used to covalently assemble collagen-like peptides into triple-helical conformation via "post-synthetic" method, which allows the purification of each peptide strands prior to trimerization thus improving the purity of final product. However, the reported assembly approach required more synthesis steps as well as a complex protection strategy for Cys residues to facilitate the chemoselective disulfide bridging of the three cysteine-peptides (Ottl et al., 1996; Ottl and Moroder, 1999).

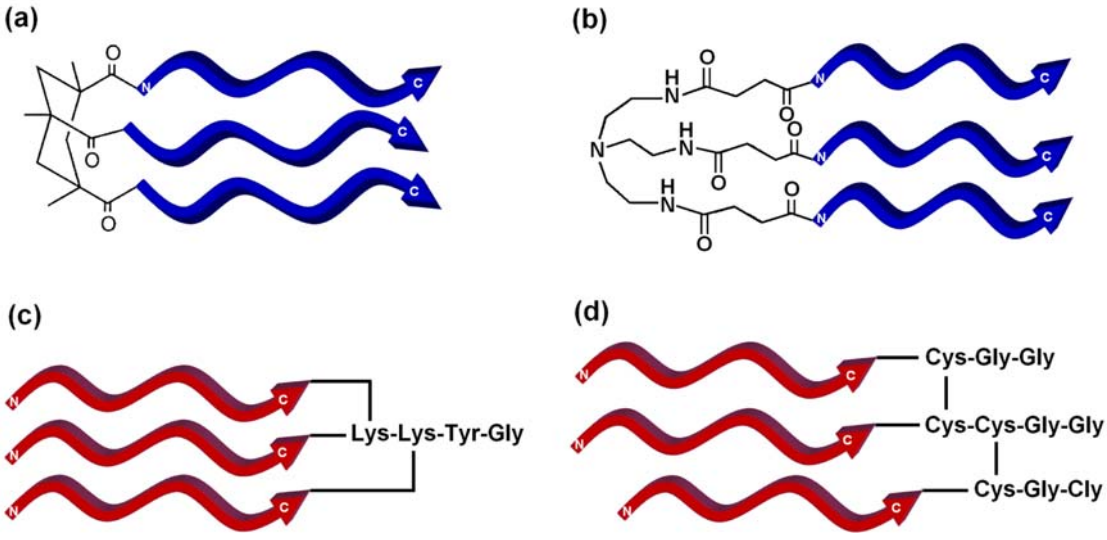

Figure 2.1. Template-assembly approach for construction of stable collagen-like triple-helical structures: a) Kemp triacid-, b) Tris(2-aminoethyl) amine-, c) lysine dimer-, and d) cysteine-disulfide-assembled collagen-mimetic peptides (Fields et al., 1993a; Ottl et al., 1996; Goodman et al., 1998; Kwak et al., 2002).

Various organic templates have also been developed for tethering collagen-mimetic peptides thus promoting the triple helix folding. Greiche and Heidemann used 1,2,3-propanetricarboxylic acid for the assembly of collagen-like peptides (Greiche and Heidemann, 1979). Goodman and co-workers successfully assembled collagen-mimetic peptides on a Kemp triacid (KTA) template thus stabilizing the triple helix of as short as three repeats of Gly-Pro-Hyp, which otherwise is in non-triple-helical random structure (Feng et al., 1996; Goodman et al., 1996). They have also reported the usefulness of Tris(2-aminoethyl) amine (Kwak et al., 2002) as a template for tethering three peptide strands in correct registration. A triacid template, cyclotriveratrylene, was also found to have comparable stabilizing effect as KTA template in facilitating the triple-helical folding of peptides (Rump et al., 2002). To reinforce the intra-molecular folding, an all-*cis*-functionalized cyclopropane template was also added into the design of collagen peptides (Yamazaki et al., 2001).

Although such synthetic collagen-like triple helices could be potential cell adhesion substrate materials (Johnson et al., 2000), the interactions of cells with these triple helices are limited to structural recognition or "RGD-independent" contact. Low levels of cell adhesion have been reported for these triple-helical collagen model peptides (Rubin et al., 1981; Zijenah and Barnes, 1990; Fields et al., 1993b). The lack of a cell binding sequence, such as RGD, may cause these synthetic triple helices to exhibit minimal cell binding activity thus limiting their application as a substrate for

supporting cell adhesion and proliferation. Nevertheless, the collagen-like structural molecules presented in these previous studies would definitely serve as a reference for the future design of artificial collagens that not only structurally but also functionally resemble their natural counterpart.

Collagen-mimetic dendrimers

Inspired by the functional significance of collagen in nature and its remarkable physiological roles, many scientists are working towards realizing an artificial collagen. New class of polymers is being developed to mimic specific variables of natural proteins. The use of dendrimers, such as poly(amidoamine) (PAMAM), in biomaterial and therapeutic applications is becoming increasingly attractive and significant (Gilmartin et al., 2005; Majoros et al., 2005). PAMAM dendrimers are highly branched macromolecules possessing a high density of surface groups, such as primary amine or carboxyl groups, which can be derivatized with various structures that drive the assembly of dendrimers to fashion protein-like structure (Figure 2.2). Furthermore, the non-cytotoxic characteristic of low generation PAMAM dendrimers makes them a desirable candidate for use as a scaffold to assemble peptides into higher order structure to develop novel protein-like biomaterials. The densely packed environment of the conjugated collagen peptides induced by the dendritic structure can promote the intramolecular folding of triple-helical conformation. The PAMAM dendrimers may also serve as a nucleation source for the interaction of intramolecular triple-helical arrays.

Many artificial proteins have been prepared by attaching peptide blocks to a template that directs the peptide helices into a protein-like packing (Mutter et al., 1992). For instance, Higashi et. al. employed a third generation PAMAM dendrimer to assemble α-helical peptides, resulting in peptide dendrimers of greatly enhanced helicity as compared to non-denrimer-assembled counterparts. The improved helicity can be attributed to aggregation of the peptide segments conjugated on the dendrimer surface (Higashi et al., 2000). This model has also been a basis for the design of artificial collagen. Goodman and co-workers reported the synthesis of 162-residue collagen-mimetic dendrimers, which exhibited enhanced triple-helical stability, based on a trimesic acid core structure and a tris-based template (Kinberger et al., 2002). This collagen model represents one of the pioneering works achieved in the formation of collagen-like supramolecular structure. Subsequently, Kinberger et. al. described the preparation and characterization of a collagen-mimetic dendrimer based on a PAMAM dendrimer core structure (Kinberger et al., 2006). The synthesis of collagen peptide-PAMAM conjugate structures resulted in a collagen-mimetic dendrimer with increased thermal stability which can be attributed to the intramolecular clustering of the triple-helical arrays about the core structure. The biological application of this collagen-mimetic dendrimer has yet to be reported.

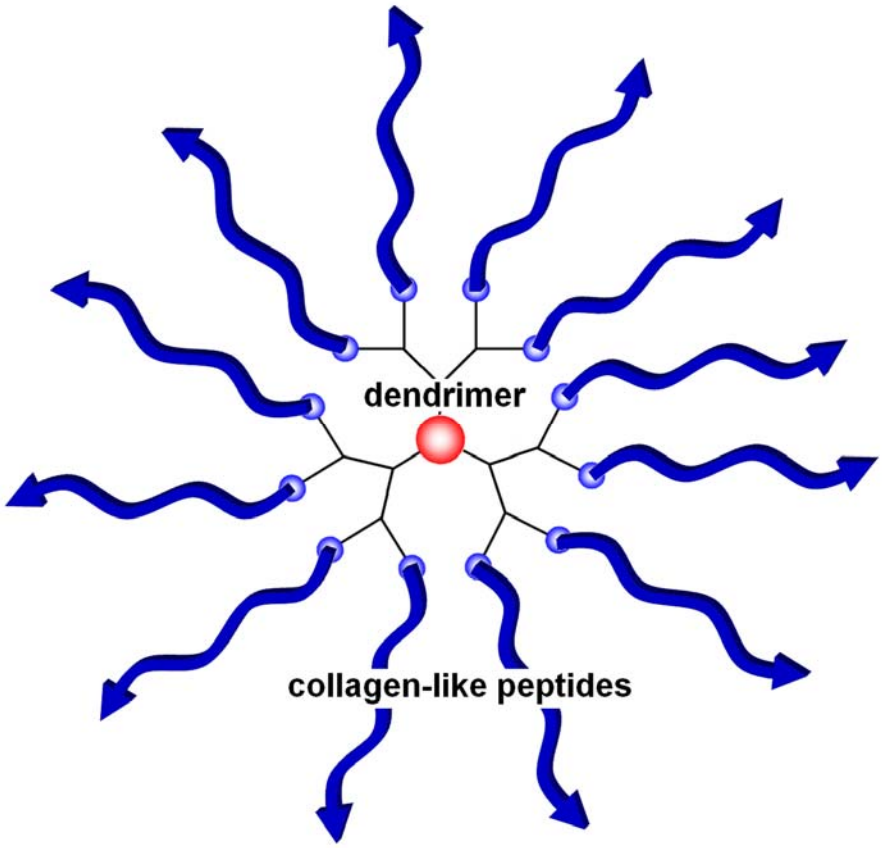

Figure 2.2 The branched dendrimers (eg. PAMAM dendrimers) with a high density of surface groups, such as primary amine or carboxyl groups, can be derivatized with collagen-like peptides to drive the assembly of dendrimers to fashion collagen-like supramolecular structure.

Although works toward realizing collagen-like peptide supramolecules has been satisfactorily achieved, especially in forming higher order molecular architectures, the biological properties of these collagen-mimetic dendrimers are still some distances away from those of the native collagen. Therefore, the supplementation of collagen-mimetic peptides or dendrimers with biologically relevant epitopes is essential to create a novel biologically active biomimetic collagen.

2.3 Integrin recognition sequences in various collagen subtypes

Collagen is recognized as an important structural support protein as well as cell adhesion matrix *in vivo*. Identification of cellular recognition sequences within this macromolecule is essential to create collagen mimics that can reproduce some, if not full, biological activities of the target collagen molecule. Over the past 30 years, a map of the distribution of numerous cell binding domains in various types of collagens has been created (Lullo et al., 2002).

Cellular recognition sequences of type I, III and IV collagens

The integrins are important cell surface receptors that mediate both cell contact and cellular recognition of the ECM. Several integrins, such as $\alpha_1\beta_1$, $\alpha_2\beta_1$, $\alpha_3\beta_1$, $\alpha_{10}\beta_1$, and $\alpha_{11}\beta_1$, have been shown to bind to collagen and activate cytoplasmic intracellular signaling pathways (Elices and Hemler, 1989; Kramer and Marks, 1989; Chan et al., 1992; Kühn and Eble, 1994; Fields, 1995; Camper et al., 1998; Velling et al., 1999; Zhang et al., 2003; White et al., 2004). Each recognizes a variety of collagen subtypes. Several regions within type I, III, and IV collagens have been identified as cellular recognition sites (see Table 2.2). For example, amino acid sequences spanning residues 434-472 and residues 1263-1277 of collagen α_1(IV) have been reported to be high affinity cell binding sites (Chelberg et al., 1990; Eble et al., 1993). Furthermore, α_1(III) 76-84 and α_1(III) 237-242 regions have also been found to display significant cell binding activity (Legrand et al., 1980; Kim et al., 2005).

Among a variety types of collagens, type I collagen is ubiquitous in all vertebrates and is among the largest and most complex macromolecules. The ubiquity and functional significance of type I collagen have interested many scientists to explore its functional domains, especially the cellular recognition sequences. Residues from 403-551 of collagen α_1(I) are found to support $\alpha_2\beta_1$-mediated adhesion and have been found to contain a binding site (DGEA) for hepatocyte $\alpha_2\beta_1$ integrin receptors (Gullberg et al., 1989; Staatz et al., 1990). Furthermore, the GFOGER sequence corresponding to residues 502-507 of collagen α_1(I) has been reported to be the major integrin-receptor binding locus within the type I collagen (Knight et al., 1998 and 2000). Xu et. al. identified a cell adhesive sequence (GLOGER) analogous to GFOGER (Xu et al., 2000). Siljander et. al. further established an affinity series for the GER-containing recognition motifs: GFOGER> GLOGER> GLSGER> GMOGER> GAOGER≈ GASGER≈ GQRGERA, strengthening the observation that GFOGER is a high affinity sequence (Siljander et al., 2004). The specific recognition sites of different collagen subtypes can be recognized by a group of cell adhesion integrin-receptors (White et al., 2004). The integrins $\alpha_1\beta_1$, $\alpha_2\beta_1$ and $\alpha_{11}\beta_1$ have been shown to recognize the GFOGER or GFOGER-like motifs found in the type I collagen (Calderwood et al., 1997; Gardner et al., 1999; Knight et al., 2000; Xu et al., 2000; Tulla et al., 2001; Zhang et al., 2003; Siljander et al., 2004).

Table 2.2. Several regions of different collagen subtypes were identified as cellular recognition sites.

Collagen subtype	Location	Sequence*	References
Type I	α_1(I) 127-134	GLOGERGR	(Xu et al., 2000)
Type I	α_1(I) 435-438	DGEA	(Staatz et al., 1991)
Type I	α_1(I) 502-507	GFOGER	(Knight et al., 1998 and 2000)
Type I	α_1(I) 772-786	GPQGIAGQRGVVGLO	(Kleinman et al., 1978; Grab et al., 1996)
Type III	α_1(III) 76-84	GKOGEOGPK	(Legrand et al., 1980)
Type III	α_1(III) 237-242	GROGER	(Kim et al., 2005)
Type IV	α_1(IV) 531-543	GEFYFDLRLKGDK	(Wilke and Furcht, 1990; Miles et al., 1994)
Type IV	α_1(IV) 1263-1277	GVKGDKGNPGWPGAP	(Chelberg et al., 1990)

* Standard one letter code is used to express amino acid sequences, except where noted. O represents Hydroxyproline residue.

Integrin-specific bioadhesive collagen-mimetic peptides

The characterization and mapping of numerous integrin binding sites within several regions of various collagen subtypes opens a way for the development of novel biologically active collagen-like biomolecules. Fields et. al. created a system in which collagen-like peptide-amphiphiles incorporating α_1(IV) 1263-1277 sequence of biological interest self-assembled into native collagen structure. Mouse melanoma cell

adhesion and spreading were promoted by the self-assembled collagen-like peptide-amphiphiles (Fields et al., 1998). This molecular design of peptide-amphiphile allows formation of lipid film or vesicles thus offering versatility for engineering bioadhesive surface as well as protein/drug delivery carrier. García and Reyes engineered an $\alpha_2\beta_1$-specific bioadhesive surface by "sandwiching" a type I collagen-derived cell adhesion sequence in a flanking host, $(GPP)_5$, which maintains the triple helix stability at above physiologic temperature. The peptide-functionalized substrate supported $\alpha_2\beta_1$-mediated cell adhesion and focal adhesion assembly (Reyes and García, 2002 and 2003). Engineering of such integrin-specific bioadhesive surfaces that specifically target certain integrin-receptors and signaling cascades may provide a biomolecular strategy for optimizing cellular response. Furthermore, a synthetic 15-residue peptide (P-15) (GTPGPQGIAGQRGVV) derived from residues 766-780 of collagen α_1(I) is reported to be 45,000 times more potent than RGD-containing peptides in competition with collagen for cell binding (Bhatnagar et al., 1997; Yang et al., 2004). P-15 has been widely used as a bioadhesive matrix to promote cell attachment, proliferation and function (Qian and Bhatnagar, 1996; Hanks and Atkinson, 2004; Yang et al., 2004; Thorwarth et al., 2005).

Several distinct sequences derived from various collagen subtypes have been characterized as cell adhesion sites. Extensive studies on both structural and biological domains of this ubiquitously expressed protein have contributed to the transition from understanding a natural system to creating a protein-like biologically

active biomaterial and applications. Another important aspect concerning the assembly of the ECM protein *in vivo* is certainly closely related to the enzyme-mediated crosslinking that plays a significant role in stabilizing the ECM proteins thus cellular activity. The crosslinking of the ECM proteins, such as collagen, to form stable supramolecular association capable of serving as protective and supporting structures is a common phenomenon in biological system.

2.4 Transglutaminases: crosslinking enzymes that stabilize proteins

Tissue transglutaminase (TGase) is a Ca^{2+}-dependent enzyme involved in the post-translational modification of proteins. It catalyzes an acyl-transfer reaction between γ-carboxamide groups of peptide-bound glutamine residues and ε-amino groups of peptide-bound lysine residues (Figure 2.3), resulting in a protease-resistant γ-glutamyl-ε-lysine isopeptide bond, thereby stabilizing protein assemblies (Greenberg et al., 1991; Lorand and Graham, 2003). Tissue TGase is expressed ubiquitously and the tissue TGase-modified proteins are evident throughout the body including extracellular matrices (ECM) as well as skin and hair. Its expression is often correlated with cellular differentiation (Greenberg et al., 1991; Aeschlimann et al., 1993), receptor signaling (Nakaoka et al., 1994), programmed cell death (Fesus et al., 1987; Greenberg et al., 1991), assembly of the ECM (Schittny et al., 1997), and several degenerative diseases (Griffin et al., 2002). Tissue TGase is also involved in

wound healing and tissue repair (Eitan et al., 1994). Owing to its various physiological functions, it is important to identify tissue TGase substrates in native proteins to better understand the physiology of tissues for diagnostic and therapeutic purposes.

The roles of tissue transglutaminase

Several lines of evidences show that tissue TGase acts physiologically in the stabilization of the ECM by crosslinking numerous ECM proteins, such as fibronectin (Fesus et al., 1986), collagen (Bowness et al., 1987; Kleman et al., 1995), and laminin (Aeschlimann et al., 1992). It plays an important role in the assembly of matrix proteins. For example, the high affinity binding and crosslinking of tropoelastin to fibrillin-1, a major fibrillin isoform in elastic fibers, confirms that the tissue TGase-mediated crosslinking is fundamental to the elastic fiber formation (Rock et al., 2004; Clarke et al., 2005). Additionally, it has been suggested that the tissue TGase-catalyzed crosslinking may play a vital role in strengthening microfibrillar networks (Qian and Glanville, 1997). The formation of crosslinks between collagen α-chains (Jelenska et al., 1980) and the crosslinking of fibronectin to specific sites in collagen types I and III (Mosher and Schad, 1979; Mosher et al., 1980) also implies an important role of transglutaminase in the organization of supramolecular structure of collagen. The irreversible crosslinking of collagen fibrils by tissue TGase may play a role in the stabilization of the ECM in the early steps of collagen fibrillogenesis (Kleman et al., 1995).

In addition to these extracellular functions, there is evidence that tissue TGase may also play a role in facilitating the interactions between cells and the ECM (Ikura et al., 1988; Gentile et al., 1992). The physiological implications related to the extracellular protein crosslinking suggest that its function is not limited to stabilizing the matrix proteins but also to facilitate cell adhesion and cell motility (Akimov and Belkin, 2001; Balklava et al., 2002). For instance, several groups demonstrated a close association of the cell surface-related tissue TGase with β1 and β3 integrins, in particular at focal adhesion sites where ECM protein fibril assembly is taking place (Gaudry et al., 1999; Akimov et al., 2000).

The collagenous domains constitute almost the entire mass of the fibrillar collagens and are usually intermingled with non-collagenous regions. The specific array of collagenous and non-collagenous domains in the nature hints several important considerations toward realizing a biologically active artificial collagen: the roles of the structural domain and the non-collagenous domain and the importance of the intermingling of the two. Collagenous domains within the ECM are unique for their stable tertiary structure, triple helix, which may play a role in the preservation of the protein activity. The non-collagenous domains normally house biologically relevant epitopes, including cell binding sequences as well as enzyme crosslinking sites. The complexation of the two domains may be the key contribution to the complete functions and activity of the natural proteins *in vivo*. Thus, presentation of these epitopes in the design of collagen mimics could further improve their properties

and bring them a little closer to the native one.

Substrate peptides for tissue transglutaminase

Of all the events that are mediated by tissue TGase, protein crosslinking is of great interest of many and is most extensively studied. The biochemical mechanism underlying the tissue TGase action involves reaction pathway that is more complicated than the simple outline presented in Figure 2.3. Briefly, the crosslinking reaction begins with transamidation of the γ-carboxamide group of a peptide-bound glutamine residue to form a thiol ester intermediate with an active-site cysteine of the enzyme (resulting in the release of ammonia). The formation of acyl-enzyme intermediate is followed by the transfer of the acyl intermediate to a nucleophilic substrate, usually the ε-amino group of a peptide-bound lysine (amine donor group). This process re-establishes the enzyme in its original form, which thereby allows it to participate in another cycle of catalysis, and results in the formation of an intermolecular isopeptide ε-(γ-glutamyl)lysine crosslink (Lorand and Graham, 2003).

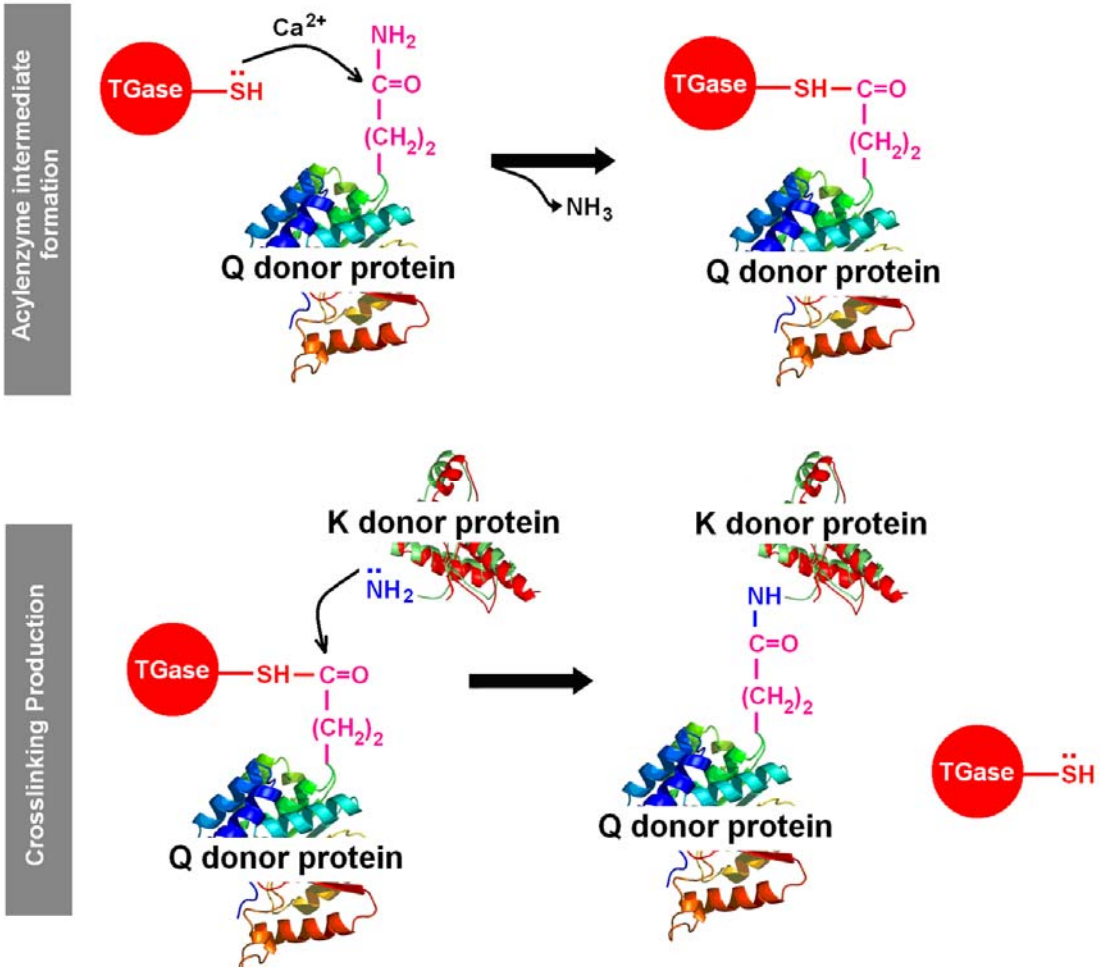

Figure 2.3 Transglutaminase-catalyzed acyl transfer and protein crosslinking. The γ-carboxamide group of a protein-bound glutamine residue (Q donor) forms a thiol ester with the active site cystein of the enzyme. The transfer of the acyl intermediate to a nucleophilic substrate, usually the ε-amino group of a protein-bound lysine (K donor group) results in the formation of intermolecular isopeptide ε-(γ-glutamyl)lysine crosslink (Lorand and Graham, 2003; Esposito and Caputo, 2004).

Although the underlying mechanism governing the enzyme recognition of the substrate is not fully understood, there is plenty of *in vitro* data indicating that there is some specific substrate requirements for tissue TGase (Esposito and Caputo, 2004). For example, one common observation in many studies was that most substrates were located at the solvent-exposed surface regions or the accessible terminal extensions of the native proteins. Additionally, the neighboring residues flanking the protein-bound glutamine and lysine residues has considerable influence on the substrate potential of the protein for tissue TGase (Grootjans et al., 1995; Esposito and Caputo, 2004). A considerable number of amine acceptor substrates have been identified in various proteins for tissue TGase (Table 2.3). Many of the amine acceptor substrates in their biotinylated or tagged form have been widely used for site-specific enzyme-directed labeling for identifying the amine donor substrate (Esposito and Caputo, 2004). In addition to serving as a probe for identifying enzyme substrate, the incorporation of the naturally-derived substrate peptides could also lead to tailoring novel protein-like crosslinkable biomimetic materials.

Table 2.3. Some previously characterized amine donor and acceptor substrates for tissue transglutaminase.

Protein	Sequence*	Reference
	Amine donor substrate, K	
βA3-crystallin	-QQELESLPTT**K**MAQTN-	(Groenen et al., 1994)
β-Endorphin	-VTLFKNAIVKNAYK**K**GE-	(Pucci et al., 1988)
Seminal vesicle protein IV	-R**K**T**K**E-, -SRRS**K**HI-, -SSYA**KKK**RSRF-	(Porta et al., 1991)
Alzheimer β/A4 amyloid	-FRHDSGYEVHHQ**K**LVFF-	(Ikura et al., 1993)
Heat shock protein 25	-PEAGKSEQSGA**K**	(Merck et al., 1993)
Glycoprotein 41	-QARILAVERYL**K**DQQLL-	(Mariniello et al., 1993)
αβ-crystallin	-EEKPAVTAAPK**K**-	(Groenen et al., 1992)
	Amine acceptor substrate, Q	
βA3-crystallin	-TV**QQ**EL-	
βB2-crystallin	-ET**Q**AG-	(Berbers et al., 1984)
βB3-crystallin	-AE**Q**HS-	
Nidogen	-GTCVAAED**Q**RPINY-	(Aeschlimann et al., 1992)
Osteonectin	-AP**QQ**EA-	(Hohenadl et al., 1995)
β-Endorphin	-GFMTSEKS**Q**TPLVTL-	(Pucci et al., 1988)
RhoA	-**Q**VELAL-, -AG**Q**EDY-	(Schmidt et al., 1998)
Osteopontin	-LKPDPS**Q**K**Q**T-	(Sorensen et al., 1994)
Tau	-V**Q**SK-, -SP**Q**LATLAD-	(Murthy et al., 1998)

* Standard one letter code is used to express amino acid sequences, except where noted. O represents Hydroxyproline residue.

Although the relationship between the matrix protein crosslinking and the roles of the tissue TGase in cell adhesion and spreading is still not fully understood, there is increasing evidence indicating that tissue TGase is externalized from cells, where it may play a key role in cell attachment and spreading as well as stabilizing the underlying protein molecules (Griffin et al., 2002). Furthermore, the tissue TGase-mediated reaction can add new properties from one substrate protein to another, thereby enhancing the function of the artificial collagen. Collagens are a diverse family of the ECM, found generally cross-linked *in vivo*. Therefore, integrating the tissue TGase substrate peptides into the molecular design of biomimetic collagen appears to be attractive for making its biological function and characteristic a little, if not significant, closer to that of the natural collagen, especially in making them crosslikable, either by exogenous or endogenous tissue TGase. Additionally, the tissue TGase-mediated protein crosslinking, a common physiological phenomenon, may be also a crucial recognition mark for cell surface receptors.

CHAPTER 3

AN INTEGRIN-SPECIFIC COLLAGEN-MIMETIC PEPTIDE APPROACH FOR OPTIMIZING HEP3B LIVER CELL ADHESION, PROLIFERATION, AND CELLULAR FUNCTION

The central hypothesis of this thesis is that the integration of collagen-like structural domain and biologically relevant epitopes, such as cell binding motif and enzyme-specific crosslinking domain, into the molecular design of collagen-mimetic biomolecule may result in a synthetic, hence pure, reproducible, and pathogen-free, crosslinkable collagen-like biomaterial that exhibits stable triple-helical conformation, cell binding activity, and substrate specificity for enzyme-mediated crossliking. We examined this hypothesis by first synthesizing and characterizing a series of collagen-mimetic peptides (CMPs) supplemented with a cell binding sequence (GFOGER) of collagen α_1(I). The aim of this study is to engineer CMPs that resemble both collagen-like molecular architecture and cell binding activity and use them as a bioadhesive matrix for optimizing cell adhesion, proliferation and functions in tissue engineering.

This chapter is modified from Khew, S.T., Zhu, X.H., Tong, Y.W. (2007) *Tissue Eng.* 13, 2451-2463.

3.1 Introduction

Mimicry of collagen structurally and biologically using various peptide sequences offers a robust strategy toward realizing an artificial collagen or novel collagen-like biomaterial. Collagen-mimetic peptides (CMPs) incorporating an integrin-specific sequence can potentially be used as a tool to specifically target certain integrin-receptor bindings and signaling cascades and thus provide a biomolecular strategy for optimizing cellular responses for tissue engineering. In this study, Gly-Pro-Pro (GPP) and Gly-Pro-Hyp (GPO) sequences were used to sandwich the integrin-specific Gly-Phe-Hyp-Gly-Glu-Arg (GFOGER) motif to assemble the peptide into a stable triple-helical conformation. The aim of this study is to engineer collagen-mimetic peptides (CMPs) that resemble both collagen-like molecular architecture and cell binding activity and use them as a bioadhesive matrix for optimizing cell adhesion, proliferation and functions in tissue engineering. We have previously reported the advantage of using Poly(3-hydroxybutyrate-*co*-3-hydroxyvalerate (PHBV) microspheres as a scaffold to engineer tissue-like constructs (Zhu et al., 2006). In this study, the effect of the CMP on regulating cell proliferation and functions was examined through a 14-day cell culture on the CMP-functionalized PHBV microspheres. This study presents an intriguing challenge to realizing a collagen-like microenvironment using mimetic peptides on a polymeric scaffold for cell culture and tissue engineering.

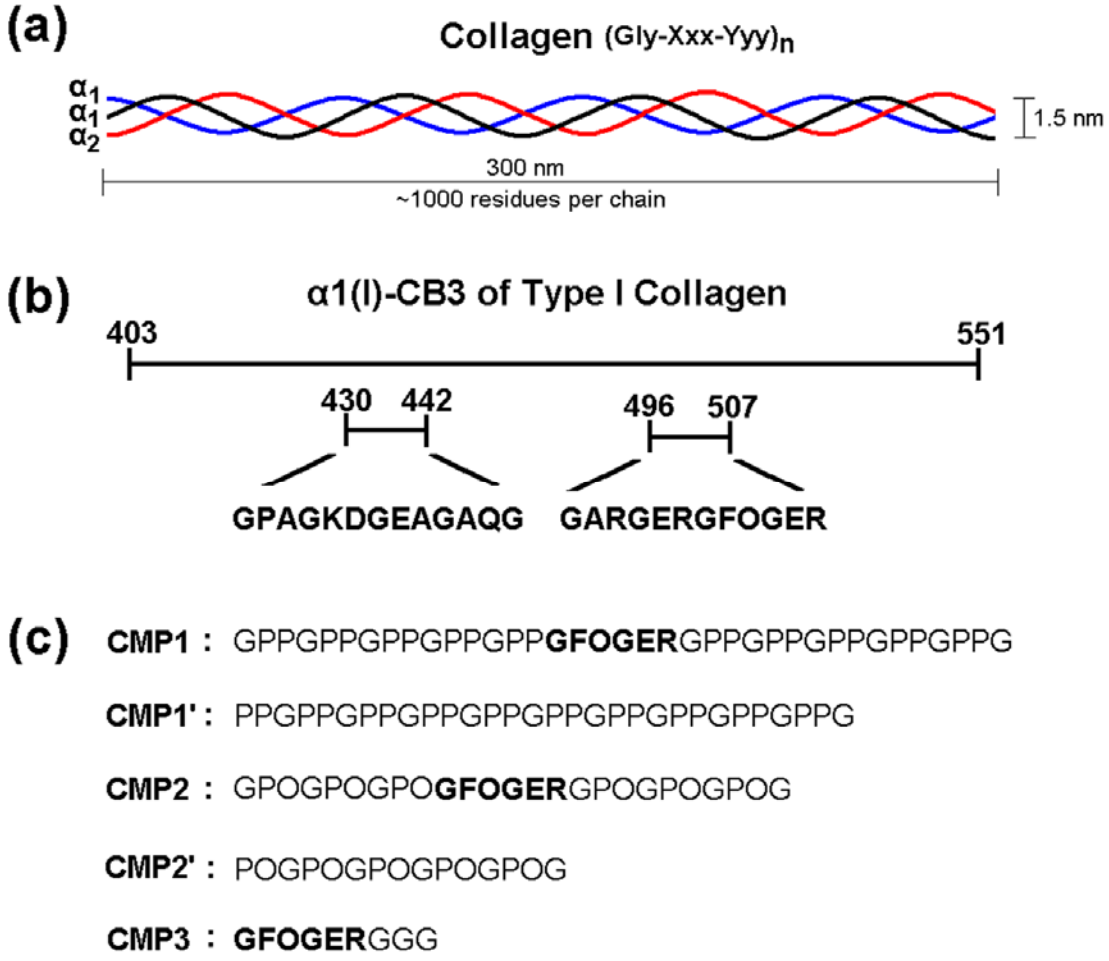

Figure 3.1. (a) Type I collagen comprises three left-handed helical polypeptide chains intertwined into a right-handed triple helix; (b) residues 502-507 of the collagen α_1(I) chain, GFOGER, is identified as the major binding locus within type I collagen (Knight et al., 1998 and 2000), (c) collagen-mimetic peptides (CMPs) consisting of various peptide sequences. The cell recognition site (GFOGER), shown in bold, was sandwiched by the repeating GPP and GPO triplets. CMP1' and CMP2' are analogous to CMP1 and CMP2, respectively, except without GFOGER. CMP3 has no repeating GPP or GPO triplets.

3.2 Experimental section

Materials

All peptide synthesis chemicals and solvents were of analytic reagent grade or better. All amino acids were of L-configuration and were purchased from Novabiochem (San Diego, CA). Chemical solvents were purchased from Sigma-Aldrich (St. Louis, MO) unless otherwise stated. Acetonitrile (high performance liquid chromatography (HPLC) grade) was purchased from Merck (Darmstadt, Germany). PHBV (8% PHV), was purchased from Sigma-Aldrich. Poly(vinyl alcohol) (PVA; molecular weight 6000) was obtained from Polysciences (Warrington, PA). RGD tripeptide was purchased from Sigma-Aldrich.

Peptide synthesis

All peptides (as shown in Figure 3.1) were synthesized in-house on an automated Multipep peptide synthesizer (Intavis, Cologne, Germany). All peptides were assembled on fluorenyl-methoxy-carbonyl (Fmoc)-Gly-Wang resin (substitution level = 0.66 mmole/g resin) at a 50-μmole scale. Stepwise couplings of amino acids were accomplished using a double coupling method with 5-fold excesses of amino acids, equivalent activator reagents, 2-(1H-Benzotriazole-1-yl)-1,1,3,3-tetramethyluronium hexafluorophosphate (HBTU) and N-Hydroxybenzotriazole (HOBt), and two equivalents of base, N-methylmorpholine (NMM). Each coupling reaction was allowed to proceed for 0.5 h at room temperature. All Fmoc-protected amino acids and

activators were dissolved in dimethylformamide (DMF), except where noted, to saturation. Fmoc-Phe and Fmoc-Pro were dissolved in 1-methyl-2-pyrrolidone (NMP). The saturation concentration of Fmoc-amino acids in DMF or NMP is 0.6 M while the saturation concentrations of HBTU and HOBt in DMF are 0.6 M and 2.2 M respectively. NMM was prepared in DMF at 45 %(v/v) concentration. The removal of Fmoc was accomplished by using 20 %(v/v) piperidine in DMF for 15 min twice. The resin was washed 4 times with DMF. Cycles of deprotection, washing, double couplings, and washing were repeated until the desired sequence achieved. The product was washed with dichloromethane twice and vacuum dried prior to cleavage from resin using a cocktail solution composed of 95 % trifluoroacetic acid (TFA), 2.5 % deionized water, and 2.5 % triisopropylsilane (v/v). The reaction was allowed to proceed for 3 h with occasional shaking. The cleavage solution was added to cold methyl tert-butyl ether dropwise to induce precipitation of the peptide. The precipitate was collected by centrifugation and was washed three times with excess of cold ether to remove any residual scavengers. The final precipitate was re-dissolved and lyophilized. The crude peptide was purified using Agilent 1100 semi-preparative HPLC (Santa Clara, CA). The purification was performed on an Agilent Zorbax 300SB-C18 reverse phase column (5 μm particle size, 300Å pore size, 25 x 1.0 cm) with a linear gradient of buffer A (0.1% TFA in water) and buffer B (0.1% TFA in acetonitrile) from 10% B to 45% B in 30 min at a flow rate of 4 ml/min. The purity of all peptides was greater than 95% according to analytical reverse phase HPLC and matrix-assisted laser

desorption/ionization time of flight (MALDI-TOF) mass spectroscopy on a Bruker AutoFlex II MALDI-TOF mass spectroscopy (Bruker, Bremen, Germany).

Biophysical studies

Circular Dichroism (CD) measurements were performed on a J-810 spectropolarimeter (Jasco, Great Dunmow, Essex, UK) using a 0.1mm quartz cylindrical cuvette (Hellma, Müllheim, Germany). All samples were dissolved in water and stored at 4 ^{o}C for at least 3 days before the test to allow for proper equilibration of triple-helical conformation. The cuvette was filled with 150 μL of samples for each measurement. The CD spectra were obtained by continuous wavelength scans (average of three scans) from 260 to 180 nm at a scan speed of 50 nm/min. Melting point temperature measurements were performed on a Cary 50Bio ultraviolet (UV) spectrophotometer (Varian, Palo Alto, CA) equipped with a Peltier temperature controller (Quantum Northwest, Spokane, WA). Before any measurement, all samples were equilibrated at the initial temperature for at least 24 h. The samples were allowed to equilibrate at least 15 min until the UV absorbance was time-independent at each subsequent temperature point. Data were collected at 225nm.

PHBV microsphere preparation

A solvent evaporation technique was used to fabricate PHBV microspheres (Yang et al., 2000). Briefly, 1 ml of 0.05 %(w/v) PVA in phosphate buffered saline (PBS,

pH=7.4) was added to 12 ml of 50 mg/ml of PHBV solution prepared in chloroform, and the mixture was emulsified using a T25B homogenizer (Ika Labortechnik, Staufen, Germany) for 15s. The homogenized mixture was immediately transferred dropwise into 300 mL of 0.05 %(w/v) PVA solution and mechanically stirred at 300 rpm for 3 h. The product was freeze-dried until a constant weight was obtained. The PHBV microspheres were sieved to obtain a size distribution of 100-300 μm as determined using an LS230 particle size analyzer (Coulter, Miami, FL) and the surface morphology was examined using a JSM-5600VL scanning electron microscope (SEM) (JEOL, Tokyo, Japan). PHBV microspheres were used in all the following experiments and assays, except the cytotoxicity assay, cell adhesion, and competition assays.

Surface modifications

PHBV microspheres were hydrolyzed in 6 M sodium hydroxide (NaOH) solution for 10 min at room temperature with constant shaking on an orbital shaker at 130 rpm to introduce carboxylic acid (COOH) groups. The hydrolyzed microspheres were washed thoroughly with excess of deionized water 5 times. The introduction of COOH was confirmed by toluidine blue O (TBO) assay (Yin et al., 2002). Briefly, 0.2 mg of hydrolyzed microspheres were incubated in 1 mL of TBO solution (0.5 m*M* in 0.1 mM NaOH, pH10) for 5 h at room temperature under constant shaking and then washed with excess amount of NaOH solution (pH 10) twice. The complexed TBO was desorbed from the surface by adding 1 mL of 50% acetic acid solution for 10 min

under vortexing. TBO concentration in the acetic acid solution was determined according to its optical density measured at 620 nm with a GENious microplate reader (Tecan, männedorf, Switzerland).

Microspheres were sterilized with 70% ethanol and washed 3 times with excess sterilized water. Carboxyl groups of the microspheres were activated using 10mM of *N*-ethyl-*N*'-(3-dimethylaminopropyl)carbodiimide (EDC)/ *N*-Hydroxysulfosuccinimide (NHS) (Sigma-Fluka, St. Louis, MO) solution sterilized by filtering through a 0.22 μm filter for 5 h with occasional shaking at room temperature. Microspheres were washed 3 times with PBS to wash away excess EDC/NHS. The CMP1 (25μg/ml or 7.7 nmol/ml) and RGD (25μg/ml or 72 nmol/ml) were covalently immobilized onto the activated microspheres by immersing the microspheres in the peptide solution at a density of 15mg microspheres /ml peptide solution at room temperature overnight.

Surface density measurement

The surface density of the immobilized peptides was determined using an amino acid analysis. The analysis was performed using AccQTag Ultra amino acid analysis kit (Waters, Milford, MA) following the manufacturer's protocol. Briefly, the peptides-functionalized microspheres were washed at least 3 times with the ultrapure water to remove the physically adsorbed and unattached peptides, and the grafted peptides were hydrolyzed in 200 μl of 6 M hydrochloric acid for 24 h. The hydrolysis

solution was then neutralized with an equal volume of 6 M NaOH. The hydrolysates (10 μl) or standard amino acid solution (10 μl) was then derivatized with 70 μl of AccQ-Fluor Borate buffer and 20 μl of AccQ-Fluor reagent for 10 min at 55 ^{o}C. The analysis was performed on Waters ACQUITY ultra performance liquid chromatography (UPLC) using an AccQ-Tag Ultra column (1.7 μm particle size, 2.1 x 100 mm) at 55 ^{o}C with a linear gradient of buffer A (AccQ-Tag Ultra eluent A1) and buffer B (AccQ-Tag Ultra eluent B) from 0% B to 60% B in 10 mins at 0.70 ml/min. The injection volume was 1.0 μl and the detection UV wavelength was set at 260 nm.

To qualitatively observe the presence of the immobilized peptides on the microspheres, fluorescein isothiocyanate (FITC) was covalently grafted to the immobilized peptides and the excess of FITC was washed away before imaging on a confocal laser scanning microscope (CLSM) (DM-IRE 2, Leica, Heidelberg, Germany). The presence of the immobilized peptides on the microspheres was also qualitatively confirmed by SEM imaging after freeze-drying.

Cell culture

L929 fibroblast cells and Hep3B liver cells (ATCC, Manassas, VA) were cultured separately in Dulbecco's modified Eagle's medium (Gibco, Grand Island, NY) supplemented with 10% fetal bovine serum (FBS) (Hyclon, Logan, UT), 110 mg/L sodium pyruvate (Sigma-Aldrich), 1% antimycotic solution (Sigma-Aldrich) and 1% non-essential amino acids (Sigma) (hereinafter called DMEM). The cells were

maintained in 2 different 75 cm^2 T-flasks and incubated at 37 ^oC in the presence of 5% carbon dioxide (CO_2) and 95% relative humidity in an Autoflow NU-4850 CO_2 water-jacketed incubator (NuAire Inc., Plymouth, MN).

Cytotoxicity assay

Samples were prepared using serum-free DMEM containing 25 μg/ml peptides. All the samples were sterilized through 0.22 μm filter and kept at 4 ^oC for at least 1 day before use to allow proper equilibration of triple-helical conformation. Serum-free DMEM was used as a reference.

L929 fibroblast cells were seeded onto a Nunclon Delta TC 96-well plate (Nunc, Roskilde, Denmark) at 2.0 x 10^4 cells/well in DMEM and incubated for 48 h. The medium was then replaced with 200 μL of the samples and each was assayed in triplicate. The cells were incubated for a further 24 and 72 h, and the viability of the cells were determined using 3-(4,5-dimethylthiazol-2-yl)-2,5-diphenyltetrazolium bromide (MTT) colorimetric assay. Briefly, the culture medium was replaced with serum-free medium/MTT solution (v/v 9:1), and incubated for 3 h. The purple formazan crystals were dissolved in dimethylsulfoxide. The absorbance was measured at 560 nm wavelength with a reference at 620 nm using a microplate reader.

Cell adhesion assay

Nunclon Delta TC Microwell plates were coated with 100 µl of 50 µg/ml solution of CMP1 (1.5 nmol), CMP2 (2.1 nmol), CMP1' (2.0 nmol), CMP2' (3.7 nmol), CMP3 (5.9 nmol) and collagen (< 0.5 nmol) at 4 ^{o}C overnight, blocked with 100 µl of 1% heat-denatured bovine serum albumin (BSA) (Sigma-Aldrich), and then washed with PBS. One hundred µl of Hep3B cell suspension in serum-free DMEM ($10x10^5$ cells/ml) was then added and incubated for 1 h at 37 ^{o}C. Unattached cells were washed away with PBS twice. Adhered cells were measured using a total deoxyribonucleic acid (DNA) quantification assay (Hoechst 33258, Sigma-Aldrich). Briefly, the cells were lysed by 3 freeze-thaw cycles in ultra-pure water and the cell lysates were mixed with 2 µg/mL bisbenzimide in 10 mM TrisHCl (pH 7.4), 1 mM EDTA and 0.2M NaCl fluorescence assay buffer and were incubated in dark for 30 min. The fluorescence was read on a microplate reader using an excitation wavelength of 360 nm and emission wavelength of 465 nm. Assays were conducted in triplicate, and the data were expressed as mean ± standard deviations (SDs). BSA-coated wells were used as a baseline reference level, and the adhesion to the collagen-coated well was used as a 100% reference level.

Competition assay

Plates were coated with 100 µl of a 50 µg/ml calf skin collagen solution as described above. Hep3B cells (10×10^5 cells/ml) were incubated with 50 µg/ml peptides in serum-free DMEM to saturate the integrin receptors on the cell surface for 30 min

before seeding. For each competition assay, 100 µl of the cell suspension was seeded to the collagen-coated well and the competitive adhesion was allowed to take place for 1 h at 37 ^{o}C. The assay was undertaken in triplicate and the data were presented as mean ± SD. The attached cells were measured by the total DNA quantification method.

Cell culture on microspheres

Hep3B cells were seeded to the microsphere at $4x10^3$ cells/ mg of microsphere, in which each well contained 1.5 mg microspheres. Cell morphology and cell-microsphere construct were observed using Leica DMIL inverted optical microscopy and SEM. Cell-microspheres constructs were washed twice with PBS and fixed with 2.5 % glutaraldehyde for 1 h. The samples were then dehydrated using ethanol gradient (50-100%) and air dried before SEM observation. At pre-determined time points (day 2, 4, 7, 10 and 14), Hep3B liver cells were checked for morphology, proliferation, viability, albumin secretion, and cytochrome P-450 activity.

Cell viability

Cell viability was assessed by a live/dead assay (Molecular Probes, Eugene, OR,) according to manufacturer's instructions. Briefly, the cells were incubated in 200 µl of live/dead Hank's balanced salt (HBSS) solution for 30 min at room temperature to label the viable and necrotic cells. The labeled cells were fixed with 4% glutaraldehyde in HBSS and observed using a CLSM

Cell proliferation

Cell number was measured using total DNA quantification. Briefly, cell-microsphere constructs were rinsed twice with PBS solution and lyzed for 2h in 60 µl of a lysis cocktail containing 0.25v/v percentage trypsin and 2.5v/v percentage lysis buffer (Promega, San Luis Obispo, CA) in ultra-pure water followed by 2 freeze-thaw cycles. The cell lysates were mixed with 2 µg/mL bisbenzimide in 10 mM TrisHCl (pH 7.4), 1 mM EDTA and 0.2M NaCl fluorescence assay buffer and were incubated in the dark for 30 min. The fluorescence was read on a GENious microplate reader (Tecan) using an excitation wavelength of 360 nm and an emission wavelength of 465 nm. Serial lysates of known cell numbers were used to calibrate the fluorescent intensity to cell number.

Albumin secretion and cytochrome P-450 activity

Albumin secretion by liver cells was measured using a human albumin enzyme-linked immunosorbent assay (ELISA) quantification kit (Bethyl, Montgomery, TX), which is based on the antibody-sandwich mechanism (Glicklis et al., 2000). At pre-determined time points (day 2, 4, 7, 10 and 14), the supernatant was aspirated from the wells and centrifuged at 13000 rpm for 5 m, filtered through a 0.45 µm Millipore filter (Milipore, Billerica, MA) and stored at –20ºC until then required for analysis.

The P-450 activity or the detoxification ability of liver cells was measured using ethoxyresorufin-O-deethylase (EROD) assay (Bhandari et al., 2001). After the

culture medium was aspirated and stored for ELISA test, the cell-microspheres construct were rinsed twice with sterilized PBS solution. Three hundred μL of medium containing 5 μM of 7-ethoxyresorufin and 20 μM of dicumarol (Sigma-Aldrich) was then added into each well and incubated for 4 h at 37ºC. The fluorescence was read at an excitation wavelength of 535 nm and an emission wavelength of 595 nm on a GENious microplate reader.

Statistical analysis

The data are presented as mean ± SDs The statistical analysis of the data was done using student's *t* test. A 95% confidence level was considered significant.

3.3 Results and discussion

Biophysical studies

The collagen-like triple-helical conformation of the CMPs was verified using CD spectroscopy. A collagen triple-helical structure exhibits a unique CD spectrum characterized by a positive peak at approximately 220nm, a crossover of approximately 213nm and a large negative peak at approximately 197nm (Brown et al., 1972; Sakakibara et al., 1972). The CD spectra of the CMPs were compared with that of the calfskin collagen to determine the presence of the collagen triple helix (Goodman et al., 2003). The CMPs, except CMP2' and CMP3, exhibited CD spectra

features characteristic of a collagen-like triple helix, including a positive peak at approximately 225 nm and a large negative trough at approximately 200 nm (Figure 3.2). These CD spectra displayed a red shift in their band positions in reference to the CD spectral band positions of collagen because of the higher percentage of imino acid contents (Rippon and Walton, 1971).

The melting curve analysis also supported the establishment of triple-helical conformations according to the CD spectra, provided additional evidence of the presence of the triple-helical conformations, and was used to determine the melting point temperatures (T_m) of the CMPs. UV absorbance of the CMPs was monitored at 225 nm as a function of temperature to obtain the melting curves as given in Figure 3.3. All CMPs, except CMP2' and CMP3, exhibited cooperative transition curves with a large transition magnitude similar to that observed for collagen, denoting the presence of some triple-helical conformations and a triple helix–to–random coil transition. The midpoint of the transition was taken as the T_m; the results are presented in Table 3.1.

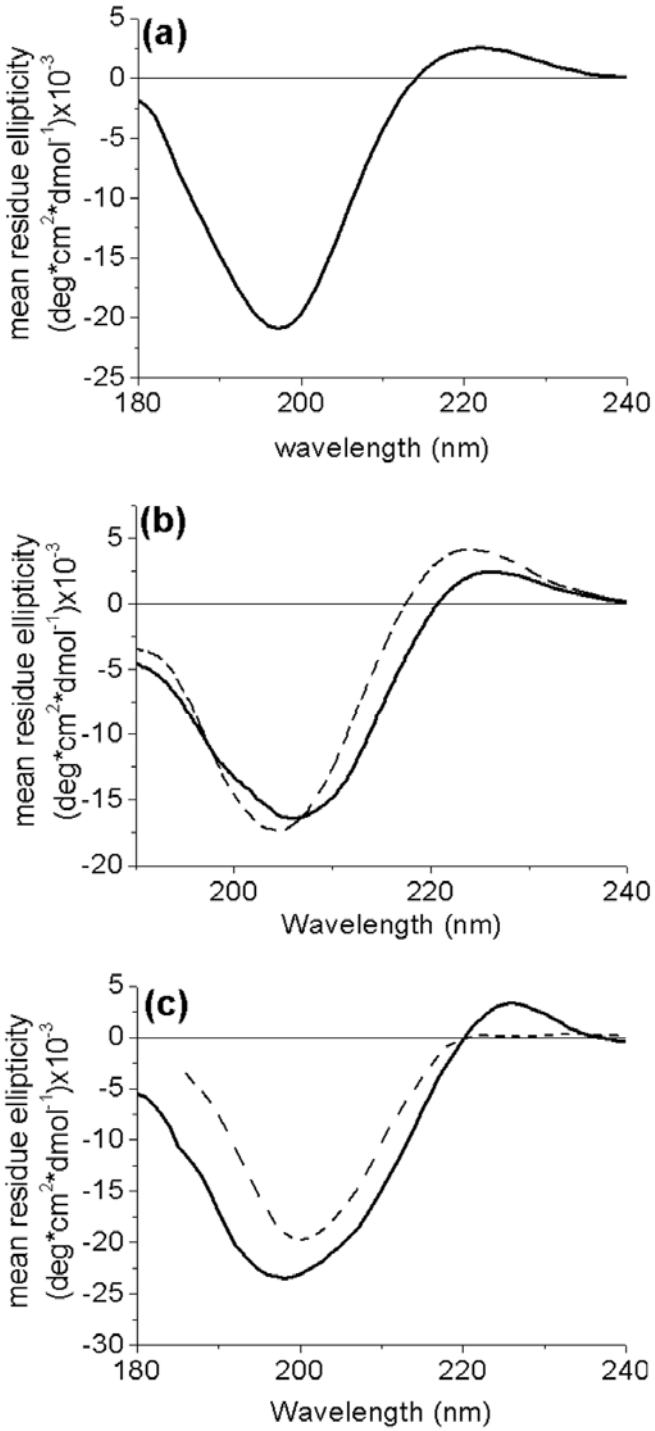

Figure 3.2. Circular dichroism spectra of (a) collagen (0.5 mg/ml), (b) collagen-mimetic peptide (CMP) 1 (0.4 mg/ml) (solid line) and CMP2 (0.4 mg/ml) (dashed line), and (c) CMP1' (0.6mg/ml) (solid line) and CMP2' (0.45mg/ml) (dashed line) in water.

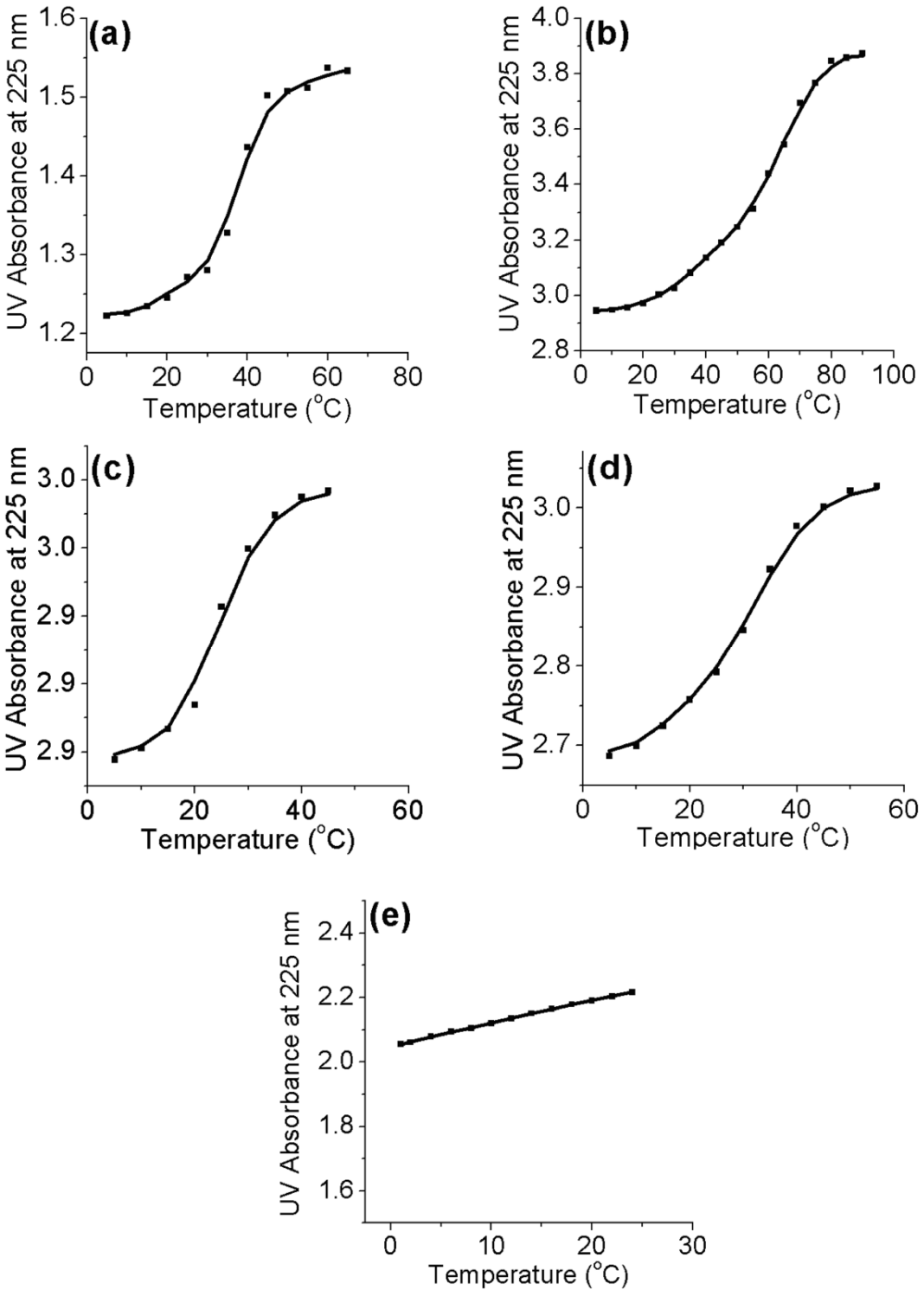

Figure 3.3. Thermal melting curves of (a) collagen (0.5mg/ml), (b) collagen-mimetic peptide (CMP) 1 (0.4mg/ml), (c) CMP2 (0.4mg/ml), (d) CMP1' (0.6mg/ml), and (e) CMP2' (0.45mg/ml), were obtained using ultraviolet (UV) absorbance measurement at 225 nm at different temperatures.

Table 3.1. Cell recognition site (GFOGER) corresponding to residues 502-507 of the collagen α_1 (I), shown in bold, was incorporated within repeat GPP or GPO triplets of the collagen-mimetic peptide (CMP).

Protein/Peptides	Sequence*	Melting point temperature (^oC)
Collagen	Calf skin collagen	37
CMP1	$(GPP)_5$**GFOGER**$(GPP)_5G$	55
CMP1'	$(PPG)_{10}$	30
CMP2	$(GPO)_3$**GFOGER**$(GPO)_3G$	25
CMP2'	$(POG)_5$	No transistion
CMP3	**GFOGER**GGG	No transistion

* Standard one letter code is used to express amino acid sequences, except for O, which is used to represent hydroxyproline residue. A single stranded GFOGER peptide was used as a reference.

Cytotoxicity

Prior to any other assay, all the peptides and collagen were assessed for their cytotoxicity. No significant changes were observed in either the cell viability (as determined by MTT) or cell morphology and appearance (result not shown) after 24-h and 72-h culture in the presence of the samples tested. The result was indicative of non-cytotoxic responses.

Recognition of the CMPs by Hep3B liver cells

To study the cellular recognition of the CMPs, we compared the promotion of cell adhesion with that of the negative (blank) and positive (collagen) controls. It can be

seen from Figure 3.4 that CMP1, CMP2, and collagen were well recognized by the Hep3B liver cells and could support the cell adhesion in a conformation-dependent manner. Biophysical studies demonstrated that the CMP1 adopts a stable triple-helical conformation, whereas CMP2 has a lower T_m value (25 ^{o}C) and thus may undergo some degree of dissociation at the cellular incubation temperature (37 ^{o}C). The difference in the stability of the triple-helical conformation resulted in a considerable loss of recognition. The percentages of the cell adhesion to CMP1, CMP2, and CMP3 were approximately 50±8%, 34±6% and 9±2% (Figure 3.4a) respectively. The triple-helical conformation appeared essential for the recognition of the CMPs by the hepatoma cells. The result is in concordance with the fact that the native collagen has noticeably higher affinity for collagen-specific receptors than the denatured collagen (Rubin et al., 1981). The denatured collagen resulted in little or no integrin-mediated adhesion (Santoro, 1986; Gullberg et al., 1992). Furthermore, it has been shown that the triple-helical conformation of collagen is essential, if not crucial, for influencing cell adhesion, spreading, migration and matrix metalloproteinase binding and human platelet adhesion and aggregation (Miles et al., 1994; Grab et al., 1996; Knight et al., 2000). Similarly, absence of the GFOGER hexapeptide in CMP1' and CMP2' caused a marked loss of activity and adverse effect on the level of Hep3B cell adhesion (< 10%). The result verified that GFOGER is one of the major binding sites within the type I collagen.

In this study, we have found that the cell binding activity of CMP1 is approximately 50% of that of collagen. The results suggested that the Hep3B liver cells recognize not only the GFOGER binding motif in the collagen, but also many other distinct adhesion domains, which are still unknown. Additionally, we have found that the presence of the integrin-specific GFOGER sequence is crucial for Hep3B cell recognition and that the 3-dimensional arrangement of the GFOGER is critical for ligand-receptor interaction.

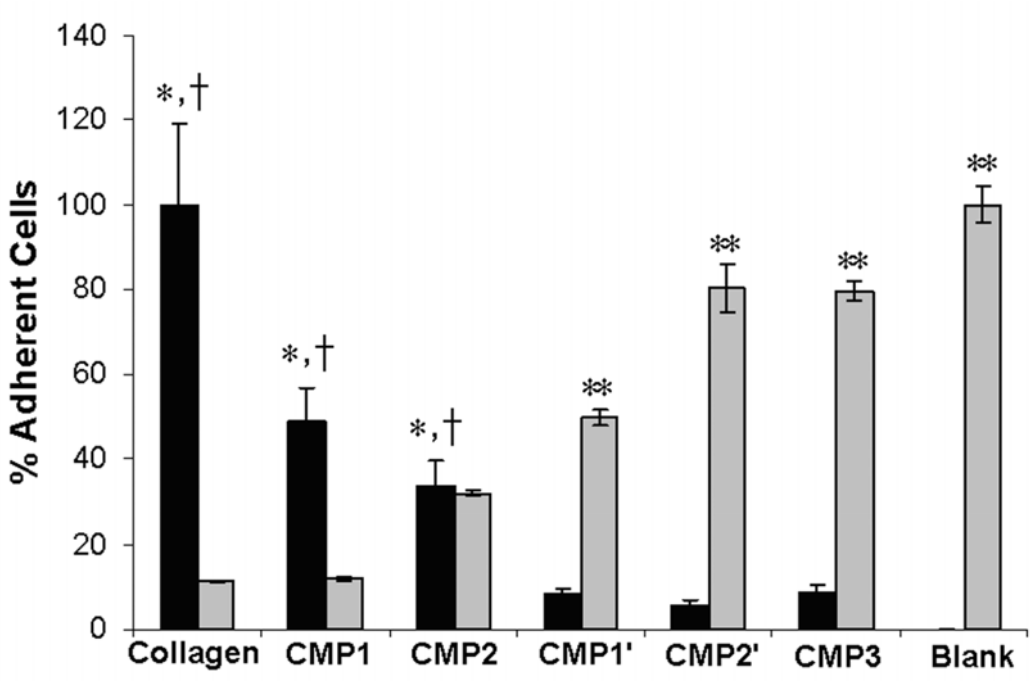

Figure 3.4. Adhesion of Hep3B liver cells (dark bars) to the collagen-mimetic peptides (CMPs) or collagen-coated surface was determined at 60 min. Cell adhesion to collagen was used as a 100% reference level, whereas adhesion to bovine serum albumin (called blank) was set as a 0% baseline. Student's *t* test with $p < 0.05$ for *significantly different from blank and †significantly different from CMP1', CMP2' and CMP3. Inhibition of the Hep3B liver cells incubated in CMP- or collagen-containing serum-free medium to the collagen-coated surface (grey bars) was assessed at 60 min. Adhesion of cells incubated in blank serum free medium was used as the 100% reference level. Student's *t* test with $p < 0.05$ for **significantly different from collagen, CMP1, and CMP2.

Hep3B cell spreading

As observed in Figure 3.5, cell spreading on CMP1 is similar to that on collagen-modified polystyrene surfaces. Cell adhesion and spreading were most extensive on collagen surfaces, followed by CMP1 and CMP2 (result not shown) surfaces. Hep3B cell spreading was most efficient when the triple helices were combined with collagen α_1(I) 502-507 sequence. This result suggested that cell migration or motility on collagen can be conformationally-dependent. Deletion of GFOGER hexapeptides or removal of the repeating Gly-Pro-Pro/ Gly-Pro-Hyp triplets caused substantially decreased Hep3B cell spreading activities. Most cells remained spherical after 60min adhesion on CMP1', CMP2', and CMP3. Cell spreading on collagen- or CMP1-modified surfaces is distinctly different from the interaction between the cells and other synthetic polymers, which merely depends on the non-specific contact between the cell membrane proteins and the functional groups of polymers (Bačáková et al., 2000a and 2000b). In fact, the extensive cell spreading was the result of the integrin-mediated extracellular-signal-transmitting cell adhesion process. As has been shown in other studies, cell motility and migration is dependent on the presence of the ECM proteins and ligands (Hynes, 1992; Fields et al., 1993b). Therefore, the results have demonstrated the potential use of the CMP to mimic a collagen-like environment for cell adhesion and development.

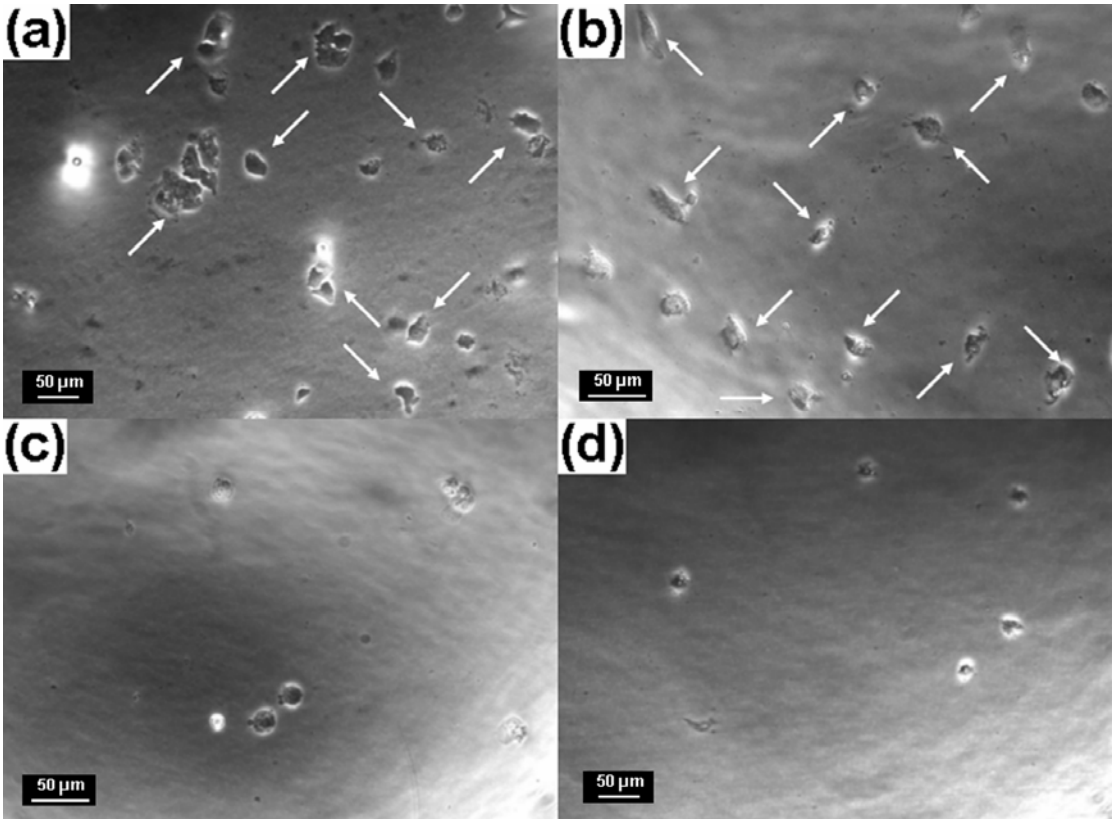

Figure 3.5. Hep3B cells were allowed to adhere and spread for 60 min on (a) collagen, (b) collagen-mimetic peptide (CMP)1, (c) CMP1', and (d) CMP3. The cells spread well (as indicated by the arrows) on collagen and CMP1. Magnification is 200x.

Inhibition of Hep3B liver cell adhesion by the CMPs

This is an indirect screening process for the cell binding activity displayed by the peptides. The cells were incubated and seeded onto collagen-coated plates in the presence of the CMP molecules. Any inhibition of cell attachment is most probably due to the specific integrin-receptor interactions between the peptides and the cells. Cell adhesion to the collagen surface is inhibited when the cell surface receptors, especially specific collagen receptors, are pre-saturated with the adhesive molecules in solution before cell seeding. The inhibitory effect of the CMP is shown in Figure

3.4. It can be seen that the GFOGER-containing triple-helical CMPs (CMP1 and CMP2) effectively inhibited Hep3B cell binding to collagen, suggesting the participation of specific collagen receptors in the cell attachment process. The inhibitory activity of CMP1 was similar to that of collagen. Removal of the Gly-Pro-Pro/ Gly-Pro-Hyp triplets or GFOGER sequence resulted in CMPs (CMP1', CMP2' and CMP3) lacking the ability to inhibit the integrin-mediated cell adhesion.

Surface modifications of PHBV microspheres

The above results indicate the cell recognition property of the CMPs used. It is well known that the integrin-mediated cell adhesion is essential for the maintenance of the viability and differentiated functions of cells (LeCluyse et al., 1996; Ben-Ze'ev et al., 2000). We have previously reported the advantage of using PHBV microspheres as a scaffold to engineer tissue-like construct (Zhu et al., 2006). In this study, CMP1 was covalently immobilized onto PHBV microspheres in order to study the effects of the CMP on regulating and promoting Hep3B liver cell growth and functions. As a control, RGD was also used to modify the PHBV microsphere surfaces as the tripeptide is an important cell binding sequence found within the fibronectin and has been reported to have high affinity for primary rat hepatocytes (Forsberg et al., 1990).

First, TBO was used to quantify the surface density of COOH groups on the modified PHBV microspheres for further peptide coupling. The number of COOH groups was found to increase 61.7% after 10 min of treatment of PHBV microspheres

with 6M NaOH. The carboxyl group density was calculated to be 97.5±7 nmol/mg of microspheres, assuming that the TBO reacted with the carboxyl groups at a 1:1 ratio (Yin et al., 2002). The surface density of the grafted peptides was determined by an amino acid analysis. The density of the grafted RGD and CMP1 on the microspheres was found to be 1.60 nmol and 0.043 nmol/mg of microspheres, respectively.

The grafted FITC-RGD was used to qualitatively observe the distribution of the immobilized peptides on the microspheres. It can readily be seen from Figure 3.6b that the grafted FITC-RGD tripeptide was homogeneously distributed on the microspheres of sizes ranged from 100-300 μm (Figure 3.6a) and thus created a surface with a 3-dimensional distribution of ligands for cell surface-integrin receptor interaction. SEM images shown in Figure 3.6c and 3.6d demonstrated that CMP1 can form into a 3-dimensional collagen-like nanofibril three-dimensional network upon being grafted onto the microspheres and freeze-dried. From the SEM images, we can clearly see that the nanofibrils were extended from the surface of the microspheres and distributed in a three-dimensional way on the microspheres. This network is physiologically similar to previously observed freeze-dried collagen networks and can serve as a bioadhesive matrix to promote cell adhesion onto the microspheres and, subsequently, cell proliferation. Integrin-mediated cell adhesion is also important for maintaining cell function and differentiation.

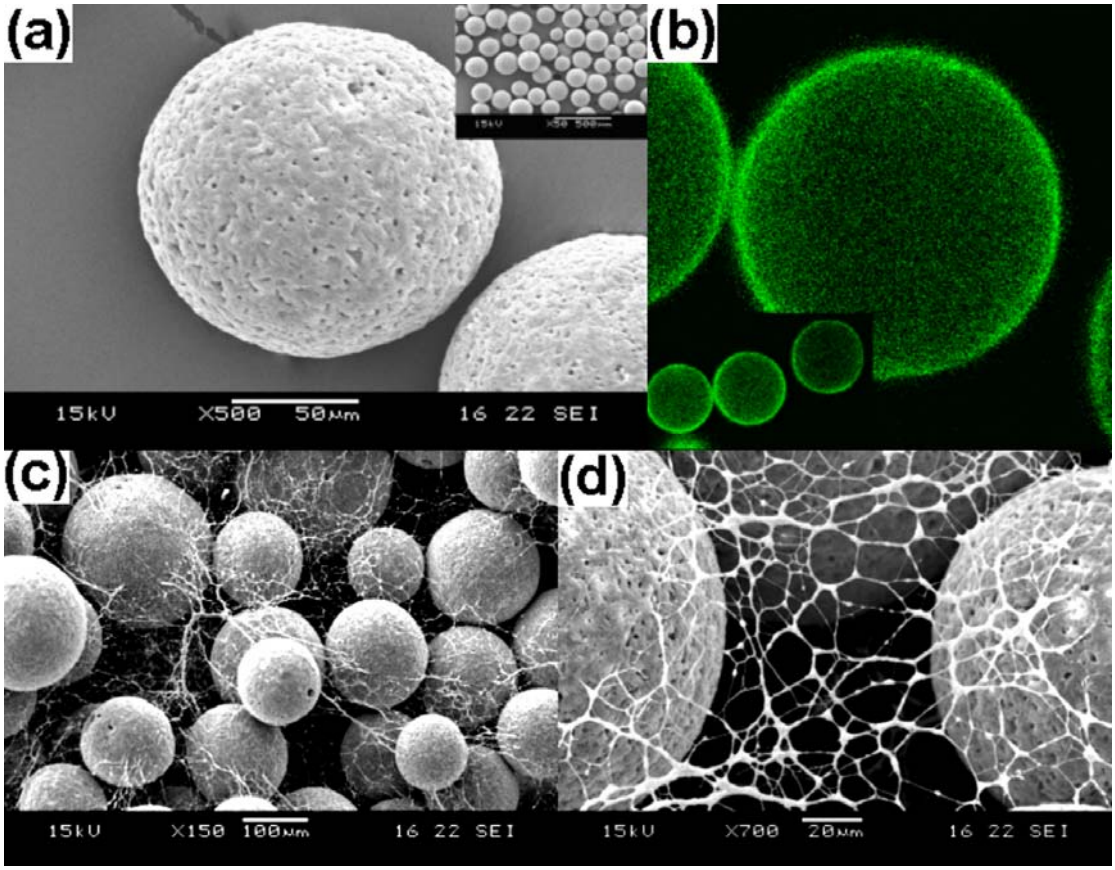

Figure 3.6. (a) Scanning electron microscope (SEM) image of the poly(3-hydroxybutyrate-*co*-3-hydroxyvalerate) (PHBV) microspheres; (b) confocal laser scanning microscope image of FITC-RGD-functionalized PHBV microspheres revealed the homogeneous immobilization of the peptides; (c) SEM image of PHBV microspheres grafted with the collagen-mimetic peptide (CMP)1. The CMP1 formed into a nanofibril collagen-like network interconnecting the microspheres; (d) an enlarged image of the CMP1 network.

Hep3B cell growth on PHBV microspheres

Hep3B liver cells were cultured on the microspheres for 14 days to study the effects of the presence of CMP1 on regulating liver cell morphology, proliferation and function. Light microscopy images of the samples were taken at day 3 to study the cell growth on different samples. It can be seen from Figure 3.7 that the cells adhered and spread on the RGD- and CMP1-grafted microspheres extensively to bridge the adjacent spheres to form 3-dimensional cell-microsphere constructs. Significantly more cells were found to attach on these microspherical scaffolds as compared to the blank microspheres. Cells had grown into multiple layers on the microspheres after 3 days of culture and were formed into a thick tissue-like structure more than 100 μm thick (Figure 3.7d). However, no significant improvement of cell attachment was observed on the blank microspheres. The observation indicated that the presence of CMP1 is capable to improve Hep3B cell growth in 3-dimensional geometry.

Confocal micrographs of Hep3B cells after 10 days of culture on CMP1-functionalized microspheres were shown in Figure 3.8. The intensive green fluorescence indicated that most of the cells were viable and the cells were well distributed within the self-assembled microspherical scaffold. An enlarged image (Figure 3.8b) showed that the cells spread expansively on the microsphere and there were strong cell-cell interactions. The CLSM images demonstrated the dense cell layer encapsulating the microspheres.

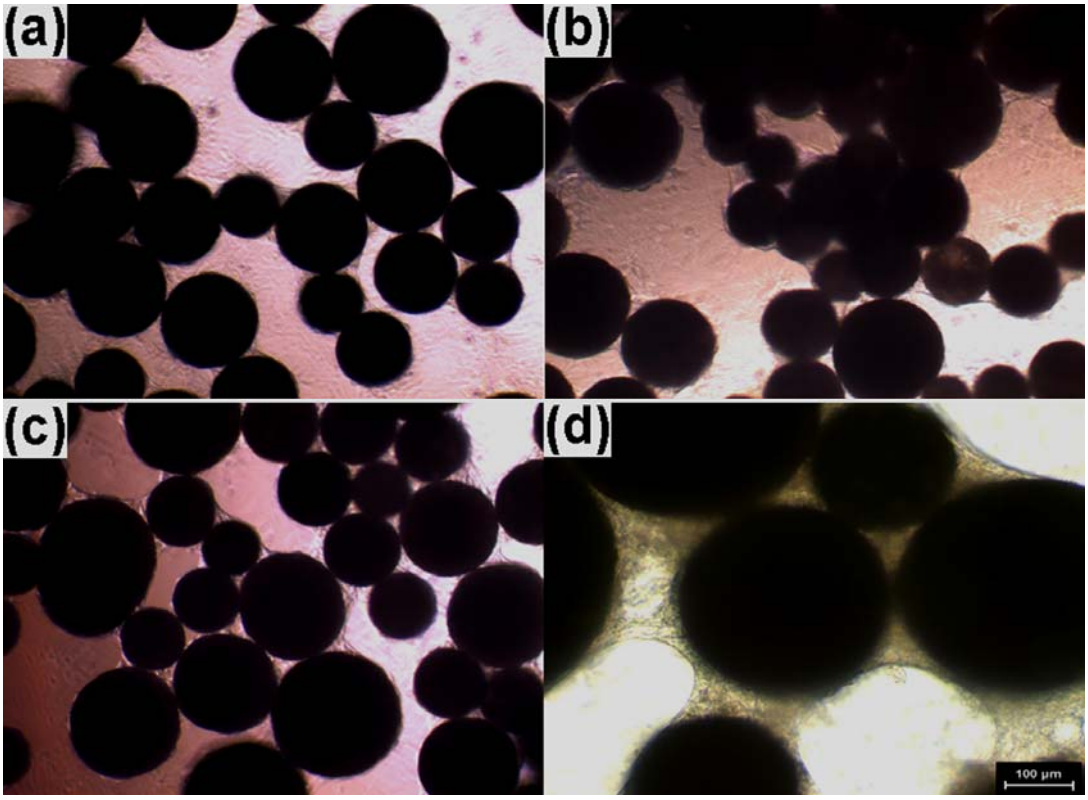

Figure 3.7. Light micrographs of Hep3B cells after 3-day culture on (a) blank microspheres, (b) RGD-functionalized microspheres, (c) CMP1-functionalized microspheres and (d) enlarged image of (c).

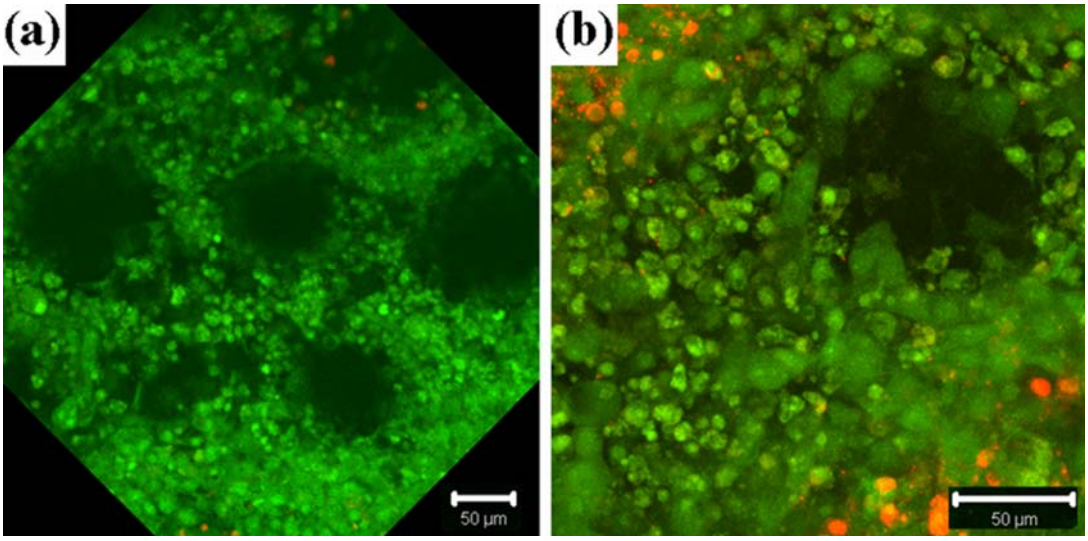

Figure 3.8. Confocal laser scanning microscope images of Hep3B cells after 10-day culture on CMP1-functionalized PHBV microspheres: (a) 200x magnification; (b) 400 x magnification. Viable cells were labeled with SYTO 10 green fluorescent nucleic acid stain, whereas the dead cells were marked with DEAD Red (ethidium homodimer-2) nucleic acid stain.

SEM images of the 10-day Hep3B cells cultured on the microspheres are shown in Figure 3.9. RGD- and CMP1-functionalized microspheres were found to be more conductive to hepatic cell growth than the blank microsphere. The cells not only covered the surfaces of the substrates but also formed a layer among the gaps and deposited an abundant of ECM materials, indicating strong cell-substrate interactions. The presence of the CMP1 matrix, although at much lower densities than the RGD tripeptide, promoted cell attachment and spreading on the microspheres, as well as extensive cell growth and cellular bridging, suggesting the potential of the CMP1 for specific integrin targeting and thus control over the growth of certain cell types.

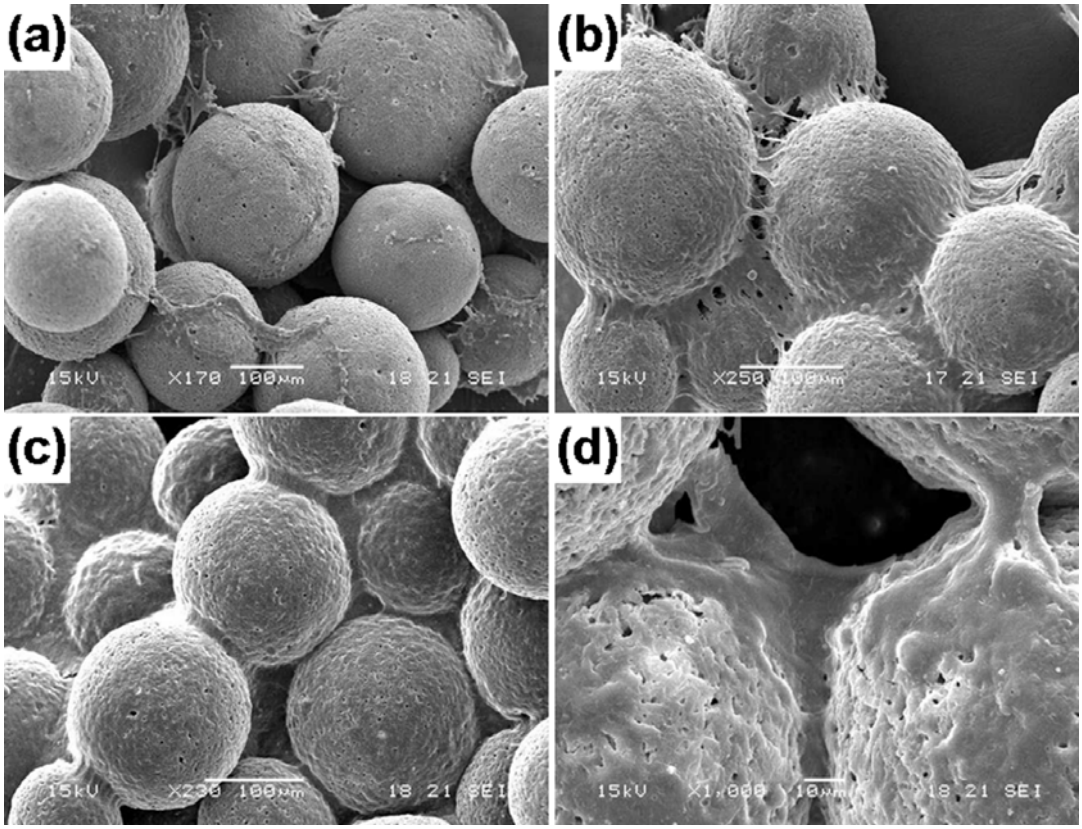

Figure 3.9. Scanning electron microscope images of Hep3B cells after 10-days culture on (a) blank microspheres, (b) RGD-functionalized microspheres, (c) CMP1-functionalized scaffold and (d) enlarged image of (c).

Cell proliferation

The cell number at pre-determined time points was quantitatively evaluated by using total DNA assay. The fluorescence of bisbenzimide correlated to the amount of DNA was normalized to cell number, as shown in Figure 3.10. Generally, it can be seen that there was a trend of increasing of cell numbers for all samples over the 2 weeks of culture. The number of Hep3B cells was significantly greater when cultured on RGD- and CMP1-functionalized microspheres than on the blank microspheres, indicating that the ligand conjugation was successful and potent for making microspheres more suitable as a scaffold. The activity of CMP1 in promoting Hep3B liver cell growth is identical to that of RGD, a well-known integrin-specific peptide for hepatocytes (Forsberg et al., 1990), although it had a much lower surface concentration.

It can be seen that the initial cell growth (day 2) on all samples was similar. The cells seeded onto blank microspheres preferred to attach to the polystyrene dish surface for survival because of the absence of cellular recognition motifs on the microspheres. This surface provided a much smaller surface area for these cells and thus promoted extensive cell-cell interactions, which resulted in more rapid cell proliferation. Alternatively, cells preferred to attach to the RGD- and CMP1-functionalized microspheres as observed under microscope (not shown). The cell number was low initially because of the lack of cell-cell interactions on the larger surface. Therefore, the initial cell number on all samples was not significantly different. There were significantly more cells after day 4 when cultured on RGD- and

CMP1-functionalized microspheres. The larger microsphere surface area and increasing cell-cell interactions helped the cells to proliferate rapidly thereafter and form into thick multiple layers as shown in Figures 3.7, 3.8, and 3.9.

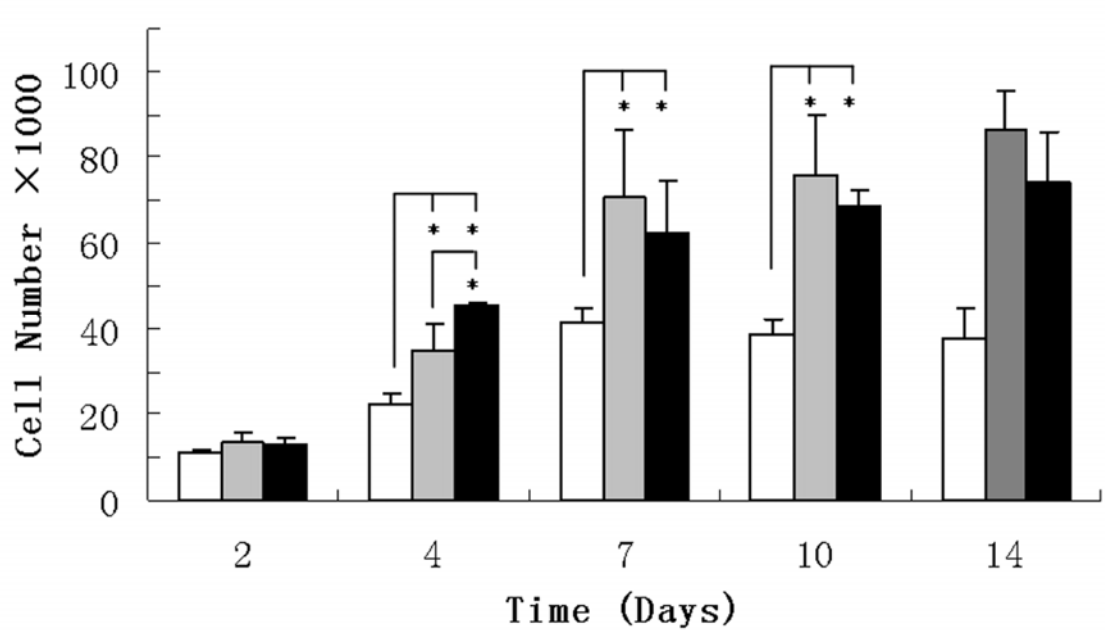

Figure 3.10. Proliferation of Hep3B cells cultured on blank (blank bar), RGD-functionalized (grey bar) (1.60 nmol RGD/mg of microspheres) and collagen-mimetic peptide (CMP)1-functionalized (black bar) (0.043 nmol CMP1/mg of microspheres) microspheres as assessed using total deoxyribonucleic acid quantification. Values represent means ± standard deviations, n=3. Statistical analysis was done using student's *t* test with *p<0.05.

Albumin secretion

Albumin secretion is an important function displayed by liver cells. The result presented in Figure 3.11 is albumin secretion on the basis of cell number at different sampling periods. Cell-ECM interactions are crucial for the maintenance of the cells' phenotypes, viability and differentiated functions (LeCluyse et al., 1996; Ben-Ze'ev et al., 2000). The cells cultured on RGD- and CMP1-functionalized samples showed significantly better albumin secretion functions, suggesting that integrin-mediated cell adhesion and signal transmission is essential for regulating cell proliferation and functions.

Albumin secretion was high initially (day 2) because of the slower initial proliferation on a lag growth phase. Subsequently, albumin secretion was observed to slow down because of rapid cell proliferation. Albumin secretion was significantly improved on days 10 and 14 than on previous days. The result is in good agreement with the cell proliferation because there is often a tradeoff between the cell proliferation and differentiation (Brieva and Moghe, 2004). The cells have grown to near confluence on the microspheres after 10 days of culture, and the proliferation rate slowed down and triggered an active differentiated function. This also explains the high levels of albumin secretion displayed by the cells grown on the blank microspheres on day 14. Cell proliferation on blank microspheres decreased after day 10, resulting in the increase in albumin secretion after day 10.

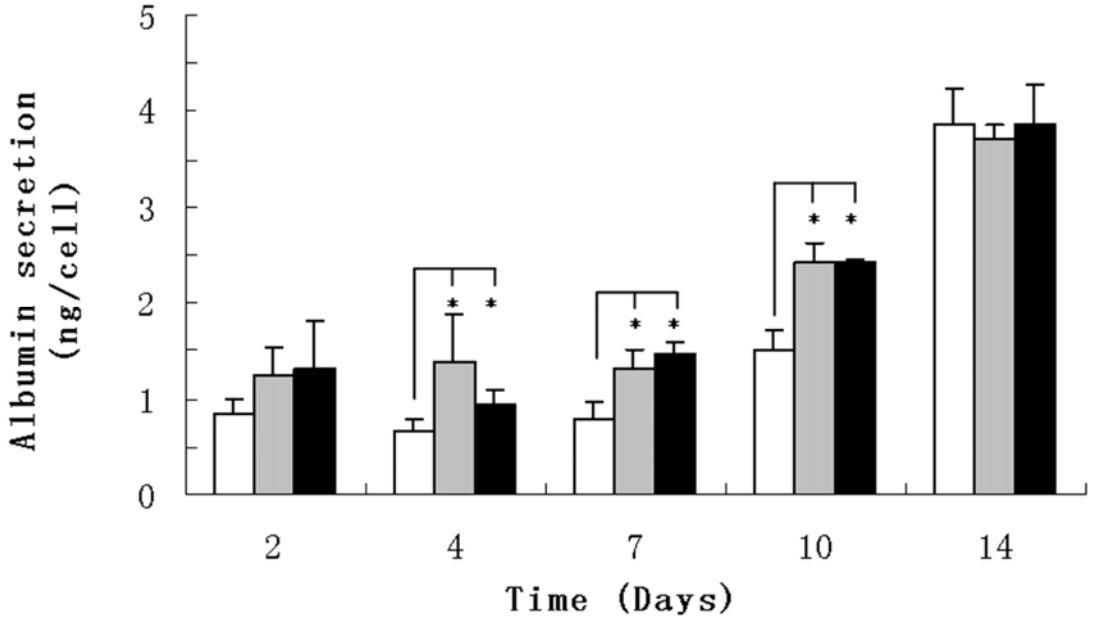

Figure 3.11. Accumulated albumin secretion by Hep3B cells cultured on blank (blank bar), RGD-functionalized (grey bar) and CMP1-functionalized (black bar) microspheres as assessed using enzyme-linked immunosorbent assay. Values represent means ± SD, n=3. Statistical analysis was done using student's *t* test with *p<0.05.

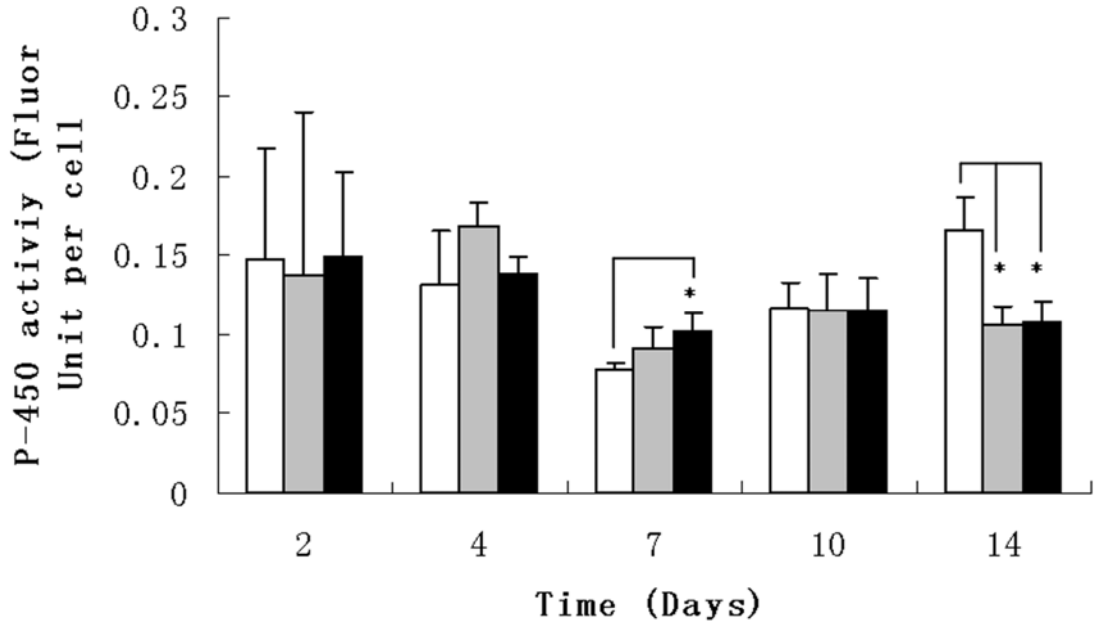

Figure 3.12. Cytochrome P-450 activity of Hep3B cells cultured on blank (blank bar), RGD-functionalized (grey bar) and CMP1-functionalized (black bar) microspheres as assessed using ethoxyresorufin-O-deethylase assay. Values represent means ± SD, n=3. Statistical analysis was done using student's *t* test with *p<0.05.

Cytochrome P-450 activity

The P-450 activities of the Hep3B cells are shown in Figure 3.12, which indicates the detoxification ability of the cells over a 4-h sampling period on the test day. Generally, the cells exhibited a similar level of P-450 activities. Slightly higher P-450 activity observed on day 2 and 4 can probably be attributed to the lower initial proliferation rates of the cells growing on a lag growth phase and thus resulted in an active differentiated function. The cells grown on RGD- and CMP1-functionalized microspheres showed much lower P-450 activities on day 14. This is possibly due to the restricted transport and diffusion of 7-ethoxyresorufin into the thick tissue-like structure formed around the microspheres that were more than 100 μm deep. The restriction reduced the concentration of the chemicals and thus resulted in a lower P-450 activity. P-450 activity on day 7 and day 14 was similar except that the P-450 activity of the cells on the blank microspheres was significantly higher on day 14. Cell proliferation on blank microspheres decreased after day 7, thus triggering an active differentiated function, as can be seen from the increase in P-450 activity on the blank microspheres from day 7 to day 14. The thickness of the cell layer on the blank microspheres was much smaller, allowing the transport of and diffusion of 7-ethoxyresorufin into the cells.

The thick multiple cell layers observed on the peptide-functionalized microspheres may limit the exchange of nutrient, oxygen and waste (Perets et al., 2003); therefore, vascularization throughout the cell-scaffold construct would be a

key step in making successful liver tissue. Vascularization could be achieved through co-culturing hepatic cells with non-parenchymal cells, such as fibroblast and endothelial cells, incorporated with a growth factor delivery strategy. The degradation of the polymeric scaffold can be controlled by using polymers with different molecular weights. The CMP-functionalized microspheres have been shown to have the potential to support cell growth for at least 14 days. Vascularization and controlled scaffold degradation would be two key factors for making long-term cell culture and tissue engineering successful.

3.4 Conclusion

In this study, we have successfully synthesized CMPs composed of mainly the repetitive GPP or GPO triplets sandwiching an integrin-specific GFOGER sequence toward realizing an artificial collagen for enhancing integrin-mediated cell adhesion, maintenance of cell phenotypes and functions, and as biomaterials to engineer well-defined bioadhesive matrix for liver tissue engineering. We have demonstrated the potential of the CMP as a cell and tissue support matrix together with the use of microspheres for enabling the *in vitro* growth of cells into large constructs of tissues. Mimicry of collagen structurally and biologically may aid in development collagen-like biomaterials and offers an alternative for animal-derived collagen.

CHAPTER 4

TEMPLATE-ASSEMBLED TRIPLE-HELICAL PEPTIDE MOLECULES: MIMICRY OF COLLAGEN BY MOLECULAR ARCHITECTURE AND INTEGRIN-SPECIFIC CELL ADHESION

Most natural proteins fold into a well-defined structure to implement their biological functions. Therefore, creation of a stable protein-like molecular architecture represents the fundamental prerequisite in realizing a novel biologically active protein-like biomaterial. Synthetic peptides consisting of Gly-Xxx-Yyy repeating sequences possess an intrinsic propensity to fold into triple-helical structures. The use of self-assembling open-chain collagen-like peptides could be the simplest way to achieve triple-helical peptides. Furthermore, the use of a template to covalently hold the collagen-mimetic peptides (CMPs) in a staggered array can reinforce and direct intramolecular folding thus stabilizing the triple-helical structures. The second part of this thesis focused on developing a template-assembly system to tether CMPs in close proximity. Template-assembly of short collagen peptides supplemented with a cell binding sequence (GFOGER) may lead to CMPs of stable triple-helical molecular architecture and cell recognition.

This chapter is modified from Khew, S.T., Tong, Y.W. (2008) *Biochemistry* 47, 585-596.

4.1 Introduction

One protein that is of wide interest to many scientists is collagen, which is the principal constituent of extracellular matrices (ECM). Various approaches have been employed to construct collagen-like triple-helical structure. For example, mimicry of collagen structure has been achieved by using various synthetic peptides primarily composed of Gly-Pro-Pro or Gly-Pro-Hyp repeating units (Sakakibara et al., 1968; Kobayashi et al., 1970). Synthetic peptides consisting of Gly-Xxx-Yyy repeating sequences possess an intrinsic propensity to fold into triple-helical structures. Thus, the use of self-assembling open-chain collagen-like peptides could be the simplest way to achieve triple-helical peptides. Additionally, various strategies have been developed to stabilize collagen-like triple-helical structures. Mutter et. al. introduced the template-assembled synthetic proteins approach for construction of stable tertiary structure of globular protein, four α-helical bundle (Mutter et al., 1992). Similarly, the idea of a template-assembled synthetic protein can also be used for the engineering of collagen-like triple helices. However, most of these approaches pose a number of challenging problems that are usually not encountered in the stepwise synthesis of linear peptides and often require a carefully designed and complex synthesis strategy (Fields et al., 1993a and 1993b; Ottl et al., 1996; Hojo et al., 1997). Although many templates have been used to assemble collagen-mimetic peptides (CMPs), few have reported the design of a fully amino acid based collagen mimics. This study focuses on establishing a template-assembly system to tether CMPs in close proximity thus

reinforcing the intra-molecular folding and stabilizing the collagen-like triple-helical conformations. This chapter describes the synthesis of a peptide template (PT), which is constituted only by amino acids, to assemble CMPs of different primary structures (Table 4.1) through a simple and direct branching protocol without complex strategies. The significance of both the triple-helical molecular architecture and specific cell-binding site was investigated.

Table 4.1. Melting point temperature (T_m) of the peptide template (PT)-assembled collagen-mimetic peptides (CMPs) and their non-templated counterparts as determined by temperature-dependent UV absorbance measurement at 225nm.[a]

Protein/Peptides	Sequence[b]	T_m (^oC)
PT-CMP1	(GFGEEG)≡[G-$(POG)_5$]$_3$	59
PT-CMP2	(GFGEEG)≡[G-$(POG)_3$]$_3$	30
PT-CMP3	(GFGEEG)≡[GG-GPO**GFOGER**GPO-GG]$_3$	20
PT-CMP4	(GFGEEG)≡[G-$(GPO)_3$**GFOGER**$(GPO)_3$-G]$_3$	44
CMP1	$(POG)_5$	No transition
CMP2	$(POG)_3$	No transition
CMP3	GPO**GFOGER**GPO	No transition
CMP4	$(GPO)_3$**GFOGER**$(GPO)_3$	25
(Pro-Pro-Gly)$_3$	$(PPG)_3$	No transition
(Pro-Hyp-Gly)$_{10}$	$(POG)_{10}$	60
Collagen	Calf-skin collagen	37

[a]Cell recognition site (GFOGER) corresponding to residues 502-507 of the collagen α_1 (I) is shown in bold. Each GFGEEG peptide template (PT) contains three carboxylic arms at its C-terminal for covalent coupling to the N-terminal of the collagen-mimetic peptides. [b]Standard one letter code is used to express amino acid sequences, except where noted. O represents hydroxyproline residue.

4.2 Experimental section

Synthesis of Fmoc-protected GFGEEG peptide template

Fmoc-GFGEEG hexapeptide (Figure 4.1) was synthesized in-house on an automated Multipep peptide synthesizer (Intavis). The peptide was assembled on Fmoc-Gly-Wang resin (substitution level = 0.66 mmole/g resin) at 50 μmole scale. Stepwise couplings of amino acids were accomplished as described previously (see "Experimental section", Chapter 3), except that the Fmoc protection group at the N-terminal of the peptide was kept intact. The product was washed with dichloromethane (DCM) twice and vacuum dried prior to cleavage from resin using a cocktail solution composed of 95 % trifluoroacetic acid (TFA), 2.5 % deionized water, and 2.5 % triisopropylsilane (TIS) (v/v). The reaction was allowed to proceed for 3 h with occasional shaking. The cleavage solution was added to cold methyl tert-butyl ether (MTBE) dropwise to induce precipitation of the peptide. The precipitate was collected by centrifugation and was washed 3 times with excess cold ether to remove any residual scavengers. The final precipitate was re-dissolved and lyophilized.

Synthesis of collagen-mimetic peptides

Collagen-mimetic peptides (CMP1, CMP2, CMP3, and CMP4) as shown in Table 4.1 were synthesized as described previously (see "Experimental section", Chapter 3). The Fmoc protection group at the N-terminal was removed by 20 %(v/v) piperidine in DMF prior to the cleavage. The crude peptide was purified using Agilent 1100

semi-preparative HPLC. The purification was performed on an Agilent Zorbax 300SB-C18 reverse phase column (5 μm particle size, 300Å pore size, 25 x 1.0 cm) with a linear gradient of buffer A (0.1% TFA in water) and buffer B (0.1% TFA in acetonitrile) from 10% B to 45% B in 30 min at a flow rate of 2.5 ml/min. Detection was set at 215 nm. The purity of all peptides was tested to be greater than 95 % by analytical RP-HPLC. The molecular weight of the peptides was verified using a Bruker AutoFlex II MALDI-TOF MS.

Synthesis of peptide template-assembled collagen-mimetic peptides

The PT-assembled CMPs (PT-CMP1, PT-CMP2, PT-CMP3, and PT-CMP4) as shown in Table 4.1 were synthesized using Fmoc-solid phase peptide synthesis method (Figure 4.2). The CMPs (CMP1, CMP2, CMP3, and CMP4) were first synthesized on the resin (50 μmole based on resin substitution level) as described above. The Fmoc protection group at the N-terminal of the peptide-resin was removed by 20 %(v/v) piperidine in DMF prior to the coupling to the peptide template manually. The resin was washed 4 times with excess of DMF. Fmoc-GFGEEG (8 μmole) was dissolved in DMF to saturation (0.3 M) and added to the reaction vessel together with 1 equiv of HBTU and HOBt, and 2 equiv of NMM, with respect to the carboxylic arms on the peptide template. The coupling of the peptide template to the N-termini of the peptide sequence proceeded for 6 h at room temperature with occasional shaking. The Fmoc protection group was removed as described above. The resin was washed with DMF and DCM twice and vacuum dried overnight. The cleavage was done as described

above. Preparative HPLC was performed to give products of purity greater than 85 %, as given by the analytical HPLC. The mass of the products was examined using MALDI-TOF MS.

Circular Dichroism (CD) spectroscopy

CD measurements were performed on Jasco Model J-810 spectropolarimeter using a quartz cylindrical cuvette (Hellma) with a path length of 0.1 mm. The cuvette was filled with 150 μL of samples for each measurement. The CD spectra were obtained by continuous wavelength scans (average of three scans) from 260 to 180 nm at a scan speed of 50 nm/min. All samples were dissolved in ultrapure water, unless otherwise stated, and stored at 4 ^{o}C for at least 7 days prior to the test to allow for proper equilibration of triple-helical conformation. The samples were equilibrated for at least an hour at the desired temperature before the CD spectrum was acquired.

Melting studies

The temperature-dependent ultraviolet (UV) absorbance of the peptides was measured on a Cary 50Bio UV Spectrophotometer (Varian) equipped with a Peltier temperature controller (Quantum North-west) (Kajiyama et al., 1995; Feng et al., 1996). Prior to any measurements, all samples were equilibrated at the initial temperature for at least 24 h. The samples were allowed to equilibrate for at least 15 min until the UV absorbance was time-independent at each subsequent temperature point. Thermal transitions of samples equilibrated in quartz cells of pathlength 1 mm were examined

by collecting data at 225 nm from 5 to 80 ^{o}C at 5 ^{o}C increments. Values of melting point temperature (T_m) were determined from the reflection point in the transition region (first derivative). All samples were dissolved in water at 0.50 mg/ml.

Nuclear Magnetic Resonance (NMR) spectroscopy

NMR spectroscopy was done on a Bruker Avance DRX500 500MHz spectrometer. NMR samples were prepared in H_2O/D_2O (2:3) (v/v) with a peptide concentration of approximately 0.10 mg/ml and stored at 4 ^{o}C for at least 24 h and equilibrated for another 1 h at specified temperature before data acquisition. 1D ^{1}H NMR spectra were recorded with a spectral width of 8012.820 Hz at 15 ^{o}C.

Cell adhesion assay

Hep3B liver cells were cultured as described previously (see "Experimental section", Chapter 3). Nunclon Delta TC Microwell plates were coated with 100 µl of 50 µg/ml peptides or calf-skin collagen solution at 4 ^{o}C overnight. The non-specific binding site of the well-plate was blocked with 100 µl of 1 % heat denatured BSA (Sigma-Aldrich), and then washed with PBS twice. A 100 µl amount of Hep3B cell suspension in serum-free DMEM (10 x 10^5 cells/ml) was then added and incubated for 1 h at room temperature (20 ^{o}C). The plates were washed with PBS two times to remove the unattached cells. Adhered cells were measured by a total DNA quantification assay Hoechst 33258 (Sigma-Aldrich) as described previously (see "Experimental section", Chapter 3). Assays were conducted in triplicate and the data

were expressed as mean ± standard deviation (SD).

Competition inhibition assay

Plates were coated with 100 μl of 50 μg/ml calf skin collagen solution as described above. Hep3B cells (10 x 10^5 cells/ml) were incubated with 50 μg/ml peptides or collagen in serum-free DMEM to saturate the cell surface receptors for 30 min before seeding. For each competition assay, a 100 μl amount of the cell suspension was seeded to the collagen-coated well, and the competitive adhesion was allowed to take place for 1 h at room temperature (20 ^oC). The assay was undertaken in triplicate and the data were presented as mean ± SD. The attached cells were measured by the total DNA quantification method. The adhesion of cells in the blank serum-free medium was used as a 100 % reference level.

Immunofluorescence Staining

Substrates were prepared as described above on a Lab-Tek chambered coverglass. Hep3B cells were allowed to adhere on the substrates at a density of 280 cells/mm^2 in serum-free medium for 3 h. Attached cells were fixed in cold 3.7% formaldehyde for 5 min, permeabilized in 0.1% Triton X-100 for 5 min, and blocked in blocking buffer (1% BSA in PBS) for 0.5 h. Direct immunofluorescence staining of the cells with monoclonal anti-vinculin FITC conjugate (Sigma-Aldrich) (1:100 dilution in PBS) was allowed to proceed for 1 h. The actin cytoskeleton and cell nucleus were stained by incubating the cells with phalloidin-tetramethylrhodamine isothiocyanate (TRITC)

(Sigma-Aldrich) (1:1000 dilution in PBS) for 1 h and with 4',6-diamidino-2-phenylindole (DAPI) (Sigma-Aldrich) (1:1000 dilution in PBS) for 5 min, respectively. A Zeiss LSM510 META confocal microscope (Zeiss, Thornwood, NY) was used for imaging.

Statistical analysis

The data of cell adhesion and competition inhibition are presented as mean ± SD. The statistical analysis of the data was done using Student's *t* test. A 95 % confidence level was considered significant.

4.3 Results and discussion

Synthesis of PT-assembled collagen-mimetic peptides

Many protein mimics have been created by incorporating non-naturally derived chemical compounds for the template or spacer (Greiche and Heidemann, 1979; Mutter et al., 1992; Feng et al., 1996; Goodman et al., 1996; Yamazaki et al., 2001; Kwak et al., 2002). To design a fully natural mimic, we propose a peptide template to engineer collagen mimetic that is only constituted with amino acids, consistent with native proteins. For the purpose of mimicking collagen more closely and in a more simplified manner, we have engineered a novel template composed of GFGEEG hexapeptide that also has the unique collagen-like primary structure (Figure 4.1), the

repeating Xxx-Yyy-Gly sequences, to assemble collagen-mimetic peptides into triple-helical conformation that resembles the native structure of collagen. This peptide template (PT) has three carboxyl groups connected to the N-termini of three CMPs (Figure 4.1).

The synthesis of template-assembled CMPs by solid phase peptide synthesis poses a number of challenging problems that are usually not encountered in the stepwise synthesis of linear peptides. Ottl et. al. utilized a complex and carefully planned strategy of orthogonal protection and deprotection of Cys residues to facilitate the chemoselective disulfide bridging of three cysteine-peptides (Ottl et al., 1996; Ottl and Moroder, 1999). Fields et. al. used a lysine-lysine based construct furnished with aminohexanoic acid spacers to template-assemble their collagen-like sequences (Fields et al., 1993a, 1993b and 1995). Branching of three peptide strands from the lysine-lysine based construct required three different protecting strategies: N^{α}-amino protection, N^{ε}-amino side chain protection which must be stable to the N^{α}-amino protecting group removal conditions, and C-carboxyl protection, which must be orthogonally stable to both N^{α}- and N^{ε}-amino protecting group removal conditions (Fields et al., 1993a, 1993b and 1995). A carefully designed branching protocol is essential to ensure the proper coupling and parallel growth of several peptide chains onto a single template and at the same time produce template-assembled collagen mimics of high purity.

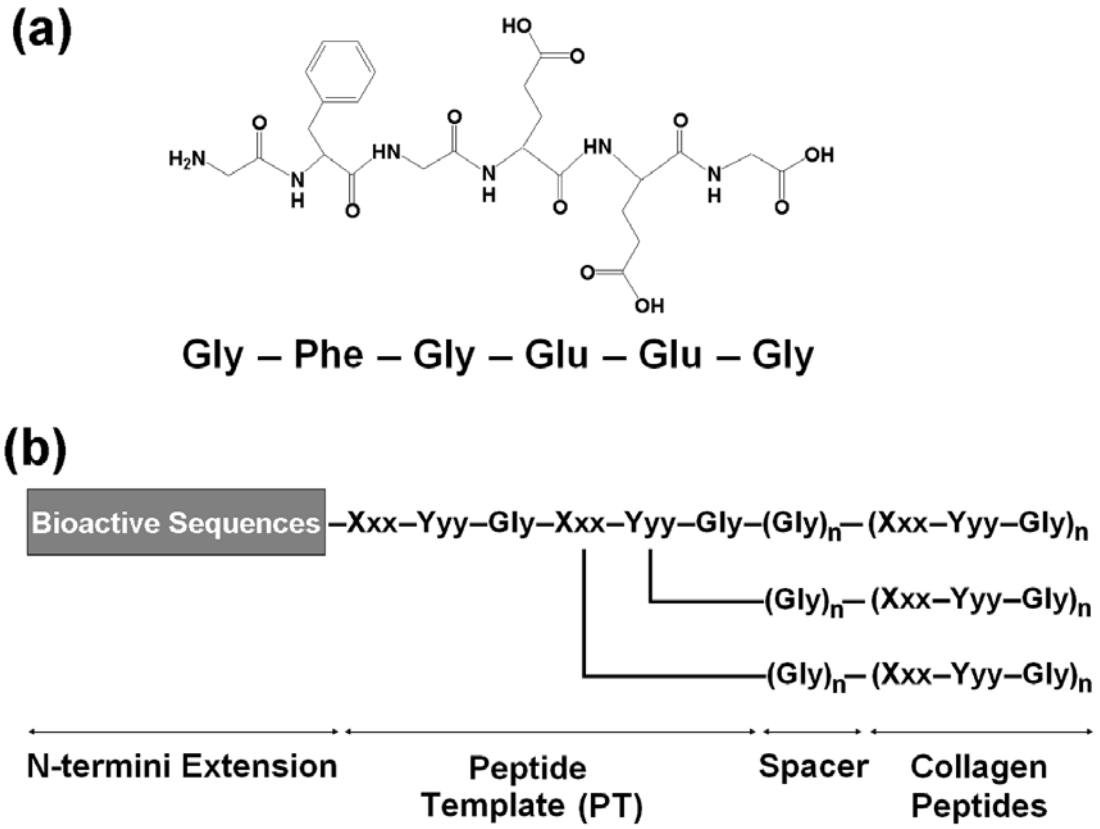

Figure 4.1. (a) Molecular structure of the GFGEEG peptide template (PT). The C-terminal of the template contains three carboxyl groups, each of which can be linked to a strand of collagen-mimetic peptide to facilitate the interactions of the three peptide chains to form the triple-helical conformation. (b) The PT-assembled collagen-mimetic peptides. The template has a fully amino acid based collagen analog, consistent with the native protein, with collagen-like primary and tertiary structure, which also allows incorporation of collagen cell binding sequences within the collagen peptide sequences as well as insertion of additional functional sequences at the N-termini extension of the template.

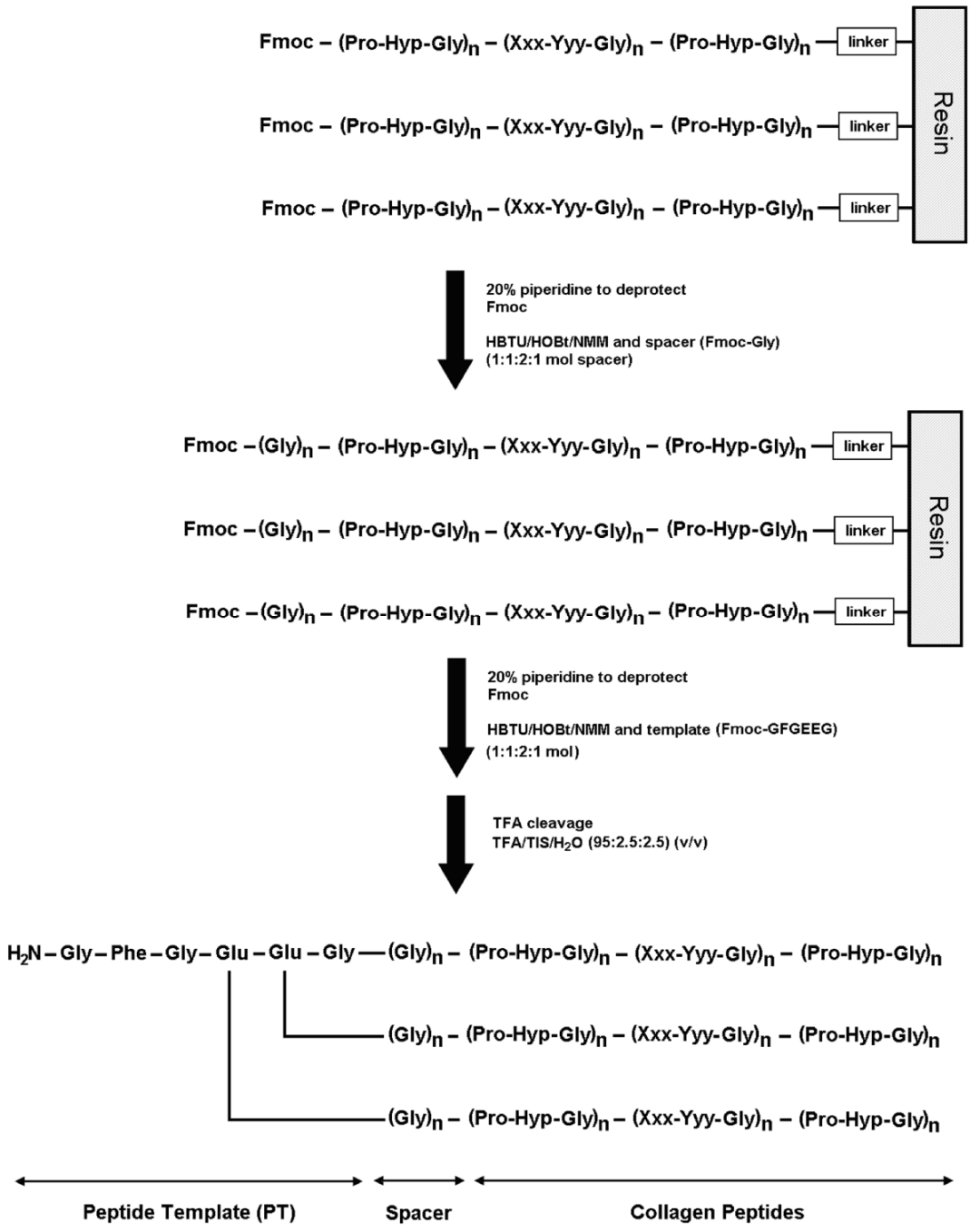

Figure 4.2. Synthesis of the peptide template (PT)-assembled collagen-mimetic peptides (CMPs). The CMPs of repeating Xxx-Yyy-Gly sequences were synthesized and coupled to the PT through a spacer by a simple fluorenyl-methoxy-carbonyl (Fmoc)-solid phase peptide synthesis method.

In this study, a rather simple and direct synthesis scheme based on a generally applicable Fmoc-solid phase synthesis method, wherein no complex strategies are required, was used to synthesize a series of PT-assembled collagen-mimetic peptides (Figure 4.2). Fmoc-GFGEEG template and CMPs were first synthesized separately on the resin. Subsequently, the Fmoc-GFGEEG were cleaved from the resin, activated, and coupled to NH_2-Gly_n-$(Xxx\text{-}Yyy\text{-}Gly)_n$-resin manually. To ensure optimum yield of the PT-assembled CMPs, Fmoc-GFGEEG was used as the limiting reagent. A cell binding motif (GFOGER) was incorporated into the PT-assembled collagen-mimetic peptides, denoted as PT-CMP3 and PT-CMP4, to mimic collagen integrin-specific adhesion. The synthesized PT-assembled collagen-mimetic peptides were harvested using mild cleavage conditions and purified. Figure 4.3 shows the analytical HPLC profiles of the purified PT-assembled CMPs and their respective MALDI-TOF MS spectra. All peptides were purified to a final purity of at least 85%. Based on the mass of the peptides obtained after HPLC purification, the yields of the PT-assembled CMP1, CMP2, CMP3, and CMP4 were approximately 2%, 8%, 9%, and 1.7%, respectively. The purified materials eluted as a single distinct peak in an analytical RP-HPLC which demonstrated the success of this synthesis protocol. The small peak shoulder may be indicative of deletion peptides of close physical properties as the parent molecules. However, the biophysical studies have indicated the formation of stable triple-helical conformations by the PT-assembled CMPs even in the presence of these deletion peptides. MALDI-TOF MS was used to verify the identity of each product, and the result showed that the molecular weight of each product obtained is

consistent with that of the desired product: PT-CMP1 $[M+H]^+$= 4776.4 (calculated= 4776.5), PT-CMP2 $[M+H]^+$= 3172 (calculated= 3172.7), PT-CMP3 $[M+H]^+$= 4864.1 (calculated= 4864.04), and PT-CMP4 $[M+H]^+$= 7729.6 (calculated= 7729.4).

These PT-assembled collagen-mimetic peptides are distinguished from other protein and collagen mimics (Greiche and Heidemann, 1979; Roth and Heidemann, 1980; Thakur et al., 1986; Fields et al., 1993a and 1993b; Feng et al., 1996; Goodman et al., 1996; Ottl et al., 1996; Ottl and Moroder, 1999; Yamazaki et al., 2001) by the use of a peptide template that has a collagen-like primary structure and the fully amino acid based contents, which closer mimics the structure of native collagen. The distinctive characteristics of our peptide (Figure 4.1b) are firstly a branching peptide composed of GFGEEG used as a template to covalently link three collagen-mimetic peptides to facilitate the folding of the triple helix. Second, a fully peptide-based template which allows the incorporation of other biologically active sequences at its extension for additional functions such as enzymatic crosslinking sites and integrin-specific adhesion domains. Third, the incorporation of phenylalanine in the template design as a chromophore for peptide concentration determination. Fourth, the EEG tripeptide at the C-terminal of the peptide template to provide three carboxylic arms for coupling with collagen-mimetic peptides. Finally, the glycine residues which were used as spacers to reduce steric hindrance and to provide flexibility to ensure proper alignment of the three peptide strands with one-residue register shift necessary for the assembly of triple helix.

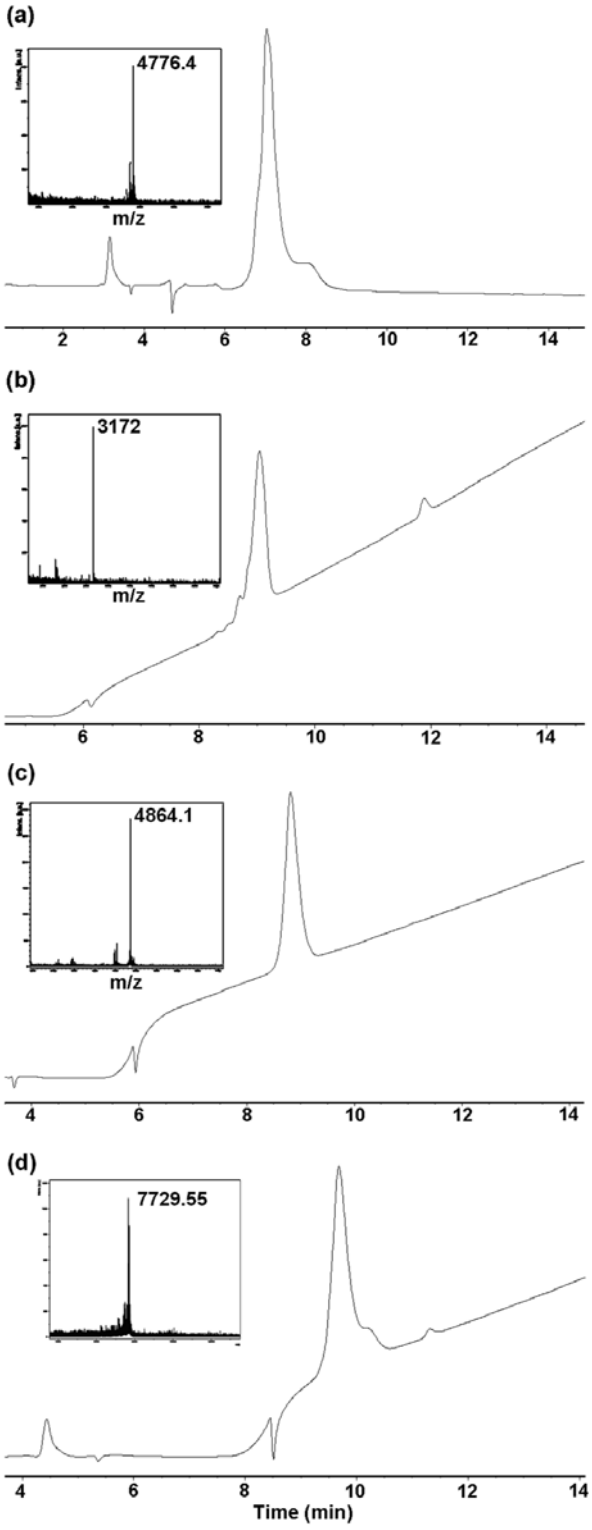

Figure 4.3. Analytical RP-HPLC chromatograms of purified (a) PT-CMP1, (b) PT-CMP2, (c) PT-CMP3, and (d) PT-CMP4 and their respective MALDI-TOF MS spectra (left). HPLC buffer gradient is from 90 %A and 10 %B to 55 %A and 45 %B in 30 min at a total flowrate of 1 ml/min, where buffer A is 0.1% TFA in H_2O and buffer B is 0.1 % TFA in acetonitrile. Injection volume was 50 µl.

CD spectroscopy

The collagen-like triple-helical conformation of the PT-assembled collagen-mimetic peptides was verified using CD spectroscopy. Natural collagen exhibits an unique CD spectrum characterized by a large negative peak at around 197 nm, a crossover near 213 nm and a positive peak at approximately 220 nm (Brown et al., 1972; Sakakibara et al., 1972). These features have been frequently used as a basis to determine the presence of synthetic collagen-like triple-helical structures in solution. The function of the peptide template in the folding of triple-helical structures was examined by comparing the CD spectra of the PT-assembled CMPs with their corresponding non-templated counterparts (CMP1, CMP2, CMP3, and CMP4). Non-templated $(Pro\text{-}Hyp\text{-}Gly)_{10}$ was used as a stable prototype of a triple helix in this study. The PT-assembled CMPs and CMP4 exhibited CD spectra features characteristic of collagen-like triple helix, including a positive peak around 220-225 nm and a large negative trough near 200 nm (Figure 4.4). These CD spectra undergo a red shift in their band positions, as compared to that of the collagen (Table 4.2), because of the higher percentage of imino acids content (Rippon and Walton, 1971). In general, the CD spectra of PT-CMP1, PT-CMP2, PT-CMP3, PT-CMP4, and CMP4 are comparable to that of natural collagen (Fig. 4.5a) and of $(Pro\text{-}Hyp\text{-}Gly)_{10}$ (Fig. 4.4a). The establishment of triple-helical conformations by CD spectral band positions was also supported by comparing the CD spectra of the PT-assembled CMPs with that of native collagen after thermal denaturation (Fig. 4.5). At elevated temperature, a significant decrease in the intensity of both positive and negative peaks of calf-skin collagen was

observed, indicating a thermal transition from the folded to unfolded state. The CD spectra of the PT-assembled CMPs exhibited similar trends at high temperature. However, the degree of conformational change is much smaller than that displayed by native collagen. This is probably due to the stabilizing effect of the template. The template effect is primarily entropic. It prevents unfolding at one end of the triple-helix and thus shifted the folding/unfolding equilibrium. This observation provides evidence for the presence of the triple helices in solution.

Conversely, the non-templated counterparts of the PT-assembled CMPs, except CMP4, displayed CD spectra (Figure 4.4) of polyproline II-like structure characterized by the shallow peak at around 200nm and the lack of the positive peak (Feng et al., 1996; Kwak et al., 2002). The patterns of these CD spectra are similar to that of $(Pro\text{-}Pro\text{-}Gly)_3$ single chain peptide as given in Figure 4.4a, which is known to have no triple-helical conformation in solution. The result is consistent with the previous studies that short synthetic $(Pro\text{-}Hyp\text{-}Gly)_n$ cannot assume triple-helical structures in water (Feng et al., 1996). Increasing the chain length of repeating Pro-Hyp-Gly triplets can help to enhance the assembly of the triple-helical conformation. Alternatively, a template can be used to induce and stabilize the assembly of the triple-helical conformation for very short peptide chains (Feng et al., 1996; Kwak et al., 2002). The formation of triple-helical conformation using short synthetic peptides represents an important breakthrough in the engineering of collagen analogues and preparation of collagen-mimetic biomaterials.

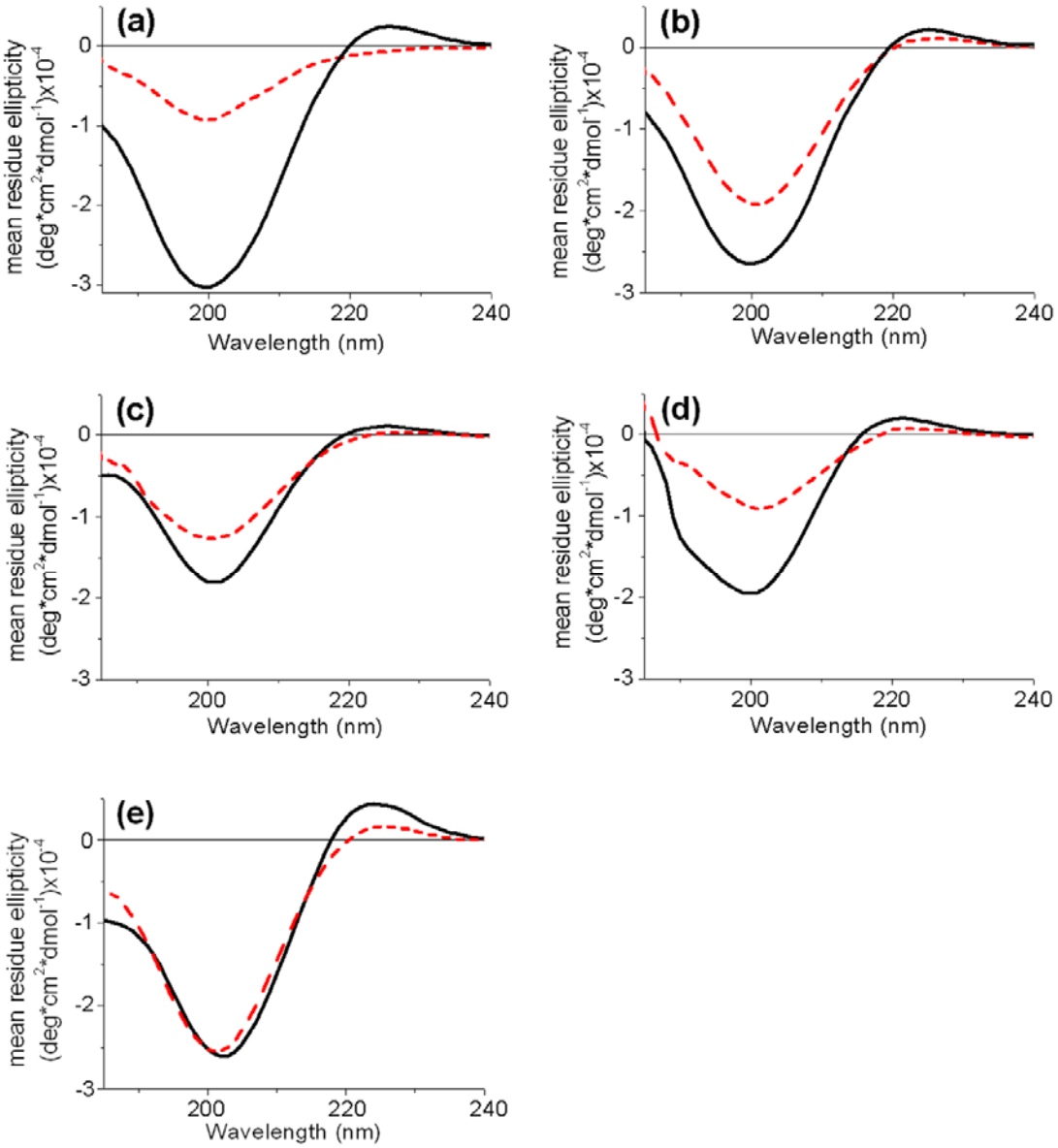

Figure 4.4. CD spectra of the PT-assembled and non-templated collagen-mimetic peptides. CD spectra of the non-templated (a) $(Pro\text{-}Hyp\text{-}Gly)_{10}$ (solid line) and $(Pro\text{-}Pro\text{-}Gly)_3$ (segmented line) in water at room temperature. CD spectra of the PT-assembled collagen-mimetic peptides (solid line): (b) PT-CMP1, (c) PT-CMP2, (d) PT-CMP3, and (e) PT-CMP4 and their non-templated counterparts (dashed line): (b) CMP1, (c) CMP2, (d) CMP3, and (e) CMP4 in water at room temperature. $(Pro\text{-}Hyp\text{-}Gly)_{10}$ was used as a stable prototype of a triple helix while $(Pro\text{-}Pro\text{-}Gly)_3$ oligopeptide was used as a negative control.

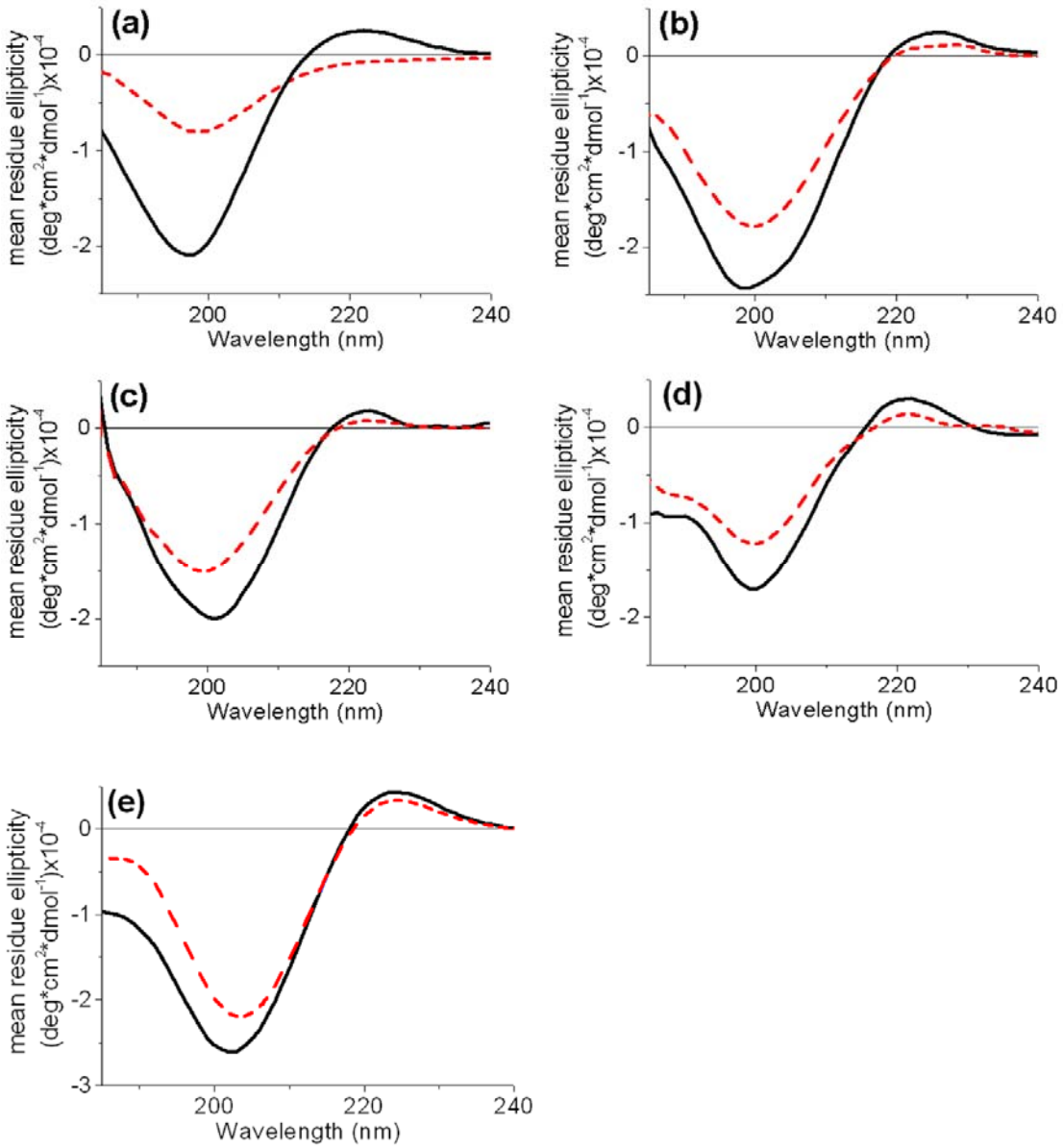

Figure 4.5. CD spectra of natural collagen and PT-assembled collagen-mimetic peptides at 20 ^{o}C (solid line) and 70 ^{o}C (segmented line): (a) calf-skin collagen, (b) PT-CMP1, (c) PT-CMP2, (d) PT-CMP3, and (e) PT-CMP4 in water.

Table 4.2. CD parameters and Rpn values of the PT-assembled collagen-mimetic peptides, non-templated collagen-mimetic peptides, $(Pro\text{-}Pro\text{-}Gly)_3$, $(Pro\text{-}Hyp\text{-}Gly)_{10}$, and calf-skin collagen.

Samples	Maximum, nm (ellipticity)	Crossover, nm (ellipticity)	Minimum, nm (ellipticity)	Rpn*
PT-CMP1	225 (0.26×10^4)	218	199 (-2.40×10^4)	0.11
PT-CMP2	223 (0.22×10^4)	217	201 (-2.02×10^4)	0.11
PT-CMP3	221 (0.31×10^4)	215	200 (-1.72×10^4)	0.18
PT-CMP4	224 (0.45×10^4)	217	202 (-2.64×10^4)	0.17
CMP1	226 (0.11×10^4)	220	201 (-1.93×10^4)	0.06
CMP2	226 (0.03×10^4)	222	200 (-1.27×10^4)	0.02
CMP3	222 (0.06×10^4)	218	202 (-1.01×10^4)	0.06
CMP4	225 (0.22×10^4)	219	201 (-2.40×10^4)	0.09
$(Pro\text{-}Pro\text{-}Gly)_3$	---	---	200 (-0.94×10^4)	---
$(Pro\text{-}Hyp\text{-}Gly)_{10}$	225 (0.32×10^4)	218	199 (-2.97×10^4)	0.11
Calf-skin collagen	222 (0.26×10^4)	214	197 (-2.11×10^4)	0.12

* Rpn represents the ratio of positive peak over the negative peak intensity in the CD spectra.

Rpn values

Rpn values denote the ratio of positive peak over the negative peak intensity in the CD spectra and have been previously used to establish the presence of triple-helical conformations in solution (Feng et al., 1996a and 1996b). The CD spectra absorbance and Rpn values of the PT-assembled collagen-mimetic peptides and CMP4, listed in Table 4.2, are comparable to that of calf-skin collagen for indications of triple-helical conformations. Rpn values of PT-CMP4 and CMP4 were 0.17 and 0.09, respectively. Higher Rpn values were obtained for PT-CMP1 (0.11), PT-CMP2 (0.11), and PT-CMP3 (0.18) as compared to their non-templated counterparts which have Rpn values ranging from 0.02-0.06. The PT-assembled CMPs and CMP4 have Rpn values close to or higher than that of natural collagen (0.12) and the triple-helical $(Pro\text{-}Hyp\text{-}Gly)_{10}$ (0.11). These data suggests that the PT-assembled CMPs contain triple-helical conformations, while the non-templated counterparts, except CMP4, do not. This conclusion is also supported by the results obtained from both CD spectroscopy and thermal melting curve analyses.

Melting curve analyses

Triple-helical conformations can be distinguished from the polyproline II-like and non-supercoiled structures based on the thermal melting characteristic (Jefferson et al., 1998). Triple helices melt in a highly cooperative manner, as the structures are stabilized by both intra- and interstrand hydrogen-bonding water networks (Bella et al., 1994 and 1995; Jefferson et al., 1998). Thermal denaturation of natural collagen

will cause a hyperchromic effect in UV absorbance and a similar effect can be observed for synthetic collagen-like peptides (Wood, 1963). The melting transition curves are given in Figure 4.6. The mid point of the transition was taken as the melting point temperature (T_m) and was presented in Table 4.1.

It can be seen from Figure 4.6a that the non-templated CMP1, CMP2, and CMP3 showed similar melting curves as the negative control $(Pro\text{-}Pro\text{-}Gly)_3$ with no transition and thus no evidence of triple helicity even at low temperature. The *R* values for the four melting curves of these nontemplated CMPs obtained by a linear fitting are greater than 0.996, suggesting that these melting curves are a linear line with no transition. The result is consistent with the CD spectroscopy that none of the nontemplated CMP1, CMP2, and CMP3 can assume stable triple-helical structures in water in the absence of a template since their chain length is too short to support a triple helix.

The use of the peptide template in promoting assembly of short peptide sequences into triple-helical conformations is clearly seen by the cooperative melting curves displayed by PT-CMP1, PT-CMP2, PT-CMP3, and PT-CMP4 as given in Figure 4.6b. While nontemplated $(Pro\text{-}Hyp\text{-}Gly)_3$ showed no transition, PT-CMP2 composed of three short $(Pro\text{-}Hyp\text{-}Gly)_3$ exhibited a cooperative melting curve in water with T_m of 30 ^{o}C. The thermal stability of the PT-assembled $(Pro\text{-}Hyp\text{-}Gly)_3$ was comparable to KTA-tethered $(Gly\text{-}Pro\text{-}Hyp)_3$, which was shown to also form

triple-helical conformation in water with a melting temperature of 30 ^{o}C (Goodman et al., 1996). As the peptide chain length increases, the thermal stability of the PT-assembled conformations increases significantly as demonstrated by PT-CMP1 composed of three $(Pro\text{-}Hyp\text{-}Gly)_5$ assembled by the peptide template (T_m = 59 ^{o}C). The melting temperature of nontemplated $(Pro\text{-}Hyp\text{-}Gly)_{10}$ in water is 60 ^{o}C as obtained from its melting curve given in Figure 4.6b, which is quite close to the T_m of PT-CMP1. Therefore, it can be seen that the stabilizing effect of the peptide template is similar and equivalent to the addition of five more Pro-Hyp-Gly repeats to the nontemplated $(Pro\text{-}Hyp\text{-}Gly)_5$ chain. This result proves the significant role of the peptide template in the assembly of short CMP chains into stable triple helices in solution. PT-CMP3 supplemented with integrin-specific GFOGER sequence (Knight et al., 1998 and 2000) was also found to have stable triple-helical conformation with T_m = 20 ^{o}C. The observation of a cooperative transition curve together with a proper CD spectrum is indicative of the presence of stable triple-helical conformation (Feng et al., 1997). It is clear that substitution of the cell binding domain into Pro-Hyp-Gly repeats may destabilize the triple helix. However, the co-oligomeric structures are still able to form triple helices.

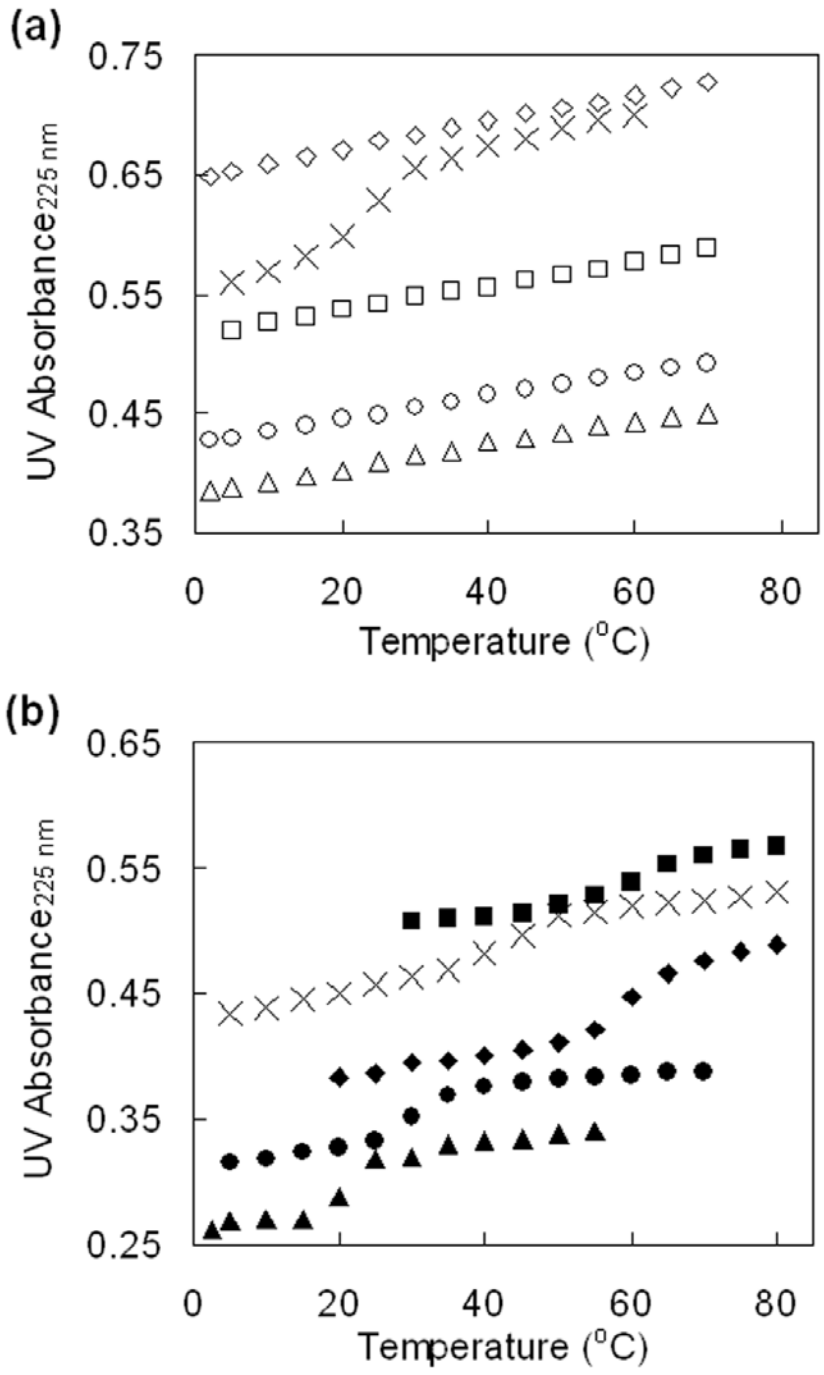

Figure 4.6. Thermal melting curve analysis. Melting transition curves of (a) non-templated: CMP1 (◇), CMP2 (○), CMP3 (Δ), CMP4 (×) and $(Pro\text{-}Pro\text{-}Gly)_3$ (□) and (b) $(Pro\text{-}Hyp\text{-}Gly)_{10}$ (■), PT-assembled collagen peptides: PT-CMP1 (◆), PT-CMP2 (●), PT-CMP3 (▲), and PT-CMP4 (×) at 0.50 mg/ml in water.

NMR spectroscopy

The presence of the triple-helical conformation in the peptide solution can also be established using NMR spectroscopy. The assembly of a triple-helical structure resulted in the appearance of a new set of NMR resonances which cannot be observed for the unassembled or unfolded collagen analogs (Brodsky et al., 1992; Li et al., 1993; Melacini et al., 1996). It is remarkable that among the resonances of the assembled triple-helical set, that of Pro $C_{\delta}H$ at 3.1 ppm is well resolved and not overlapped by any resonance of the unfolded structure sets. The resonance at 3.1 ppm can therefore be used unambiguously to identify the triple-helical structure (Melacini et al., 1996).

Figure 4.7 showed the 1D ^{1}H-HMR spectral region containing the assembled Pro $C_{\delta}H$ resonance for collagen analogs $(Pro\text{-}Hyp\text{-}Gly)_{10}$, PT-CMP1, and PT-CMP2. It can be seen from Figure 4.7 that both $(Pro\text{-}Hyp\text{-}Gly)_{10}$ (used as a stable prototype of triple helix in this study) and PT-CMP1 displayed a strong peak signal at near 3.1 ppm. This is consistent with the previous CD and UV melting curve analyses that both the collagen analogs adopt stable triple-helical conformation in solution. Also in agreement with the previous analyses, PT-CMP2 with lower triple helix stability showed a relatively lower peak signal with dispersion at near 3.1 ppm (Figure 4.7c). The result showed that three triplets are minimally sufficient to form an assembled structure. Goodman et. al. proposed that the resonance dispersion is induced by the triple helix end effect and is more significant in shorter peptides (Melacini et al.,

1996). This interpretation is consistent with the wide broadening of the Pro $C_{\delta}H$ signal at near 3.1 ppm observed for PT-CMP2 as compared to PT-CMP1 and $(Pro\text{-}Hyp\text{-}Gly)_{10}$. On the other hand, it is known from our previous results that CMP1 is not stable in the assembled form and therefore the set of triple-helical resonance at near 3.1 ppm is absent in CMP1 (Figure 4.7d).

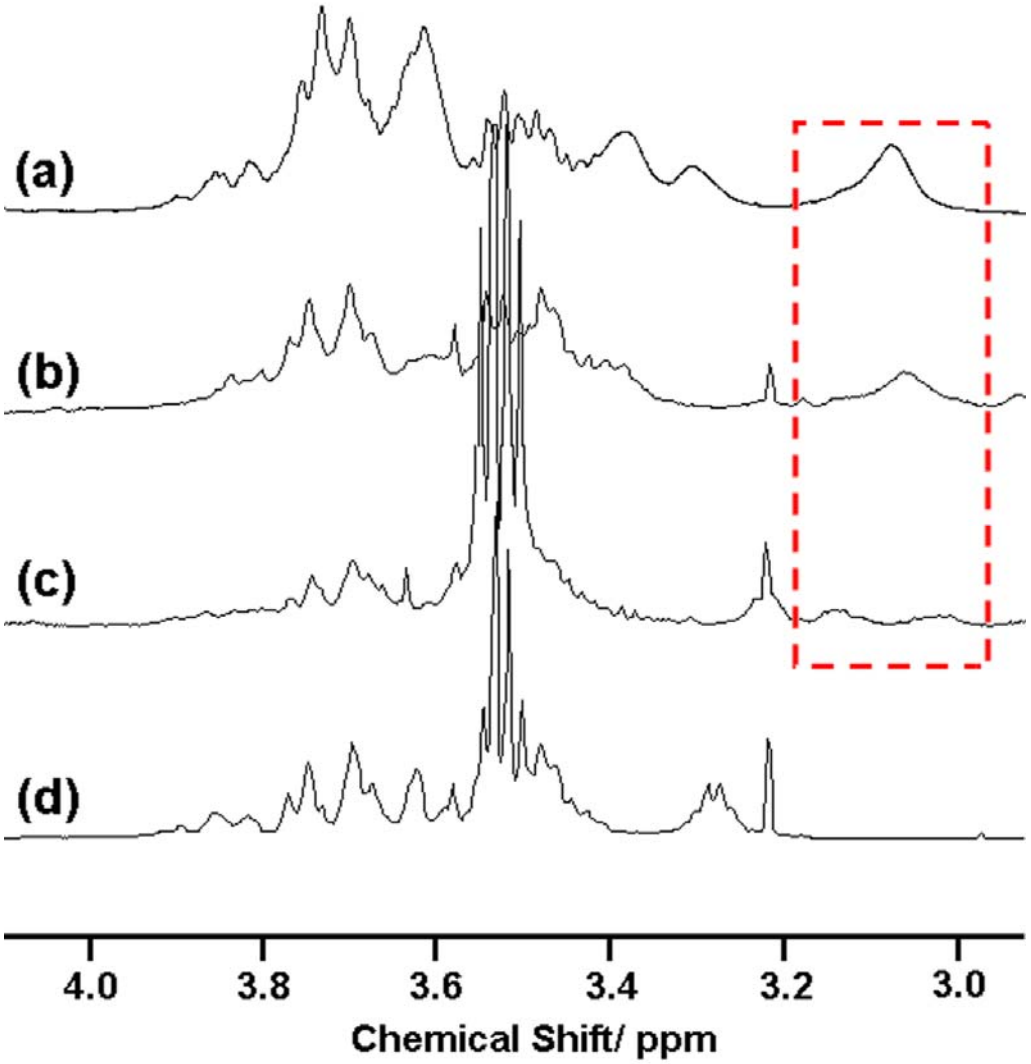

Figure 4.7. 1D ^{1}H-NMR spectra of (a) $(Pro\text{-}Hyp\text{-}Gly)_{10}$, (b) PT-CMP1, (c) PT-CMP2 and (d) CMP1. The boxed spectral regions contain a peak signal representative of the assembled Pro $C_{\delta}H$ signal at 3.1-3.0 ppm. All spectra were acquired at 15 ^{o}C.

Collagen peptide activity

Cell adhesion assay was performed to study the cell binding activity of PT-CMP3 and PT-CMP4 and to understand the specific functions of the protein structure in correlation with specific amino acid sequences in the cell binding process. Collagen and heat-denatured BSA were used as a positive and negative control, respectively. The human carcinoma Hep3B cell line has a high constitutive activity in adhesion to collagen and therefore was used as the model cell type (Masumoto et al., 1999).

The cell adhesion result is presented in Figure 4.8a. The cell-binding activity of PT-CMP3 and PT-CMP4 was found to be 36±5% and 62±1% of that of natural collagen, respectively. The presence of both PT-CMP3 and CMP4 promoted modest but significant adhesion of Hep3B at a similar level (~40%). The cell adhesion can be observed to be conformation-dependent by comparing the differences in cell adhesion levels on PT-CMP4, PT-CMP3, CMP4, and CMP3. The above studies have demonstrated that while PT-CMP4 adopts stable triple-helical conformation, PT-CMP3 and CMP4 have lower T_m values (20 and 25 ^{o}C, respectively) and thus may undergo some degree of dissociation. Conversely, CMP3 cannot assume a triple helix structure. These conformational differences resulted in a considerable loss of recognition. It is interesting to note that both PT-CMP2 and CMP3 promoted cell adhesion at a comparable level probably because of their similar triple helicity. The result is consistent with the fact that native collagen has a noticeably higher affinity for collagen specific receptors than denatured collagen (Santoro, 1986; Gullberg et al.,

1992). Furthermore, the triple-helical conformation of collagen has been shown to be essential, if not crucial, for influencing cell adhesion, spreading, migration, matrix metalloproteinase (MMP) binding, and human platelet adhesion and aggregation (Fields, 1991; Miles et al., 1994; Grab et al., 1996; Knight et al., 2000). It has been reported that $(Gly\text{-}Pro\text{-}Hyp)_9$ and $(Gly\text{-}Pro\text{-}Pro)_{10}$ can serve as substrates for rat hepatocytes at least to some extent (Rubin et al., 1981), suggesting the repeating tripeptide units composed of Gly and Pro might be recognized by the hepatocyte-binding sites. However in this study, a low degree of cell attachment to the triple-helical PT-CMP1, with reference to the cell adhesion to the blank (BSA) surface, was observed, which we attribute to the lower number of tripeptide repeats found in PT-CMP1. PT-CMP1 also lacks a GFOGER cell adhesion sequence which similarly would have an adverse effect on the level of Hep3B cell adhesion, thus indicating the specific recognition of the GFOGER sequence by cells. In all, cell recognition of collagen peptides appeared to be both conformation and sequence-specific dependent, and the absence of either resulted in a marked loss of cell adhesion. These findings may have great impact for biological chemists in their biomolecular design: shorter, and hence less expensive, CMPs could be used as a stable triple-helical molecular architecture with our template assembly strategy to improve their cell recognition by supplementing them with a specific cell-binding sequence.

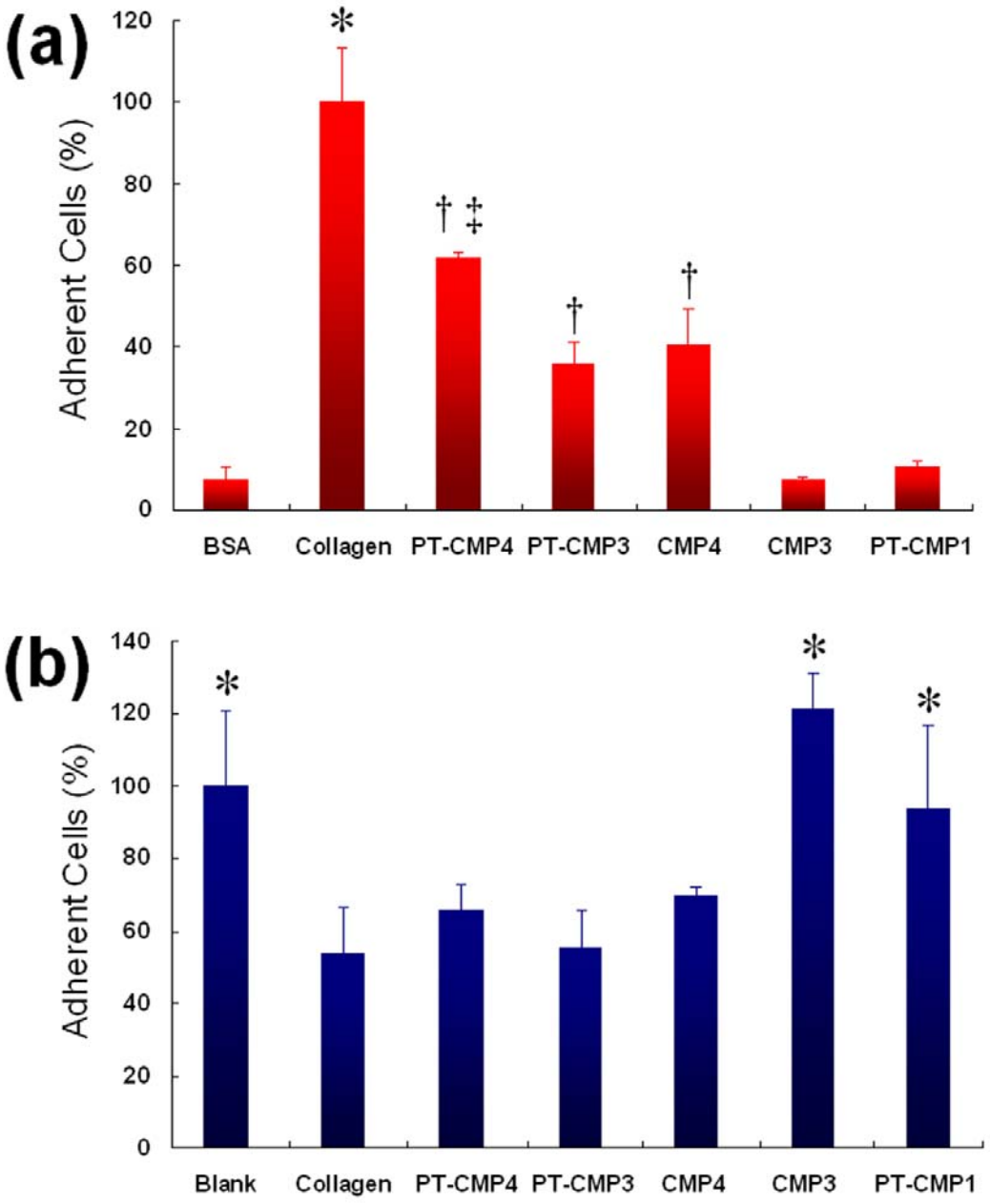

Figure 4.8. (a) Adhesion of Hep3B cells as a function of surface composition: 1% heat-denatured BSA (BSA), calf-skin collagen (Collagen), PT-CMP4, PT-CMP3, CMP4, CMP3, and PT-CMP1. Cells in serum-free medium were allowed to adhere to peptide- or protein-coated well plate for 1 hour at 20 ^{o}C.. Student's *t* test with *p < 0.001: significantly different from all other samples, with †p < 0.001: significantly different from BSA, CMP3, and PT-CMP1, and with ‡p < 0.05: significantly different from PT-CMP3 and CMP4. (b) Competition inhibition of Hep3B cell adhesion to collagen-coated surface. Cells in serum-free medium were incubated with 50 μg/ml peptide or collagen for 30 mins prior to seeding. Cell adhesion in blank serum-free medium was used as a positive control. Student's *t* test with *p < 0.05: significantly different from blank, CMP3, and PT-CMP1.

Hep3B cells seeded on PT-CMP4, PT-CMP3, PT-CMP1, and collagen substrates were fixed and stained for actin stress fibers (TRITC-phalloidin; red), nuclei (DAPI; blue), and vinculin (FITC-anti-vinculin; green), a major membrane-cytoskeletal protein present in focal adhesion plaques that is involved in the linkage of integrins to actin cytoskeleton (Ezzell et al., 1997), to study the cytoskeletal organization and focal adhesion formation. The confocal images are shown in Figure 4.9. It can be observed that the cells seeded on PT-CMP4 and PT-CMP3 exhibited distinct actin stress fibers, indicating the formation of strong cytoskeleton organization in the cells. The extensive cell spreading could be a result of the integrin-mediated cell adhesion process (Hynes, 1992; Fields et al., 1993b). The clustering of vinculin at cell periphery and center indicated that the cells formed strong focal adhesion contacts on both PT-CMP4 and PT-CMP3 surfaces (Figure 4.9). It can be qualitatively seen from the vinculin staining that the cells on both PT-CMP4 and PT-CMP3 surfaces exhibited higher concentrations of vinculin, and thus more focal contacts than the cells seeded on CMP3 (result not shown) and PT-CMP1 surfaces, indicating a more firm adhesion and more rapid interaction between the cell surface receptors and GFOGER sequence. Conversely, the collagen-like adhesion profile was not observed for the cells seeded on CMP3 (result not shown) and PT-CMP1, as can be seen from the obscure actin organization. Furthermore, most of them remained in spherical morphology on CMP3 and PT-CMP1. The less pronounced vinculin observed for the cells seeded on CMP3 and PT-CMP1 indicated the absence of strong focal adhesion contacts.

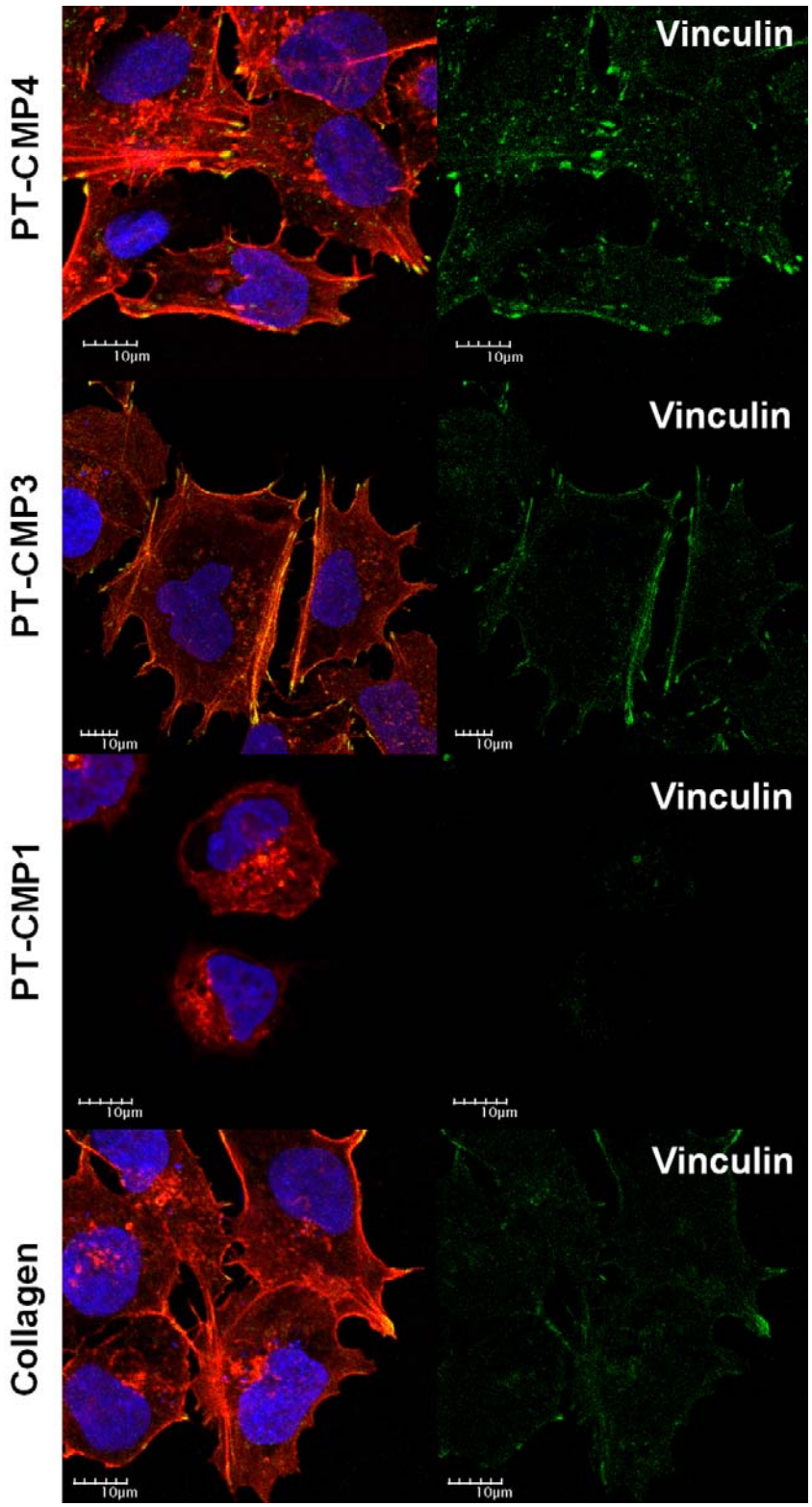

Figure 4.9. Immunofluorescence images of Hep3B cells on PT-CMP4, PT-CMP3, PT-CMP1, and calf-skin collagen. Confocal images were taken after the cells, in serum-free medium, were seeded on different surfaces for 3 h.

The competitive inhibition assay is an indirect screening for the cell binding activity displayed by the peptides. Cell adhesion to the collagen surface was inhibited when the cell surface receptors, especially specific collagen receptors, are presaturated with the adhesive molecules prior to cell seeding. The inhibitory activity of PT-CMP4 and PT-CMP3 was similar to that of collagen and is shown in Figure 4.8b. It can be seen that both PT-CMP4 and PT-CMP3 effectively inhibited Hep3B cell binding to collagen. The inhibition was most probably due to the specific interactions between the adhesive peptides and the cell surface receptors, suggestive of the participation of specific collagen receptors in the adhesion process. Removal of GFOGER sequence or loss of the triple helix structure resulted in CMPs lacking the ability to inhibit the integrin-mediated cell adhesion process.

4.4 Conclusion

A simple strategy for making a peptide template composed of GFGEEG hexapeptide to assemble collagen-like peptide sequences into proper triple-helical molecular architecture was successfully developed. The biological assays demonstrated the successful imitation of collagen integrin-specific adhesion by the PT-assembled CMPs supplemented with a GFOGER sequence. This peptide template assembly strategy appears to be versatile for creating and stabilizing desired collagen-like molecular architectures. Such template-assembly system could be used to further study protein

folding, to create novel protein mimetics, to insert additional specific functions into the protein mimetics by incorporating bioactive sequences at the extension of the peptide template, or to coat biomaterials to engineer integrin-specific surfaces.

CHAPTER 5

THE SPECIFIC RECOGNITION OF A CELL BINDING SEQUENCE DERIVED FROM TYPE I COLLAGEN BY HEP3B AND L929 CELLS

In the previous chapter, we have established a template-assembly strategy to tether collagen-mimetic peptides (CMPs) in close proximity thus reinforcing the intramolecular folding and stabilizing the triple-helical structures. The template-assembled CMPs supplemented with the GFOGER cell binding sequence exhibited significant cell adhesion activity. To understand the recognition of Hep3B and L929 cells toward the GFOGER sequence and the structural basis of the recognition, a series of PT-assembled CMPs of different triple-helix stabilities were synthesized as a model for natural collagen. The integrin-specific GFOGER sequence was incorporated into the collagen peptides not only to promote cell adhesion but also to study its specific recognition by the two cell types. Although several distinct sequences derived from various collagen subtypes have been characterized as cell adhesion sites, little is known about the specific recognition of a collagen sequence by different cell types. This study may contribute to a better understanding of the specific recognition of Hep3B and L929 cells toward the GFOGER sequence.

This chapter is modified from Khew, S.T., Tong, Y.W. (2007) *Biomacromolecules* 8, 3153-3161.

5.1 Introduction

Cell adhesion is crucial for the assembly of individual cells into three-dimensional tissues, as most cells grown *in vitro* must adhere to a substrate to survive and proliferate (Rubin et al., 1981). Among the ECMs, type I collagen can directly promote the adhesion and migration of numerous cell types, including hepatocytes, fibroblasts, melanoma, keratinocytes and neural crest cells (Rubin et al., 1981; Faassen et al., 1992; Grzesiak et al., 1992; Scharffetter-Kochanek et al., 1992; Perris et al., 1993). Several cell binding domains within the type I collagen macromolecules have been identified and used to engineer bioadhesive surfaces (Staatz et al., 1991; Gullberg et al., 1992; Grab et al., 1996; Knight et al., 1998; Reyes and García, 2003; Renner et al., 2004). However, little has been done to compare the specific recognition of different cell types to a specific collagen or ECM protein sequence. Most cell integrin-receptors interact in a conformation-independent manner with specific peptide sequences derived from ECM proteins, such as RGD (Ruoslahti and Pierschbacher, 1987; Massia and Hubbell, 1991) and YIGSR (Graf et al., 1987; Massia et al., 1993). Conversely, the collagen integrin-receptors, such as $\alpha_1\beta_1$, $\alpha_2\beta_1$, $\alpha_3\beta_1$, $\alpha_{10}\beta_1$, and $\alpha_{11}\beta_1$ (Kramer and Marks, 1989; Kuhn and Eble, 1994; Fields, 1995; Camper et al., 1998; Velling et al., 1999; Zhang et al., 2003), bind to several regions within the triple-helical domain of collagen in a conformation-dependent manner (Staatz et al., 1991; Vandenberg et al., 1991; Miles et al., 1994; Knight et al., 1998; Knight et al., 2000). Both conformation-dependent and conformation-independent

sites may coexist within type I collagen (Fields, 1995; Grab et al., 1996). Recent studies have revealed that GFOGER hexapeptide derived from residues 502-507 of collagen α_1(I) is a major cell-binding site within type I collagen (Knight et al., 1998; Knight et al., 2000). To understand the recognition of different cell integrin receptors to this specific cell-binding sequence (GFOGER) and the structural basis of the recognition, a series of PT-assembled collagen-mimetic peptides (CMPs) of different triple-helix stability were synthesized. This study may contribute to a better understanding of the specific recognition of a cell binding sequence by different cell types and the need to use specific cell binding sequences for precisely controlling adhesion of a particular cell type.

5.2 Experimental section

Peptide synthesis

The PT-assembled CMPs (PT-CMP1, PT-CMP3, and PT-CMP4) and the nontemplated peptides (CMP1, CMP3, and CMP4) as shown in Table 4.1 were synthesized using Fmoc-solid phase peptide synthesis method as described previously (see "Experimental section", Chapter 4).

Cell adhesion assay

Hep3B and L929 cells were cultured separately as described previously (see "Experimental section", Chapter 3). Nunclon^{TM} Delta TC 96-well plates were coated with 100 µl of 50 µg/ml peptides or calf-skin collagen solution at 4^{o}C overnight, blocked with 100 µl of 1% heat denatured bovine serum albumin (BSA) (Sigma-Aldrich), and then washed with phosphate buffered saline (PBS) two times. Denatured collagen peptides and collagen substrates were prepared in a similar way, except that the samples were first heated to 70 ^{o}C for 3 h immediately before incubation in the microwell plate at 70 ^{o}C overnight (Rubin et al., 1981). 100 µl of the cell suspension in serum-free DMEM (10 x 10^5 cells/ml) was then added and incubated for 1 h at room temperature (20 ^{o}C). The plates were washed with PBS two times to remove the unattached cells. Adhered cells were measured by a total DNA quantification assay Hoechst 33258 (Sigma-Aldrich), as described previously. For all substrates, n = 6 and the data were expressed as mean ± standard deviation (SD).

Competition inhibition assay

Plates were coated with 100 µl of 50 µg/ml calf-skin collagen solution as described above. Cells (10 x 10^5 cells/ml) were incubated with 50 µg/ml peptides or collagen in serum-free DMEM to saturate the cell surface receptors for 30 min before seeding. For each competition assay, 100 µl of the cell suspension was seeded to the collagen-coated well and the competitive adhesion was allowed to take place for 1 h at room temperature (20 ^{o}C). The assay was undertaken in triplicate and the data were

presented as mean ± SD. The attached cells were measured by the total DNA quantification method as described previously.

Immunofluorescence staining for actin organization and focal adhesions

Substrate preparation was done as described above on a Lab-Tek chambered coverglass. Cells were seeded at a density of 280 cells/mm^2 in serum-free medium for 3 h. Attached cells were fixed in cold 3.7 % formaldehyde for 5 min, permeabilized in 0.1% Triton X-100 for 5 min, and blocked in blocking buffer (1% BSA in PBS) for 0.5 h. Direct immunofluorescence staining was done as described previously (see "Experimental section", Chapter 4)

Statistical Analysis

The data of cell adhesion and competition inhibition are presented as mean ± SD. The statistical analysis of the data was done using Student's *t* test. A 95% confidence level was considered significant.

5.3 Results and discussion

Hep3B liver and L929 fibroblast cell adhesion on PT-assembled and nontemplated collagen-mimetic peptides

A cell adhesion assay was performed to study the recognition of Hep3B liver cell and L929 fibroblast cell for a specific cell binding sequence (GFOGER) derived from residue 502-507 of collagen α_1(I). The cell adhesion result is presented in Figure 5.1. Calf-skin collagen and heat-denatured BSA were used as a positive and negative control in this assay, respectively.

It can be seen from Figure 5.1 that the maximum adhesion of both Hep3B (~60%) and L929 (~90%) cells occurred on the PT-CMP4 surface. PT-CMP3 and CMP4 supported cell adhesion at a comparable level. The presence of both PT-CMP3 and CMP4 promoted modest but significant adhesion of Hep3B (average ~40%) and L929 (average ~73%) cells. The cell adhesion to GFOGER appeared to be conformation-dependent, as can be observed from the cell adhesion level on PT-CMP4, PT-CMP3, CMP4, and CMP3. Biophysical studies (see "Results and discussion", Chapter 4) demonstrated that PT-CMP4 adopts stable triple-helical conformation while PT-CMP3 and CMP4 has a lower T_m value (20 and 25 ^{o}C, respectively) and thus may undergo some degree of dissociation. Conversely, CMP3 cannot assume a triple helix structure. These conformation differences resulted in a considerable loss of recognition by both Hep3B and L929 cells. It is interesting to

note that both PT-CMP3 and CMP4 promoted cell adhesion at a comparable level, probably because of their similar triple helicity. The result indicates that the activity of different CMPs supplemented with the same binding motif (GFOGER) may be similar if their triple helicity is comparable, highlighting the importance of triple-helical conformation in preserving the GFOGER cell binding site. The triple helix structure has been shown to be essential, if not crucial, for influencing cell adhesion, spreading, migration, matrix metalloproteinase binding, and human platelet adhesion and aggregation (Fields, 1991; Miles et al., 1994; Grab et al., 1996; Knight et al., 2000). Similarly, absence of the GFOGER hexapeptide in PT-CMP1 caused a marked loss of activity and had an adverse effect on the level of cell adhesion, thus indicating the specific recognition of the GFOGER sequence by both cell types.

Although the presence of PT-CMP4 promoted both Hep3B and L929 cell adhesion considerably, the two cell types displayed a significant difference in their recognition for the GFOGER sequence, as can be seen from the cell adhesion to PT-CMP4, PT-CMP3 and CMP4. In all cases, the cell-binding activity displayed by L929 cells was notably higher than that exhibited by Hep3B cells, suggesting that the collagen mimetics may have greater affinity for fibroblast receptors and that the mimicry of collagen cell adhesion by using a specific cell-binding sequence may be different for various cell types. Although GFOGER has been shown as a major cell-binding site in collagen (Knight et al., 1998 and 2000), it is not the only cell adhesion site within macromolecules, and it is not universally recognized by all cell

integrin receptors. This could be one possible reason for the lack of recognition displayed by Hep3B cells. The integrins $\alpha_1\beta_1$, $\alpha_2\beta_1$ and $\alpha_{11}\beta_1$ have been shown to bind GFOGER and the GFOGER-like motifs found in collagen (Knight et al., 2000; Xu et al., 2000; Zhang et al., 2003; Siljander et al., 2004). The difference in cell recognition is thus probably because of the differences in their expression of these specific integrins for GFOGER. Both hepatocytes and fibroblast cells have been shown to attach to natural collagen (Rubin et al., 1981; Grab et al., 1996; Jokinen et al., 2004). However, the repertoire of integrins expressed by hepatocytes is strikingly different from that of most other fibroblast cells. Platelets, epithelial cells, and fibroblasts have been shown to express high levels of $\alpha_2\beta_1$, which is the primary receptor for GFOGER and type I collagen (Knight et al., 1998 and 2000; Siljander et al., 2004). In contrast, collagen receptors $\alpha_2\beta_1$ usually expressed by epithelial cells are undetectable in normal adult hepatocytes (Nejjari et al., 1999). Primary rat hepatocytes and fibroblasts both express the integrin $\alpha_1\beta_1$ that can function as a collagen receptor (Gullberg et al., 1992), with the adult hepatocytes expressing only low levels of $\alpha_1\beta_1$ integrin, which is also true for Hep3B cells (Nejjari et al., 1999). It is likely that the restricted expression of integrins by normal adult hepatocytes is an adaptation to their particular microenvironment (Nejjari et al., 1999). In contrast to most epithelial cells, hepatocytes lack an organized basement membrane. Conversely, fibroblasts are the cells of connective tissues and are responsible for maintaining the structural integrity of the tissue by continuously secreting precursors of the ECM, especially collagen. Thus, the significant difference in the expression of integrins $\alpha_1\beta_1$ and $\alpha_2\beta_1$ by Hep3B

and L929 cells may be a result of their adaptation to the different extracellular microenvironment and therefore result in the different cell binding activity of Hep3B and L929 cells on the GFOGER surfaces. A specific cell binding motif may not be recognized by a wide range of integrin-receptors expressed on a specific cell type, and thus the use of a combination of cell-binding sequences is necessary to better mimic ECM cell adhesion for optimized cell and tissue engineering. A combination of peptide models of collagen integrin-binding sequences and other ECM sequences has been studied previously and found to have potential to mimic biological activities of an ECM (Malkar et al., 2003; Baronas-Lowell et al., 2004).

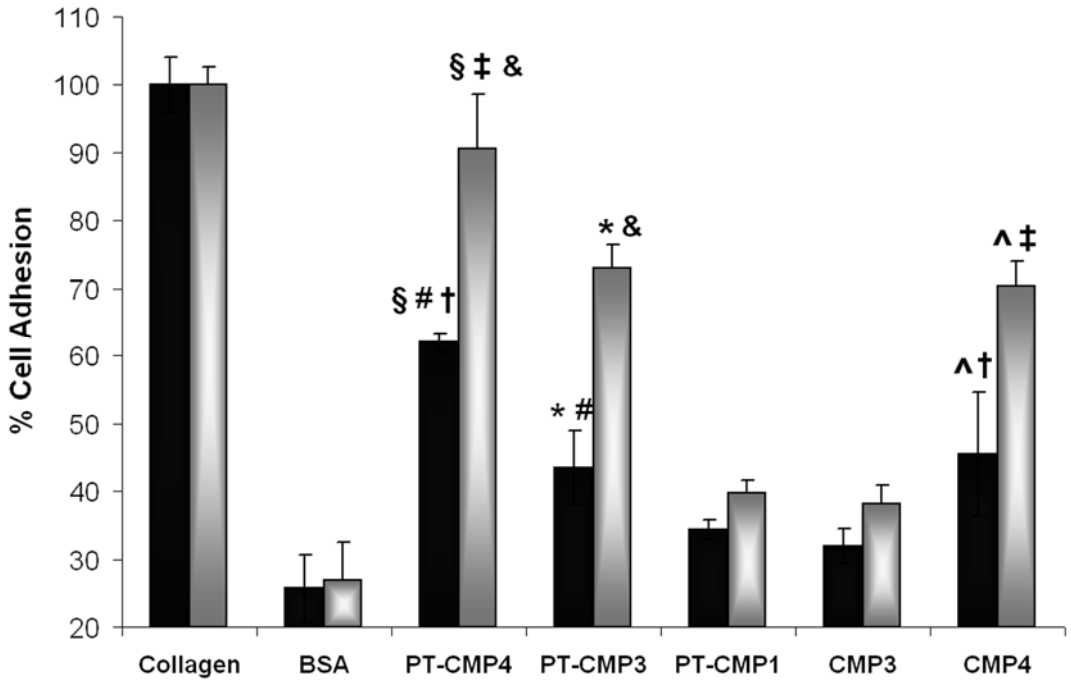

Figure 5.1. Adhesion of Hep3B (dark) and L929 (grey) cells as a function of surface composition: calf-skin collagen (Collagen), 1% heat-denatured BSA (BSA), PT-CMP4, PT-CMP3, PT-CMP1, CMP3, and CMP4. Cells in serum-free medium were allowed to adhere to peptide- or protein-coated well plate for 1 hour at 20^{o}C. Student's t test with $p < 0.05$: §,*, #, †, ^, &, and ‡ are significantly different from each other respectively. Each histogram represents the mean ± SD with n = 6.

Competitive inhibition of Hep3B and L929 cell adhesion to collagen

The competitive inhibition assay is an indirect screening for the cell binding activity displayed by different cell types for the collagen or collagen peptides. The cells were preincubated with soluble collagen or collagen peptides prior to being seeded onto collagen-coated plates. Cell adhesion to the collagen surface is inhibited when the cell surface receptors, especially specific collagen receptors, are pre-saturated with the adhesive molecules prior to cell seeding. Adhesion of cells onto the collagen surface in blank serum-free medium was used as the 100% reference level.

It can be seen from Figure 5.2 that both cell types displayed specific interactions with the soluble collagen, and thus the cell adhesion to the collagen surface was significantly inhibited by the presence of soluble collagen molecules in the competitive inhibition assay. The inhibition of adhesion of both cell types to collagen surface by soluble collagen was comparable, indicating that both cells may recognize native collagen at a similar level and suggesting that GFOGER is not the only major cell adhesion sequence within the collagen macromolecules. In fact, both cell types may express similar integrins for other cell binding sequences of collagen, as demonstrated in the following cell adhesion assay.

The inhibitory activity of PT-CMP3 and PT-CMP4 was comparable to that of collagen for L929 cell adhesion. The GFOGER-containing triple-helical PT-CMP3 and PT-CMP4 effectively inhibited L929 cell binding to collagen. The inhibition was

most probably due to the specific interactions between the GFOGER and the specific surface receptors, suggestive of the participation of specific collagen receptors in the adhesion process. The inhibition of Hep3B cell adhesion by the PT-assembled CMPs, however, was not comparable to the collagen. Hep3B cells displayed higher cell binding activity than L929 cells during the competitive inhibition, indicating the lack of specific interaction between the GFOGER sequences with the cell surface receptors. The result is in agreement with the cell adhesion assay, which showed that Hep3B and L929 cells may express integrins involved in the specific interaction with GFOGER, such as $\alpha_1\beta_1$ and $\alpha_2\beta_1$, at different levels. Removal of the GFOGER sequence or loss of the triple helical structure resulted in collagen peptides lacking the ability to inhibit the integrin-mediated cell adhesion process, as can be seen from the lower inhibitory activity displayed by PT-CMP1 and CMP3.

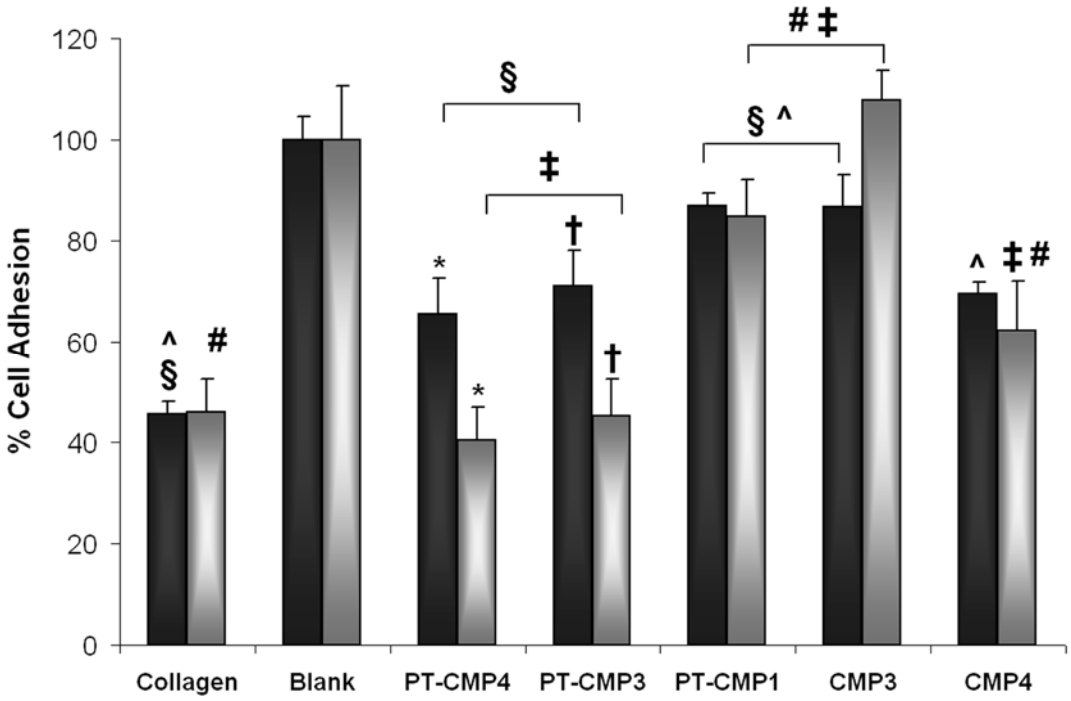

Figure 5.2. Competition inhibition of Hep3B (dark) and L929 (grey) cell adhesion to the collagen-coated surface. Cells in serum-free medium were incubated with 50 μg/ml peptide or collagen for 30 min prior to seeding. The competitive adhesion was allowed to take place for 1 h at 20°C. Cell adhesion in blank serum-free medium was used as a positive control. Student's *t* test with $p < 0.05$: §,*, #, †, ^, and ‡ are significantly different from each other respectively. Each histogram represents the mean ± SD with n = 3.

Cell adhesion to native and denatured collagen and PT-assembled collagen-mimetic peptides

Several cells have been shown to recognize native and denatured collagen (Rubin et al., 1981; Tuckwell et al., 1994). Here, we studied the specific cell binding activity of Hep3B and L929 cells to the native and denatured collagen and the PT-assembled CMPs supplemented with GFOGER. The triple-helical structure has been shown to be important for both Hep3B and L929 cell attachment to GFOGER through the cell adhesion assay using a series of PT-assembled CMPs of different triple helicities as a model for natural collagen. However, the recognition of the cells over a specific substrate, such as collagen or PT-CMP3, when the substrate is heat-denatured is not fully known. This study was performed to further investigate the role of the triple-helical molecular architecture in the specific recognition of Hep3B and L929 cells over the GFOGER sequence and collagen. The denatured substrates were prepared by heating collagen or PT-assembled CMP solutions at 70 ^{o}C for 3 h immediately before incubation in the microwell plate at 70 ^{o}C overnight (Rubin et al., 1981).

The collagen triple helix appears to be an important recognition element for both Hep3B and L929 cells, as can be seen from the reduction of the cell adhesion to the denatured collagen substrate. The result is consistent with the fact that native collagen has a noticeably higher affinity for collagen-specific receptors than denatured collagen (Santoro, 1986; Gullberg et al., 1992). The cell adhesion of both

cell types was reduced at a similar degree to ~55% (Figure 5.3), suggesting a similar recognition of both cells over the denatured collagen. The cell adhesion to denatured collagen, although lower, is still significant, indicating that the triple helix is important, but not crucial, for cell adhesion to collagen. This result suggests that both Hep3B and L929 cells express integrins that are involved in the adhesion to denatured collagen, such as $\alpha_5\beta_1$ and $\alpha_v\beta_3$ (Davis, 1992; Gullberg et al., 1992; Pfaff et al., 1993; Tuckwell et al., 1994), but are not involved in adhesion to triple-helical GFOGER at a similar level. The sequences involved in cell adhesion to denatured collagen are probably DGEA (Yamamoto and Yamamoto, 1994) and RGD (Davis, 1992; Gullberg et al., 1992). Conversely, the receptors that are responsible for adhesion to GFOGER, such as $\alpha_1\beta_1$, $\alpha_2\beta_1$ and $\alpha_{11}\beta_1$ (Knight et al., 2000; Xu et al., 2000; Zhang et al., 2003; Siljander et al., 2004), were expressed by Hep3B and L929 cells at different levels.

While the adhesion of both Hep3B and L929 cells was reduced by approximately 50% on the denatured collagen, the cell binding activity to the denatured PT-assembled CMPs, especially PT-CMP4, was better preserved, which we attribute to the stabilizing effect of the PT in promoting the assembly of the short CMPs into the triple-helical conformation. In contrast, the cell adhesion to the non-triple-helical GFOGER (CMP3) was significantly reduced (Figure 5.1). It has been demonstrated that the degree of conformational change of the PT-assembled CMPs is much smaller as compared to that of the calf-skin collagen at elevated temperatures (Figure 4.5), probably because of the stabilizing effect of the template,

which promotes interactions between the peptides and overcomes the unfavorable entropy. This result suggests that CMPs can be used as a stable triple-helical molecular architecture with a proper template assembly strategy to improve their cell recognition by supplementing them with a specific cell-binding sequence. It is also interesting to note that the L929 cells displayed a higher binding activity than the Hep3B cells in adhering to the denatured PT-assembled collagen-mimetic peptides, consistent with the result of the cell adhesion assay, suggesting that the expression of integrins for collagen GFOGER may be different by various cell types.

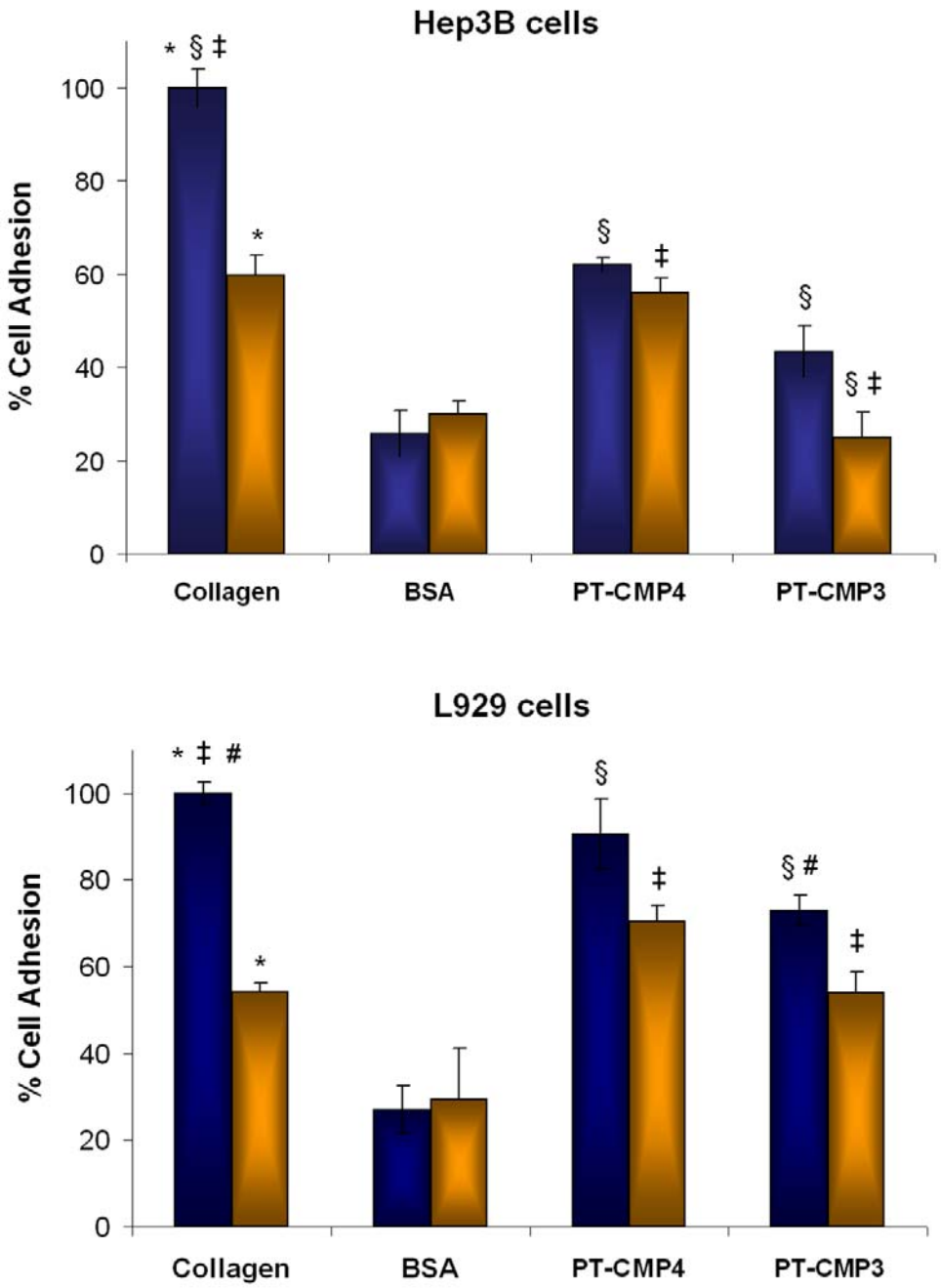

Figure 5.3. Adhesion of Hep3B (a) and L929 (b) cells as a function of surface composition coated at different temperatures overnight: 4°C (dark) and 65°C (grey). Cells in serum-free medium were allowed to adhere to peptide- or protein-coated well plate for 1 hour. Student's *t* test with $p < 0.05$: §,*, #, and ‡ are significantly different from each other respectively.

Cytoskeletal organization and focal adhesion immunofluorescence staining for Hep3B and L929 cells

Hep3B and L929 cells seeded on collagen, PT-CMP4, and CMP3 substrates were fixed and stained at 3 h for actin stress fibers (TRITC-phalloidin; red), nuclei (DAPI; blue), and vinculin (FITC-anti-vinculin; green), a major membrane-cytoskeletal protein present in focal adhesion plaques that is involved in the linkage of integrins to actin cytoskeleton (Ezzell et al., 1997).

It can be seen from the confocal images (Figure 5.4) that both cell types displayed well-developed actin cytoskeletal structure and collagen-like adhesion profiles on PT-CMP4 surface. Both Hep3B and L929 cells exhibited distinct actin stress fibers when seeded on collagen and PT-CMP4 surfaces. The assembled elongated actin filaments indicated the formation of strong actin cytoskeleton organization in both cell types. Conversely, the actin organization became less pronounced on the cells seeded on non-triple-helical GFOGER (CMP3) surfaces. While both Hep3B and L929 cells spread and developed extensive actin stress fibers on collagen and PT-CMP4 surfaces, most of them remained in spherical morphology after 1 and 3 h adhesion on CMP3 and PT-CMP1 (result not shown). Deletion of GFOGER sequence or loss of triple helical structure caused a substantial decrease in cell spreading activities.

Focal adhesions are sites where integrin-mediated adhesion links to the actin cytoskeleton. It can be seen from the vinculin staining (Figure 5.4) that both cells formed strong focal adhesion contacts on the collagen surface. Most of the focal adhesions were found at both the cell periphery and center, associated with the ends of stress fibers of the cells. Although the recognition of GFOGER sequence by different cell types cannot be measured quantitatively by immunofluorescence staining, it can be seen from the confocal images qualitatively that L929 cells exhibited a higher concentration of vinculin and thus more focal contacts compared to Hep3B cells on the PT-CMP4 surface, indicating a more firm adhesion and more rapid interaction between the cell surface receptors and the GFOGER sequence. The localization of vinculin on the periphery and center, with a sharp spike at the termination points and across the actin stress fibers, of both cell types seeded on PT-CMP4 suggests that the collagen peptides promoted the integrin-mediated cell adhesion in a pattern similar to that observed on the collagen surface. Conversely, both Hep3B and L929 cells displayed very few focal adhesion points when seeded on the CMP3 surface. Cells did not form strong focal contacts on non-triple-helical GFOGER, as the vinculin are observed at relatively low densities at the periphery of the cells. The focal adhesion position at the convergence of integrin adhesion, signaling and the actin cytoskeleton generally involve integral membrane protein integrins, which bind to extracellular proteins via specific amino acid sequences, such as the RGD motif. Therefore, we hypothesize that cell adhesion and spreading on collagen and PT-CMP4 surfaces are unlike the interaction between cells and synthetic polymers, which merely depends on

the non-specific contact between the cell membrane proteins and the functional groups of polymers (Bačáková et al., 2000a and 2000b). The extensive cell spreading could, in fact, be a result of the integrin-mediated cell adhesion process (Hynes, 1992; Fields et al., 1993b). Cell focal adhesion is important in regulating cellular behavior, including adhesion, signaling, migration, proliferation, and differentiation. Different cell types may recognize a specific cell-binding sequence at a different degree. Therefore, mimicry of an ECM microenvironment using a specific or combination of various cell-binding sequences to target a particular cell type is important to optimize a specific cell and tissue engineering.

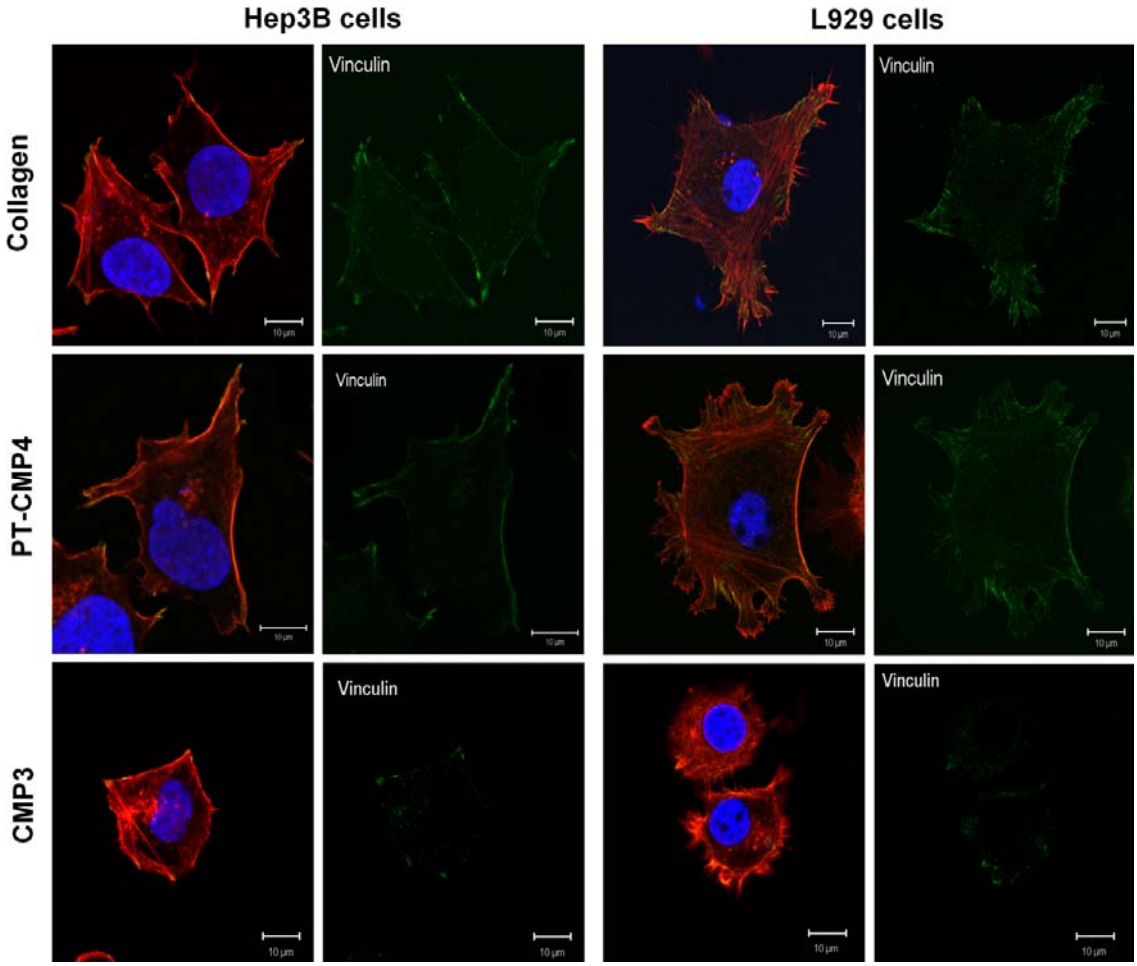

Figure 5.4. Cytoskeletal organization and focal adhesions of Hep3B and L929 cells as a function of substrates: calf-skin collagen, PT-CMP4, and CMP3. Cells were fixed and stained for actin stress fibers (TRITC-phalloidin; red), nuclei (DAPI; blue), and vinculin (FITC-antivinculin; green) after 3 h adhesion in serum-free medium and examined by confocal microscopy (60x magnification).

5.4 Conclusion

PT-CMP4 was shown to promote both Hep3B and L929 cell adhesion considerably. Cell recognition of the collagen peptides supplemented with GFOGER appeared to be both conformation- and sequence-specific, the absence of which resulted in a marked loss of cell recognition. It was also shown in this study that different cell types may recognize the GFOGER sequence at different levels. Although the GFOGER sequence appears to be a general cell adhesion-promoting site, there are differences in the levels of cell binding activity based on the cell types. A specific cell-binding motif may not fully mimic an ECM microenvironment, and the use of a combination of two or more cell-binding sequences, such as RGD, DGEA, and GFOGER, may be necessary for targeting a wide range of integrin receptors expressed on a specific cell type to better mimic ECM cell adhesion.

CHAPTER 6

CHARACTERIZATION OF AMINE DONOR AND ACCEPTOR SITES FOR TISSUE TRANSGLUTAMINASES USING A SEQUENCE FROM THE C-TERMINUS OF HUMAN FIBRILLIN-1 AND THE N-TERMINUS OF OSTEONECTIN

In the previous chapters, we have synthesized and characterized a series of collagen-mimetic peptides that exhibited both collagen-like triple-helical conformation and cell binding activity. Toward achieving an enzymatically crosslinkable biomimetic collagen, the study that naturally follows these previous works would be the characterization of amine donor and acceptor substrates for tissue transglutaminase (TGase), a naturally occurred enzyme involved in the post-translational modification (crosslinking) of proteins. This chapter describes the characterization of a specific region on human fibrillin-1, spanning from residues 2800-2806 (EDGFFKI), as an active amine donor substrate for tissue TGase. A previously characterized APQQEA derived from osteonectin was used as an amine acceptor probe. The identification of the naturally-derived substrate peptides for tissue TGase could eventually lead to tailoring novel protein-like crosslinkable biomaterials.

6.1 Introduction

Because tissue transglutaminase (TGase) is expressed ubiquitously, the tissue TGase-modified proteins are evident throughout the body including extracellular matrices (ECM) as well as skin and hair. However, the biological role of tissue TGase is varied. It has been implicated in many biological processes, such as cellular differentiation (Greenberg et al., 1991; Aeschlimann et al., 1993), receptor signaling (Nakaoka et al., 1994), programmed cell death (Fesus et al., 1987; Greenberg et al., 1991), assembly of ECM (Schittny et al., 1997), and several degenerative diseases (Griffin et al., 2002). The clarification of the physiological function of tissue TGase requires identification of its acceptor and donor substrate sites from natural proteins. Fibrillin-1 is the major fibrillin isoform in elastic fibers. Though the molecular mechanisms of elastic fibers formation are unknown, it has been reported that the TGase crosslinking between fibrillin-1 (amine acceptor) and tropoelastin (lysine donor) is fundamental to the elastic fiber formation (Rock et al., 2004; Clarke et al., 2005) and also between fibrillin molecules (Qian and Glanville, 1997). Additionally, it has been suggested that the tissue TGase-mediated crosslinking plays a vital role in strengthening microfibrillar networks (Thurmond and Trotter, 1996). To advance the understanding of the role of tissue TGase crosslinks, it is important to exactly identify the substrate peptide involved. While a considerable number of reactive glutamine residues have been identified in various proteins (Aeschlimann et al., 1992; Coussons et al., 1992), only a limited number of amine donor substrates have been characterized

(Pucci et al., 1988; Porta et al., 1991; Groenen et al., 1992 and 1994; Ikura et al., 1993; Mariniello et al., 1993; Merck et al., 1993). Even less information is available about the amine donor sites of fibrillin-1 for tissue TGase. To fill this gap, we identified a specific region on human fibrillin-1, spanning from residues 2800-2806 (EDGFFKI), as an active amine donor substrate for tissue TGase. In this study, we have also looked into the potential of EDGFFKI to serve as a tracer peptide to detect endogenous transglutaminase activity and as a probe for enzyme-directed site-specific labeling of potential amine acceptor sites in native proteins.

6.2 Experimental section

Peptide synthesis

Peptides were synthesized on an automated Multipep peptide synthesizer (Intavis, Cologne, Germany), using solid-phase method. Briefly, the peptides were assembled on fluorenyl-methoxy-carbonyl (Fmoc)-Gly-Wang resin, as described previously. The purity of all peptides was greater than 95% as determined by Shimadzu analytical HPLC (Kyoto, Japan). The peptide mass was verified by LC-mass spectroscopy (MS) (Bruker) and MALDI-TOF MS (Bruker). The peptides were dissolved in 100 mM Tris/HCl buffer (pH 7.4) at 2 mM and stored at -20°C before use.

Enzymatic crosslinking and analysis

A previously characterized APQQEA was used as an amine acceptor probe (Hohenadl et al., 1995). The reaction volume (25 μL) contained 0.5 mM APQQEA, 0.5 mM EDGFFKI or EDGFFRI or FEKDIFG or MDC (Sigma-Aldrich), 100 mM Tris/HCl (pH 7.4), 10 mM $CaCl_2$, and 0.5 *U*/ml guinea pig liver tissue TGase (Sigma-Aldrich). A control reaction mixture contained similar compositions, except with no tissue TGase added. The reaction cocktail was incubated at 37 °C and stopped by adding ethylenediaminetetraacetic acid (EDTA) to a final concentration of 10 mM and diluted 2x by using 100 mM Tris/HCl (pH 7.4) at predetermined time points.

To quantify the reactivity of EDGFFKI, EDGFFRI, FEKDIFG, and MDC towards the amine acceptor probe, the reaction mixtures were analyzed by analytical HPLC on an Agilent Zorbax 300SB-C18 reverse phase (RP) column (5 μm particle size, 300Å pore size, 25 x 0.46 cm) with a gradient of buffer A (0.1% TFA in water) and buffer B (0.1% TFA in acetonitrile) from 5% B to 60% B in 20 min at a flow rate of 1 ml/min. Injection volume was 5 μL and the UV detector was set at 220 nm. LC-MS was used to identify each peak. The peak area of the unreacted peptide substrate was compared to that of the respective control (without tissue TGase) to determine the reaction conversion. MALDI-TOF mass spectroscopy was used to accurately identify the peptide substrates and the crosslinked peptides.

Detecting endogenous transglutaminase activity in human skin tissue

A previously reported novel *in situ* detection method for the TGase activity in the skin was used (Raghunath et al., 1998). Briefly, cryostat sections (5μm) of human skin were air-dried for 10 min at room temperature, re-incubated with 1% BSA in 0.1 M Tris/HCl (pH 7.4) for 30 min at room temperature and then incubated for 1.5 h at room temperature with substrate buffer (10 μL of 10 mM biotinylated EDGFFKI or biotinylated APQQEA or biotinylated cadaverine + 10 μL 200 mM $CaCl_2$ + 965 μL Tris Buffer) at pH 7.4. A control was treated similarly, except that $CaCl_2$ was replaced with 25 mM ethyleneglycoltetraacetic acid (EGTA) to inhibit the Ca^{2+}-dependent TGase. After 3 times of washing in PBS, the sections were incubated for 30 min at room temperature with streptavidin-dichlorotriazinylaminofluorescein (DTAF) (1:100 in PBS), counter-stained with 4',6-diamidino-2-phenylindole (DAPI) to identify cells, and washed 3 times in PBS for 15 min and mounted in polyvinyl alcohol mounting medium with anti-fading agent (Sigma). Images were captured using Zeiss axio observer in ApoTome mode, 40x objective and 300 ms exposure time.

Specific labeling of amine acceptor sites in human skin tissue by exogenous tissue transglutaminase using EDGFFKI as a probe

To irreversibly inhibit endogenous TGase activity, skin sections were incubated with 10 mM solution of TGase inhibitor iodoacetamide (Sigma, US) in 100 mM Tris/HCl, pH 7.4, for 1.5 h and washed six times in PBS for 30 min. Assay of residual intrinsic TGase activity was performed by similar procedures used for detecting the

endogenous TGase activity. Iodoacetamide-treated sections were then incubated for 1.5 h at room temperature with enzyme + substrate buffer (200 µL of 1.25mg/ml guinea pig liver tissue TGase + 10 µL 10 mM of biotinylated-EDGFFKI or biotinylated APQQEA or biotinylated cadaverine + 10 µL 200 mM $CaCl_2$ + 765 µL Tris buffer) at pH 7.4. A control was treated similarly, except that $CaCl_2$ was replaced with 25 mM ethyleneglycoltetraacetic acid (EGTA) to inhibit the Ca^{2+}-dependent tissue TGase. The slides were washed thrice in PBS for 15 min, incubated for 30 min at room temperature with streptavidin-DTAF 1:100 in PBS, counter stained with DAPI, washed 3 times in PBS, and mounted in Polyvinyl alcohol mounting medium with anti-fading agent. Images were captured using Zeiss axio observer in ApoTome mode, 40x objective and 300 ms exposure time.

6.3 Results

EDGFFKI as an amine donor substrate for tissue TGase

The partial length peptide EDGFFKI derived from the C-terminal of human fibrillin-1 contains a lysine residue at position 2805 for tissue TGase crosslinking. Coupling of EDGFFKI to the amine acceptor probe was monitored by HPLC. The tissue TGase-mediated crosslinking resulted in an additional peak on the HPLC as shown in Figure 6.1, which was identified as a conjugation of the two peptides by LC-MS. In contrast, no crosslinking was observed in the control reaction (without tissue TGase),

confirming that the coupling of EDGFFKI to the amine acceptor substrate APQQEA was a tissue TGase-catalyzed reaction. The changes in the molecular mass were examined by MALDI-TOF mass spectroscopy. It can be seen from the mass spectra (Figure 6.2) that the crosslinking was only observed between the EDGFFKI and APQQEA in the presence of tissue TGase. The result confirmed the intermolecular conjugation between EDGFFKI and APQQEA.

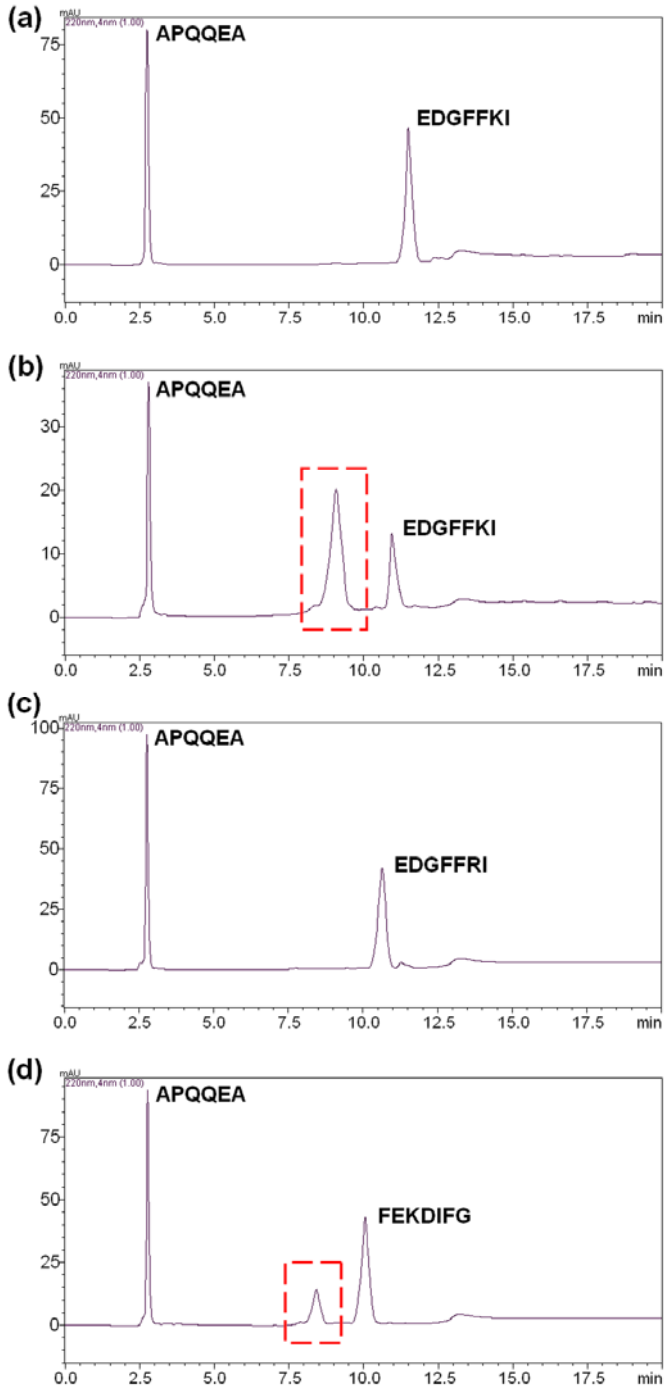

Figure 6.1. Tissue transglutaminase (tissue TGase)-mediated crosslinking reactions as monitored by reverse-phase HPLC after 60 min. A previously characterized APQQEA was used as an amine acceptor probe. The reaction volume (25 µL) contained 100 mM Tris/HCl (pH 7.4), 10 mM $CaCl_2$, and 0.5 mM APQQEA incubated with (a) 0.5 mM EDGFFKI, (b) 0.5 mM EDGFFKI + 0.5 *U*/ml tissue TGase, (c) 0.5 mM EDGFFRI + 0.5 *U*/ml tissue TGase, and (d) 0.5 mM FEKDIFG + 0.5 U/ml tissue TGase. The HPLC peak identity was confirmed by LC-MS/MS. The boxed peak represents the reaction product with molecular weight corresponding to the crosslink of the two substrate peptides.

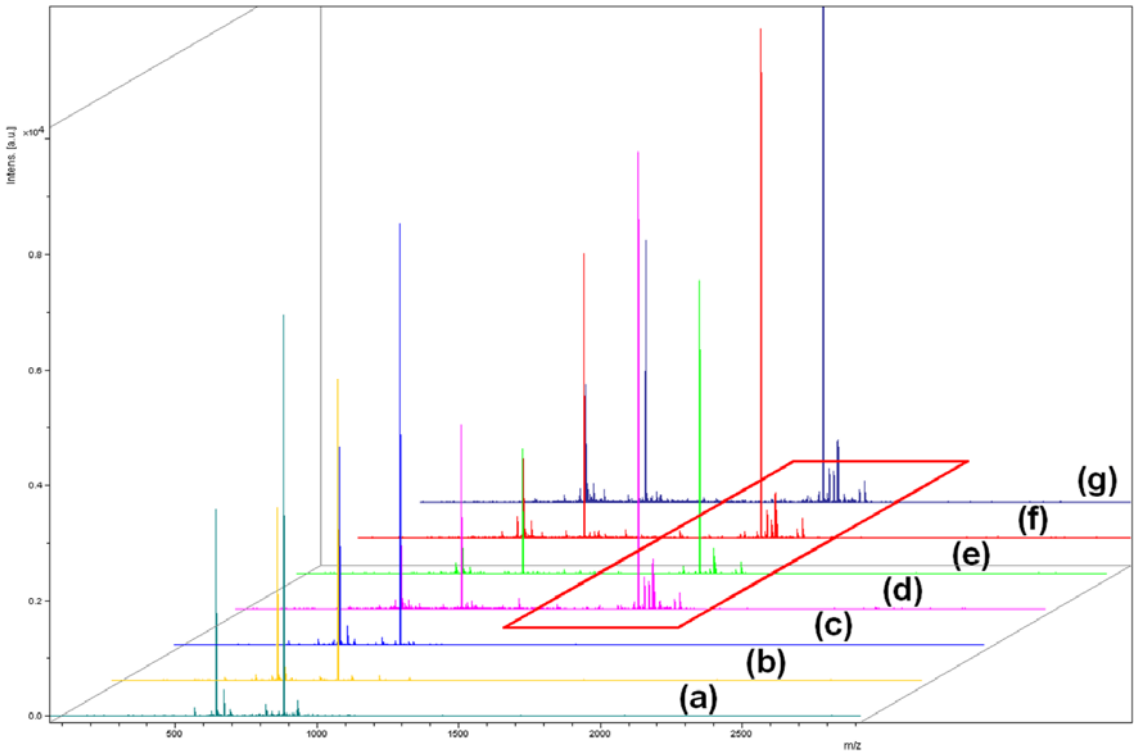

Figure 6.2. MALDI-TOF mass spectroscopy was used to accurately identify the unreacted peptide substrates as well as the crosslinked product, if any. A previously characterized APQQEA was used as an amine acceptor probe. After 60 min incubation at 37°C, (a) no crosslinking was observed when EDFGGKI was replaced by EDGFFRI (Lys → Arg); (b) no reaction was observed between EDGFFKI (MW: 855) and APQQEA (MW: 643) in the absence of tissue TGase; (c) no crosslinking between FEKDIFG (MW: 883.1) and APQQEA was detected in the absence of tissue TGase; and (d) a crosslink product (MW: 1481) between FEKDIFG and APQQEA was observed. Extensive crosslinking between APQQEA and EDGFFKI was observed at (e) 60 min, (f) 120 min, and (g) 360 min, resulting in a branch peptide of molecular weight of 1481. The boxed peak represents the reaction product with molecular weight corresponding to the crosslink of two substrate peptides.

A widely used amine donor probe for TGases, MDC (Lorand and Campbell, 1971; Lorand et al., 1979; Jeitner et al., 2001; Zhang et al., 2002), was used as a control to study the reactivity of the substrate peptide towards the tissue TGase. MDC itself can be incorporated into the enzyme-specific γ-glutaminyl or acceptor residues, blocking the lysine donors from participating in the formation of protein-to-protein crosslinks. Although the molecular size of EDGFFKI is much larger than the widely-used lysine-mimic MDC, the reactivity or conversion of the native protein-derived EDGFFKI is always comparable to, if not better than, that of the latter (Figure 6.3). It can be seen from Figure 6.3 that the incubation of the substrates with tissue TGase for an hour caused the disappearance of more than half of the substrate peptides, suggesting that the peptide is an active substrate for the enzyme. Transglutaminases are short-lived enzymes (Verderio et al., 1998; Griffin et al., 2002). Although the enzymatic reaction was allowed to proceed for 6 h, the reaction appeared to be completed within 2 h and the reaction rate decreased thereafter, probably due to the instability and inactivation of the enzyme in long time-period experiments (Kahlem et al., 1996) and also the subsequent decrease in the substrate concentration. The loss of the enzyme activity with time may also explain the incomplete conversion (70%) of the peptide substrate. Kahlem et. al. suggested the addition of fresh TGase repeatedly during the reaction to retain the enzymatic activity in long-term experiments (Kahlem et al., 1996).

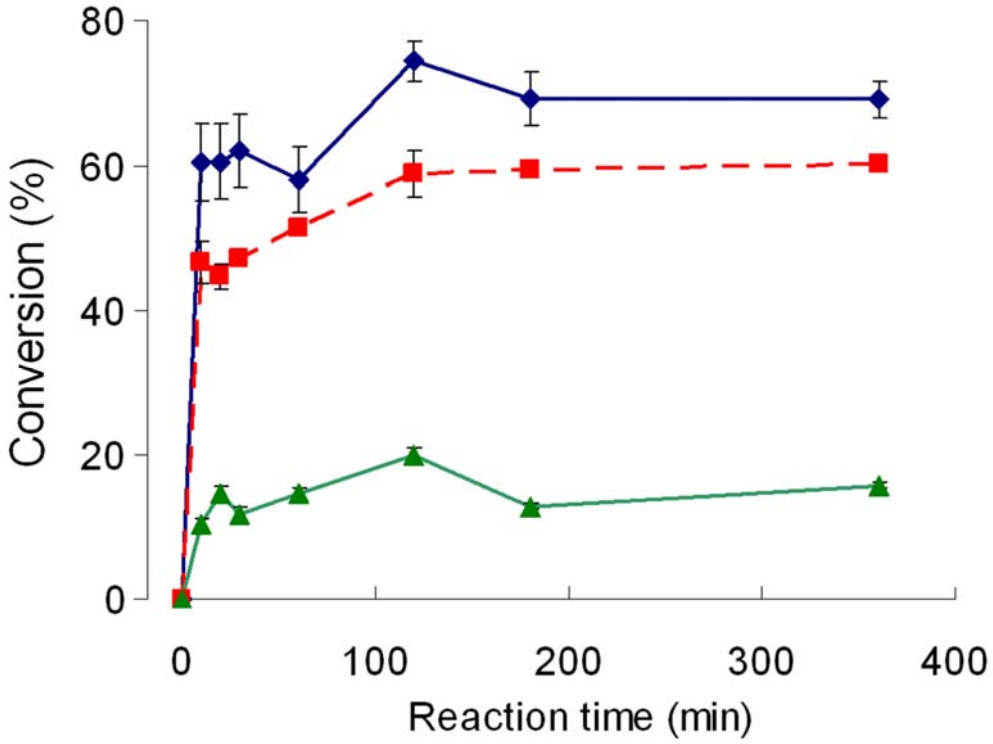

Figure 6.3. Reactivity of EDGFFKI (◇), FEKDIFG (▲), and monodansylcadaverine (MDC) (□) towards the tissue TGase-mediated crosslinking was determined based on the substrate conversion, using APQQEA as an acceptor probe. The unreacted substrates were quantified using HPLC. A control, which has a similar composition except without tissue TGase, was used as a baseline to calculate the conversion of the substrates. Data were presented as mean ± standard deviation.

Identification of the reactive glutamyl residue in APQQEA substrate

A previously characterized APQQEA was used as an amine acceptor probe. EDGFFKI substrate was shown to bind only to one of the Gln residues, resulting in the conjugation of EDGFFKI and APQQEA at 1:1 ratio (Figure 6.1 and 6.2). However, the affinity of EDGFFKI for Gln^3 and Gln^4 was not known. Two alternative substrate peptides, APQNEA and APNQEA, were used to verify whether EDGFFKI bound specifically to one Gln residue or randomly to one of the two adjacent Gln residues. It can be seen that both EDGFFKI and MDC were readily coupled to the Gln-substituted APQNEA substrate by tissue TGase (Figure 6.4 and 6.5) while neither EDGFFKI nor MDC can be enzymatically conjugated to APNQEA. It is also interesting to note that a low but significant signal for addition of two MDC to one APQQEA was detected on MALDI-TOF MS (MW: 1280) while APQQEA with one conjugated MDC (MW: 961.5) was the most common product (Figure 6.5). MS/MS analysis (Table 6.1) of APQQEA with one conjugated MDC gave a new sequence: Ala-Pro-X-Gln-Glu-Ala, where X was not a usual amino acid but probably represented the glutaminyl residue with the MDC substitution, indicating that exclusive crosslinking occurred at Gln^3 position. Based on the crosslinking of EDGFFKI and MDC to APQQEA, APQNEA, and APNQEA and the MS/MS analysis, it appears that of the two adjacent Gln residues in the APQQEA substrate peptide, the one closer to the N terminus was probably the susceptible target site while Gln^4 could serve as a secondary acyl donor only in the presence of Gln^3.

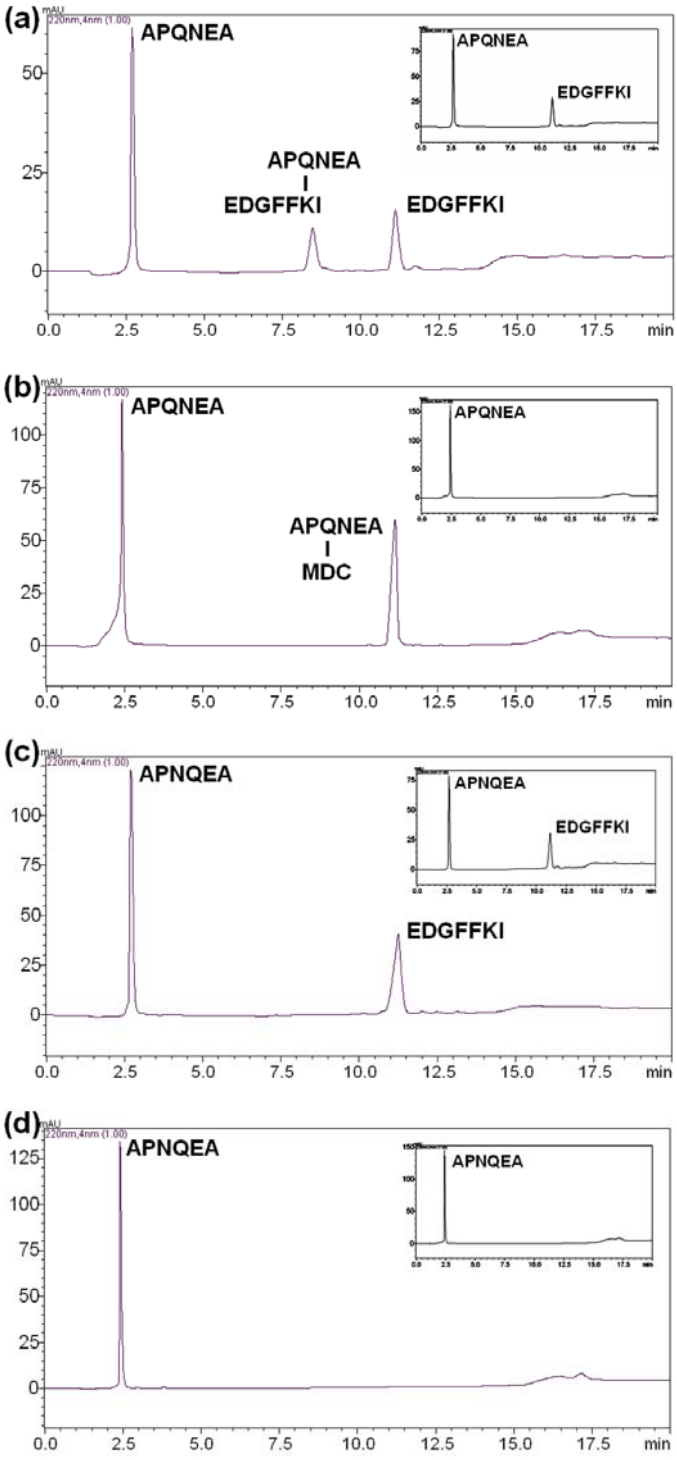

Figure 6.4. Two Q-substituted substrate peptides, APQNEA and APNQEA, were used to verify the active acyl donor site of APQQEA. HPLC chromatograms for reaction mixtures containing: (a) EDGFFKI and APQNEA, (b) MDC and APQNEA, (c) EDGFFKI and APNQEA, and (d) MDC and APNQEA, in the presence of tissue TGase after 60 min incubation at 37^{o}C. The insets are the respective control without tissue TGase. Chromatograms were collected at 220 nm for peptide amide bonds. Detection was set at 280 nm for dansylcadaverine (chromatograms not shown). Only product with conjugated dansyl groups absorbed at 280 nm.

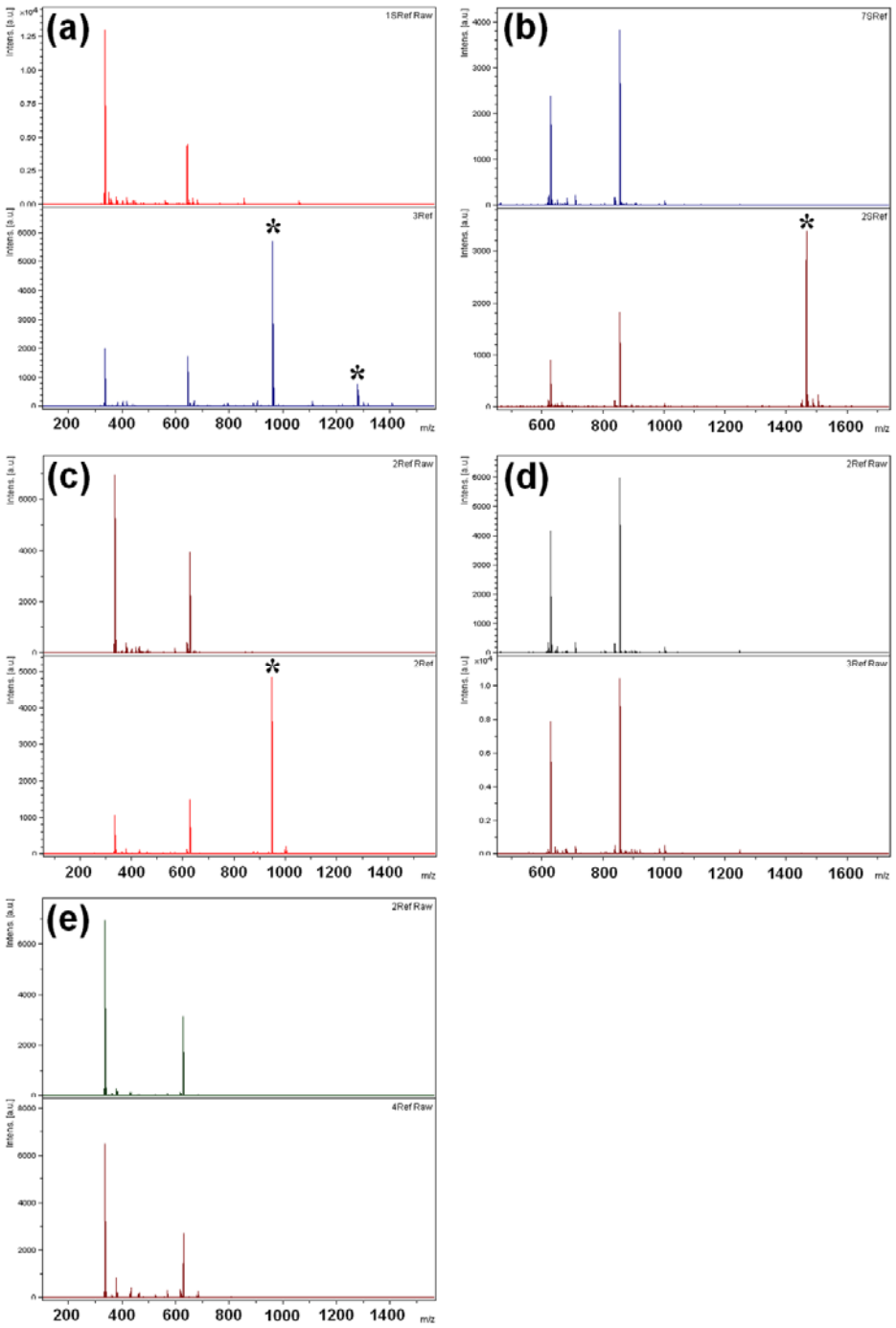

Figure 6.5. MALDI-TOF MS was used to accurately identify the crosslinking between substrate peptides mediated by tissue TGase, if any. Peaks marked with asterisk (*) denoted the crosslink products. APQQEA with one conjugated MDC (MW: 961.5) was the primary crosslink product. Low but significant amount of APQQEA with two conjugated MDC (MW:1280) was also detected (a). EDGFFKI (MW: 855) (b) and MDC (MW: 335.5) (c) were readily coupled to the mutated APQNEA (629) substrate to give a product of MW of 1467 and 947.5, respectively. Neither EDGFFKI (d) nor MDC (e) can be enzymatically conjugated to APNQEA (MW: 629). The respective control (without tissue TGase) for each sample was included above the individual spectra.

Table 6.1. Monoisotopic mass list for the peptide fragment ions obtained from the MS/MS analysis of the crosslinked product between monodansylcadaverine and APQ^{3}Q^{4}EA. X is unknown residue. The mass of X corresponds to Q^{3}-MDC.

Sequence	B series	B ions (Da)	Y series	Y ions (Da)
A	1	72.1 (not detected)	6	961.4
P	2	169.1	5	890.4
X	3	615.3	4	793.4
Q	4	743.4	3	347.2
E	5	872.4	2	219.1
A	6	943.4	1	89.1 (not detected)

Specific recognition of EDGFFKI by tissue TGase

Replacing the lysine in the sequence of EDGFFKI with an Arg residue abolished the substrate specificity (Figure 6.1 and 6.2), verifying the specific recognition of the lysine residue by the tissue TGase. A randomly ordered FEKDIFG peptide was used to examine the specific recognition of the C-terminal partial length peptide of human fibrillin-1, EDGFFKI. Interestingly, the random FEKDIFG peptide also displayed significant but lower substrate activity towards tissue TGase (Figure 6.3). The enzymatic crosslinking between FEKDIFG and APQQEA resulted in an additional peak on the HPLC chromatogram (Figure 6.1) and the change in molecular mass was observed by mass spectroscopy (Figure 6.2).

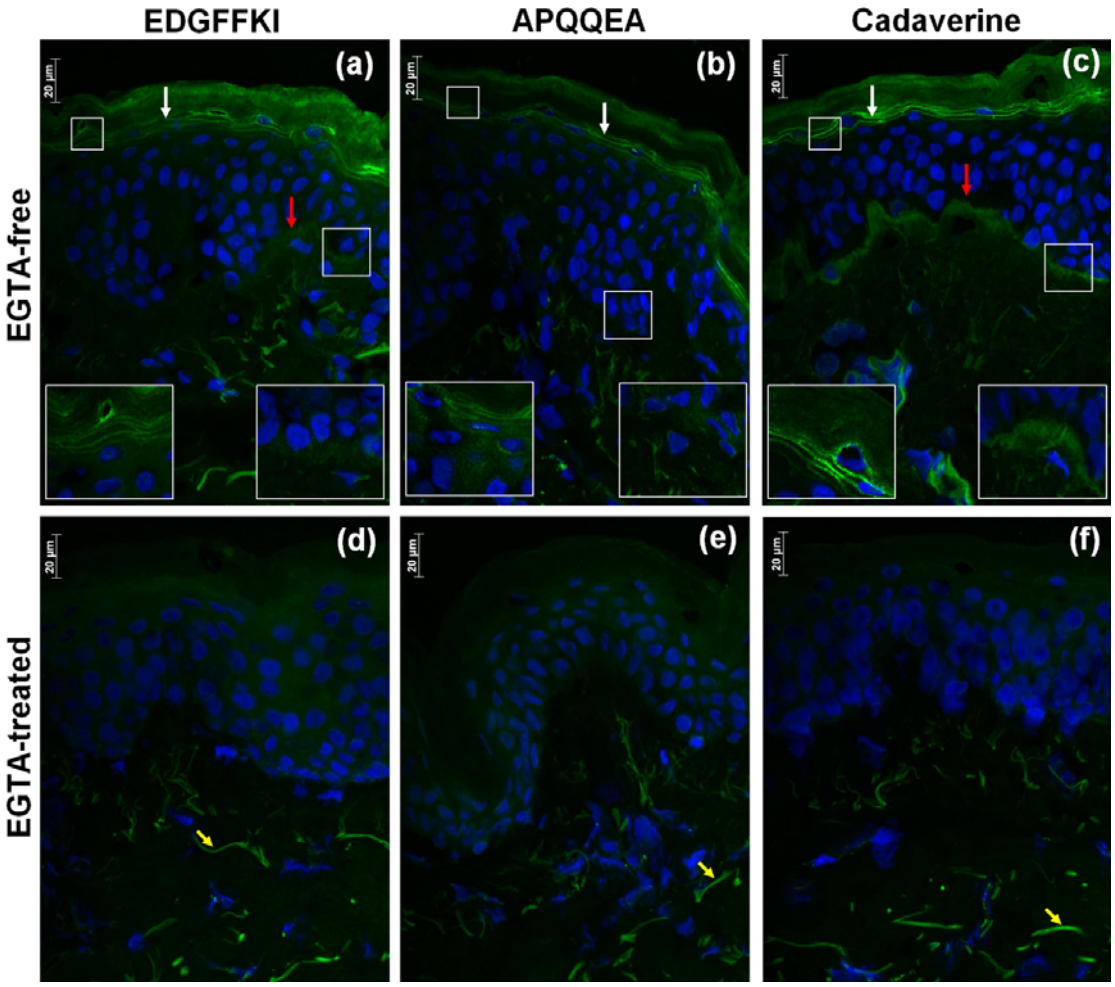

Figure 6.6. Transglutaminase (TGase) activity was detected in human skin cryostat sections by incubating the skin tissue with the biotinylated amine donor substrate biotin-EDGFFKI (a) and biotinylated amine acceptor substrate biotin-APQQEA (b) in the presence of Ca^{2+}. Biotinylated cadaverine was used as a control for EDGFFKI (c). Incorporation of the biotinylated substrates was visualized using streptavidin-DTAF. Cell nucleus was stained with DAPI (blue). Intrinsic TGase activity in human skin incorporated both EDGFFKI and APQQEA substrates peptides as well as cadaverine into stratum granulosum layer of epidermis (white arrow) and epidermal-dermal junction (red arrow). Pretreatment of skin tissues with EGTA completely inhibited the endogenous TGase activity and thus no enzymatic incorporation of EDGFFKI (d), APQQEA (e), and cadaverine (f) was observed. Picture insets in (a), (b), and (c) shows 63x magnification of stratum spongiosum (left side) and epidermo-dermal junction (right side). Yellow arrows indicate autofluorescence.

In situ localization of endogenous transglutaminase activity using EDGFFKI as a tracer peptide

Incorporation of small primary amines into tissue proteins is still the main way of detecting endogenous TGase activity (Lorand and Graham, 2003). To trace the intrinsic TGase activity, cryostat sections of human skin were incubated with biotinylated EDGFFKI and APQQEA, separately. The incorporation of these peptides to the TGase-active site was subsequently identified by streptavidin-DTAF. It can be seen from Figure 6.6 that the two biotinylated substrates were readily incorporated into the human skin sections. Biotin-EDGFFKI incorporation was detected in the stratum granulosum layer of epidermis and epidermal-dermal junction (Figure 6.6a). No activity was detected in the dermal zones. Biotin-APQQEA gave similar result after 1.5 h incubation (Figure 6.6b), but was weakly incorporated into the stratum granulosum and epidermal-dermal junction, suggesting that there may be less amine donor substrates in the skin tissue. We have also used biotinylated cadaverine as a control for the novel EDGFFKI substrate (Figure 6.6c). The intrinsic enzyme-directed labeling was similar to that obtained by using EDGFFKI, verifying the coupling of primary amines in the incorporation of biotin-EDGFFKI. The incorporation of the biotinylated EDGFFKI, APQQEA, and cadaverine into the skin tissue must have been due solely to the endogenous TGase activity. All substrates, when incubated with the skin tissue, were incorporated into the stratum granulosum and along basement membrane, but remained intact in the presence of EGTA, which completely inhibited the Ca^{2+}-dependent enzyme activity (Figure 6.6d, 6.6e, and 6.6f). Autofluorescence

was detected in dermis layer containing collagen fibers. The extracellular matrices in tissues, such as collagen, are likely to contribute to the autofluorescence emission. Incorporation of both EDGFFKI and APQQEA to the similar sites of the human skin tissue confirmed the presence of active endogenous TGase in the stratum granulosum layer.

Enzyme-directed site-specific labeling of potential amine acceptor sites in native proteins using EDGFFKI as a probe

The observation that the C-terminal partial peptide of human fibrillin-1, EDGFFKI, can serve as a lysine donor substrate for tissue TGase offered an opportunity to identify the potential amine acceptor sites in native proteins by enzyme-directed site-specific labeling. We demonstrated this function of EDGFFKI using human skin tissue as a model. Figure 6.7 showed the exogenous tissue TGase-mediated crosslinking of biotinylated EDGFFKI to both epidermis and dermis of the skin tissue. The labeling pattern by biotin-EDGFFKI (Figure 6.7a) was similar to that obtained with the biotinylated cadaverine (Figure 6.7c). One important observation was that the guinea pig liver tissue TGase-directed labeling pattern of proteins with biotinylated APQQEA (Figure 6.7b) was quite different from that obtained with the biotinylated EDGFFKI. Apparently, biotin-APQQEA substrate marked the potential donor sites, whereas the biotinylated EDGFFKI specifically labeled the acceptor substrate in the proteins. Isolating and sequencing the potential acceptor substrates for transglutaminases was not in the scope of this study. As previously noted for the *in*

situ localization of endogenous transglutaminase, the different degrees of modifications of the same tissue protein indicated that the number of reactive amine donor and acceptor sites in the native proteins may be significantly different. A comparison of the exogenous enzyme-directed labeling profiles with the biotinylated EDGFFKI and the glutamine-containing biotinylated peptides suggested that the amine donor subunits, marked with the latter probe, may have less population in the native biological system or at least in skin tissues as compared to the amine acceptor subunits, and may in some respects explain the phenomenon that only very few donor substrates have been characterized.

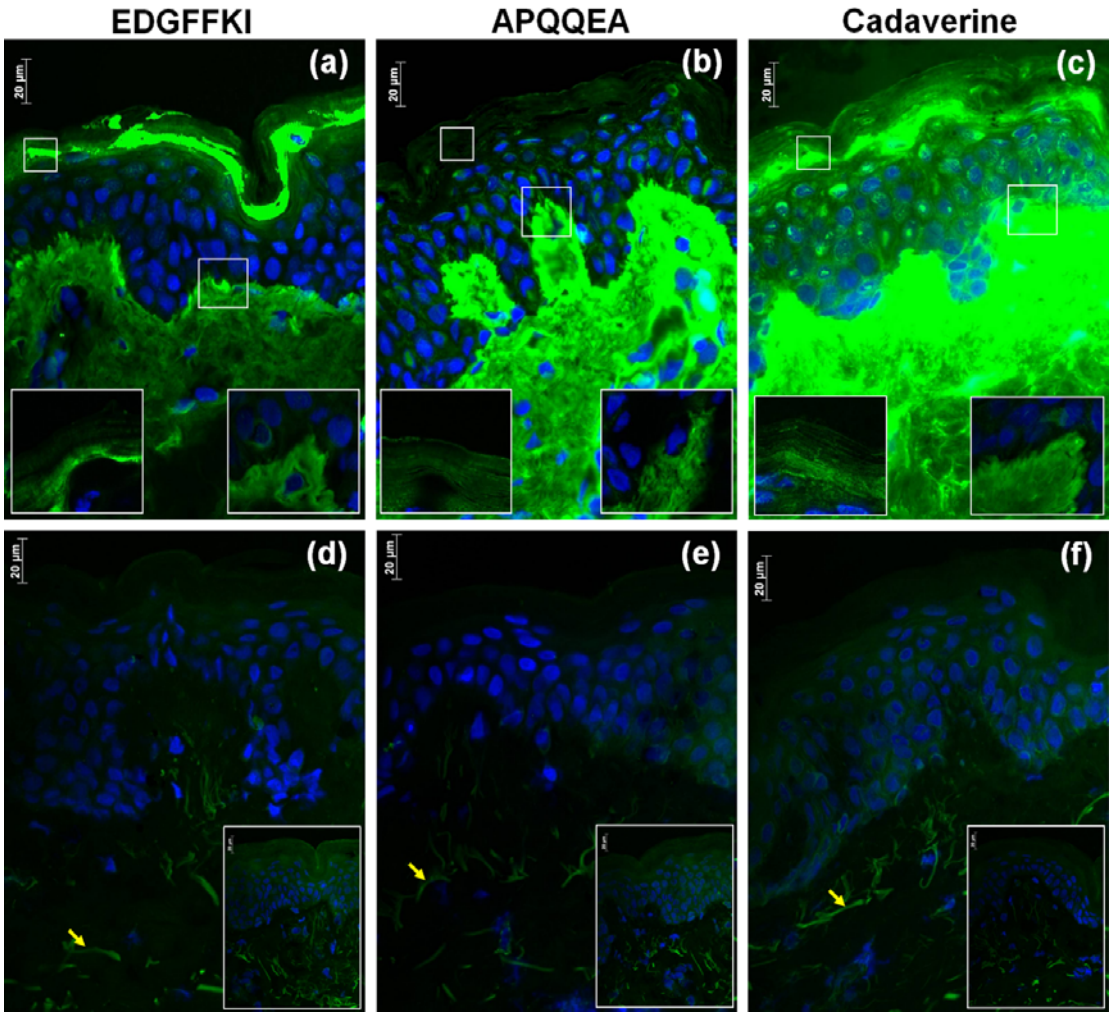

Figure 6.7. Potential amine acceptor sites in native proteins can be labeled via an enzyme-directed site-specific labeling using EDGFFKI as a probe. Human skin tissue was used as a model. Exogenous tissue transglutaminase (TGase) mediated incorporation of biotinylated EDGFFKI to the potential amine acceptor sites in both epidermis and dermis of the skin tissue (a). The labeling pattern by biotin-EDGFFKI was similar to that obtained with the biotinylated cadaverine, a control for EDGFFKI (c). Biotinylated APQQEA marked the potential amine donor sites (b). No enzymatic incorporation of substrates was observed in the presence of EGTA, in the respective control (d, e, and f). Picture insets in (a), (b), and (c) shows 63x magnification of stratum spongiosum (left side) and epidermo-dermal junction (right side) while the picture insets in (d), (e), and (f) indicate residual endogenous TGase activity after irreversible inhibition by iodoacetamide treatment. Green and blue fluorescence indicate the enzymatically incorporated DTAF-tagged EDGFFKI, APQQEA, or cadaverine and cell nucleus, respectively. Yellow arrows indicate autofluorescence.

6.4 Discussion

Thus far, only a few amine donor substrates for tissue TGase have been characterized (Table 2.3). One common observation in many studies was that most substrates were located at the accessible terminal extensions of the native proteins (Mulders et al., 1987; Groenen et al., 1992 and 1994; Lorand et al., 1992; Merck et al., 1993). For example among the many lysine residues present in αB-crystallin, the C-terminal lysine residue was found to serve as the sole amine donor for TGase (Groenen et al., 1992; Lorand et al., 1992). These limited data obviously suggested that the location of substrate lysine residues for TGase should be accessible to the enzyme.

The structure and organization of fibrillin-1 are poorly understood because of its complexity, and many details are still undefined. Because of the large size and bulky nature of fibrillin-1, it has been necessary to explore individual region of the protein. The recent observations that the C-terminal arm of this protein contained a cell binding site available for cell attachment (Ritty et al., 2003) and was accessible for enzymatic cleavage (Raghunath et al., 1999) offer an opportunity to search for the potential amine donor substrates from this region. On this basis, we speculated that in fibrillin-1, a lysine at position 2805 in the C-terminus, which extends from the calcium-binding EGF-like domain of this protein, is the amine donor site for tissue TGase.

The identification of high affinity interactions between EDGFFKI and a previously reported amine acceptor, APQQEA, confirms this region of human fibrillin-1 as an amine donor site. However, much more data from diverse biological systems is required to show whether it is a rule or an exception that most amine donor substrates of fibrillin-1 must be also located in the terminal extensions. Extensive studies on substrate requirements for TGases have demonstrated that the presence of a glycine or aspartic acid residue before the lysine donor had a significant adverse effect on the substrate reactivity (Groenen et al., 1994; Grootjans et al., 1995). Replacing a hydrophobic residue, such as leucine and phenylalanine, for a glycine residue preceding the amine donor lysine considerably enhanced the substrate activity toward the enzyme (Grootjans et al., 1995). It is noteworthy that the sequence of EDGFFKI, with Phe residues directly preceding the substrate lysine, is accord with the pattern of preference established and observed for these limited number of characterized amine donor substrates. Furthermore, the C-terminal EDGFFKI sequence of fibrillin-1 is conserved in human, murine, bovine, and porcine, except an alteration in the position 2801 (Asp → Asn) of the latter two (Table 6.2). The preservation of the C-terminus of fibrillin-1 in higher vertebrates, which encloses the TGase crosslinking sequence, implies a specific function of this domain in these species. This could be related to its role in elastic fiber formation and tissue stabilization.

Table 6.2. A comparison of residues 2791-2806 of C-terminal of fibrillin-1 from different species (Biery et al., 1999).

Protein	Species	Sequence
Fibrillin-1	Human	-NRYLIESGN**EDGFFKI**-
	Murine	-NRYLIESGN**EDGFFKI**-
	Bovine	-NRYLIESGN**ENGFFKI**-
	Porcine	-NRYLIESGN**ENGFFKI**-

Hohenadl and co-workers reported that both Gln^3 and Gln^4 of APQQEA substrate peptide were the amine acceptor sites for TGases, with no preference for either of these Gln residues but modified only one of them in each molecule (Hohenadl et al., 1995). No exclusive modification of one of the adjacent residues has been observed (Berbers et al., 1984; Simon and Green, 1988; Hohenadl et al., 1995). However, we have shown different observations in our study with MDC and EDGFFKI as an amine donor substrate. MDC showed tendency to bind Gln^3 specifically even though a low but significant amount of MDC was found to also conjugate Gln^4 and thus modified both Gln residues simultaneously in one APQQEA molecule. EDGFFKI substrate bound preferentially to one specific Gln residue in APQQEA. Unlike the mutant APQNEA, the mutated acceptor probe, APNQEA, did not accept both EDGFFKI and MDC to form γ-glutamyl-ε-lysine isopeptide bonds. In summary, the result indicated that the first of the two adjacent Gln residues was

probably the preferred target of enzymatic modification. The result was accord with the observation that only the first Gln residue of the N-terminal sequence of fibronectin, EAQQIV, was an amine acceptor site (Parameswaran et al., 1990). It appears that no consensus on the preferential pattern of conjugation of amine donor substrate to adjacent glutamyl residues has been reached thus far. Most previous characterizations were done by using synthetic lysine mimics, such as MDC and putrescine, as an amine donor substrate. The modes of interactions of TGases with small primary amines and with native protein-derived substrates are likely to be different. Steric hindrance could be one possible reason that EDGFFKI could not be conjugated to two adjacent Gln residues in one acceptor molecule simultaneously as MDC did. However, although unrevealed, it cannot be excluded that the preferential and specific coupling of EDGFFKI to the first Gln residue of APQQEA was probably due to the native characteristic and affinity of the two native protein-derived substrates. The result may indicate that identification of more naturally occurring substrate peptide, rather than synthetic lysine mimic, for sorting out the γ-glutamine crosslinking sites in native biological system is necessary. More studies remain to be done to unveil the mechanism of the selective coupling of native peptide substrate to a specific position of the amine acceptor substrate.

Although EDGFFKI patterned on the C-terminal sequence of human fibrillin-1 has been shown to function as a tissue TGase substrate, it has been demonstrated that many scattered Lys residues in peptides or small proteins may also

act as amine donors. Although none of the characterized reactive lysine residues in proteins is preceded by acidic amino acid residues such as glutamate and aspartate (Groenen et al., 1994; Grootjans et al., 1995), it clearly and unexpectedly appears that a random sequence of FEKDIFG did also react with the amine acceptor probe, strengthening the common notion that TGases are less selective toward amine donor lysine residues. But in native proteins, the nature of the neighboring residues and the protein conformation may present appreciable influence on the reactivity of a lysine residue, and thus some lysine residues are greatly preferred to others. This conjecture is supported by previous studies on substrate requirements in native protein using a series of recombinant protein mutants (Grootjans et al., 1995). Our results also demonstrated that the random FEKDIFG was not as attractive to TGases as the naturally occurring EDGFFKI substrate peptide. Little is known about the manner in which the TGases operate on macromolecular substrates in biological systems. The conformational factors may play an important role in the enzyme-substrate interaction, and thus causing differences in substrate specificities. Further studies are required to reveal the possible modulating effects of the protein conformation in comparison with the small model substrate.

As TGases participate in various cellular and extracellular processes, it is thus expected that perturbations in the enzyme activity, through genetic deficiencies, autoimmune disorders, or abnormal expression, are closely associated with some human diseases (Huber et al., 1995; Benedetti et al., 1996; Lorand and Graham, 2003).

Therefore, identification of suitable probes to assess the endogenous TGase activity in tissues is important and is of high medical values in disease diagnosis. The identification of a short peptide substrate containing a lysine donor and an easily recognizable reporter group made it possible to detect the intrinsic TGase activity in tissues as demonstrated in this study. Use of such biotinylated lysine donor substrate could also aid in an enzyme-directed site-specific labeling of potential amine acceptor substrates for TGase in skin tissues as well as other biological systems.

6.5 Conclusion

It has been shown that the C-terminal EDGFFKI sequence spanning residues 2800-2806 of human fibrillin-1 is an active lysine substrate and displaying good donor substrate reactivity towards tissue TGase. Identification of more native amine donor as well as acceptor substrates will eventually contribute to a better understanding of the *in vivo* TGase-mediated crosslinking in relation to their biological functions and diseases. The use of short naturally-derived substrate peptides could also lead to tailoring novel protein-like crosslinkable biomaterials. From the present result, it appears that some works remain to be done before the exact enzyme-substrate interaction and recognition under normal and pathological conditions will be fully understood.

CHAPTER 7

ENZYMATICALLY CROSSLINKED COLLAGEN-MIMETIC DENDRIMERS THAT PROMOTE INTEGRIN-SPECIFIC CELL ADHESION

The primary interest of this thesis is to develop an enzymatically crosslinkable collagen-like biomaterial, namely a biomimetic collagen that resembles the native molecular architecture and cell binding activity of collagen. In the previous chapters, we have synthesized and characterized collagen-mimetic peptides capable of assembling into stable triple-helical structures and exhibiting cell binding activity. Additionally, we have characterized amino donor and acceptor sites for tissue transglutaminase (TGase). With these as the foundation, we now explore how the structural domain, cell binding motif, and the enzyme crosslinking sequence can be integrated and conjugated to a dendrimer to engineer collagen-mimetic dendrimers that exhibit enhanced triple-helical stability, cell binding activity, and substrate specificity for tissue TGase-mediated crossliking. Collagens are a diverse family of the ECM, found generally crosslinked *in vivo*. This study may contribute to bringing the biological function and characteristic of the artificial collagen a little, if not significant, closer to that of the natural collagen.

This chapter is modified from Khew, S.T., Yang, Q.J., Tong, Y.W. (2008) *Biomaterials*, In press.

7.1 Introduction

Inspired by the functional significance of collagen in nature and its remarkable physiological roles, many scientists are working toward realizing an artificial collagen using different strategies and designs. Although works toward realizing collagen-like peptide supramolecules has been greatly achieved, especially in forming higher order molecular architectures, the biological properties of these collagen mimics are still some distances away from those of the native collagen. One important aspect concerning the assembly of the ECM protein *in vivo* is closely related to the enzyme-mediated crosslinking that plays a significant role in stabilizing the ECM proteins thus cellular activity. The crosslinking of the ECM proteins, such as collagen, to form stable supramolecular association capable of serving as protective and supporting structures is a common phenomenon in biological system. Collagens are a diverse family of the ECM, found generally crosslinked *in vivo*. We speculate that protein crosslinking, a common physiological phenomenon, may also play an important role in cellular recognition process. While many different collagen mimics have been successfully synthesized (Goodman et al., 1998; Koide, 2005), none have incorporated the enzymatic crosslinking characteristic into the synthetic collagen. In this study, we focused on establishing a molecular strategy to engineer a functional "biomimetic collagen" that exhibits stable collagen-like molecular architecture, cell binding activity, and substrate specificity for tissue TGase. This study may contribute to taking us one step further toward realizing an artificial collagen.

7.2 Experimental section

Peptide synthesis

All peptides, including Ala-Pro-Gln-Gln-Glu-Ala (APQQEA), Glu-Asp-Gly-Phe-Phe-Lys-Ile (EDGFFKI), $(GPO)_3GFOGER(GPO)_3$ (CMP), $(GPO)_3GFOGER(GPO)_3APQQEA$ (CMP-Q), and $(GPO)_3GFOGER(GPO)_3EDGFFKI$ (CMP-K), where O represents hydroxyproline, were synthesized in-house on an automated Multipep peptide synthesizer (Intavis) and purified as described previously (see "Experimental section", Chapter 3). The purity of all peptides was greater than 90% according to analytical reverse phase HPLC. The mass of the peptides was examined using a Bruker AutoFlex II MALDI-TOF MS.

Synthesis of collagen-mimetic dendrimers

A generation 1.5 PAMAM dendrimer (PAMAM G1.5) (Sigma-Aldrich) containing 16 sodium carboxylate groups (COONa) was used to synthesize PAMAM-CMPs conjugates. The COONa groups of the PAMAM G1.5 were converted to free carboxylic groups (COOH) using TFA (1 mol COONa: 1.5mol TFA). The salts were removed by column chromatography using pre-packed Isolute Si (20 g) column (International Sorbent Technology, Mid Glamorgan, UK) with 70% methanol as mobile phase. The collected PAMAM G1.5 was concentrated using rotary evaporator and lyophilized and redissolved in water. The COOH groups of the PAMAM G1.5 were activated using freshly prepared *N*-ethyl-*N*'-(3-dimethylaminopropyl)

carbodiimide (EDC)/ *N*-hydroxysulfosuccinimide (NHS) solution (1 mol PAMAM G1.5 (≡16 mol COOH): 16 mol EDC: 16 mol NHS). To 1 mol of activated PAMAM G1.5 (≡16 mol COOH), 24 mol of CMP-K or CMP-Q was added and the reaction was allowed to proceed for 12 h at room temperature with occasional shaking. The product, PAMAM G1.5-CMP-Q (CMD-Q) or PAMAM G1.5-CMP-K (CMD-K) was purified through dialysis of molecular weight cut off point of 10 kDa to remove unreacted peptides before passing through reverse phase high performance column chromatography (HPLC) for purification as described previously.

Biophysical studies

CD measurements were performed on a J-810 spectropolarimeter (Jasco) using a 1 mm quartz cuvette (Hellma). All samples were dissolved in water (0.25 mg/ml) and stored at 4 ^{o}C for at least 3 days before the test to allow for proper equilibration of triple-helical conformation. The cuvette was filled with 200 μL of samples for each measurement. The CD spectra were obtained by continuous wavelength scans (average of three scans) from 250 to 180 nm at a scan speed of 50 nm/min.

The temperature-dependent UV absorbance of the samples was measured on a Cary 50 Bio UV Spectrophotometer (Varian) equipped with a peltier temperature controller (Quantum Northwest) (Kajiyama et al., 1995; Feng et al., 1996). Prior to any measurements, all samples were equilibrated at the initial temperature for at least 24 h. The samples were allowed to equilibrate at least 15 min until the UV absorbance

was time-independent at each subsequent temperature point. Data were collected at 225 nm. Values of melting point temperature (T_m) were determined from the reflection point in the transition region. All samples were dissolved in water at 0.25 mg/ml.

Enzymatic crosslinking of collagen-mimetic dendrimer

A reaction volume (25 μL) contained 0.1 mM CMD-Q, 0.1 mM CMD-K, 100 mM Tris/HCl (pH 7.4), 10 mM $CaCl_2$, and 0.5 *U*/ml guinea pig liver tissue TGase (Sigma-Aldrich). A control reaction contained similar compositions, except with no tissue TGase added. The reaction cocktail was incubated at 37 °C for 2 h. The crosslinking was observed using MALDI-TOF MS.

Cell culture and biological assays

L929 fibroblast cells and Hep3B liver cells (ATCC) were cultured separately in Dulbecco's modified Eagle's medium (Gibco, Grand Island, NY) supplemented with 10% fetal bovine serum (FBS) (Hyclon, Logan, UT), 110 mg/L sodium pyruvate (Sigma-Aldrich), 1% antimycotic solution (Sigma-Aldrich) and 1% non-essential amino acids (Sigma) (hereinafter called DMEM) as described previously. Cytotoxicity assay, cell adhesion assay, competitive inhibition assay, and immunofluorescence staining were done as described previously. All samples were assayed in triplicate

7.3 Results and discussion

Collagen-mimetic dendrimers

The collagenous domains constitute almost the entire mass of the fibrillar collagens and are usually intermingled with non-collagenous regions. The specific array of collagenous and non-collagenous domains in nature hints several important considerations toward realizing a biologically active artificial collagen: the roles of the structural domain and the non-collagenous domain and the importance of the intermingling of the two. Collagenous domains within the ECM are unique for their stable tertiary structure, triple helix, which may play a role in the preservation of the protein activity. The non-collagenous domains normally contain biologically relevant epitopes, including cell binding sequences as well as enzyme crosslinking sites. The complexation of the two domains may be of key contribution to the complete functions and activity of the natural proteins *in vivo*. Thus, presentation of these epitopes in the design of collagen mimics may further improve their properties and bring them a little closer to that of the native one. Herein, we reported the synthesis of collagen-mimetic dendrimers by conjugating collagen-mimetic peptides (CMP-Q or CMP-K) onto a PAMAM G1.5 dendrimer (Figure 7.1). The dendrimer was used as a template to enhance intramolecular folding thus stabilizing the triple-helical structures. The cell binding sequence (GFOGER) was sandwiched between the structural domains, repeating Gly-Pro-Hyp triplets, whereas the Q-donor (APQQEA) or the K-donor (EDGFFKI) substrate peptides were placed at the extension of the C-termini

of the collagen-mimetic peptides, exposed to solvents as commonly observed for the naturally occurring tissue TGase substrates (Mulders et al., 1987; Groenen et al., 1992 and 1994; Lorand et al., 1992; Merck et al., 1993).

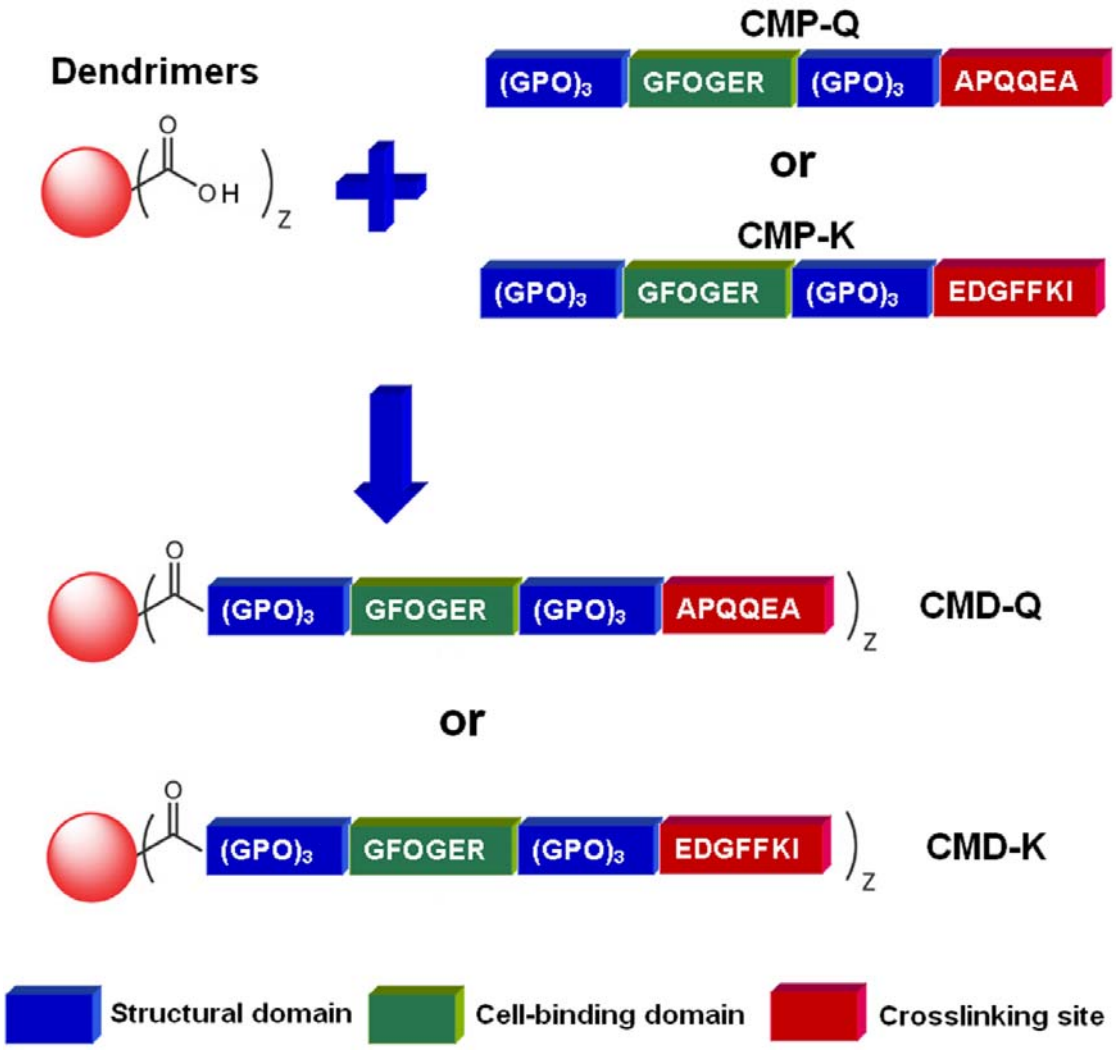

Figure 7.1. Collagen-mimetic peptides (CMP-Q or CMP-K) supplemented with a cell binding sequence (GFOGER) and the identified EDGFFKI or APQQEA substrate sequence were conjugated onto a PAMAM dendrimer to create a crosslinkable "biomimetic collagen". Z denotes the number of peripheral functional groups of the dendrimers available for tethering peptides covalently in a close proximity thus promoting intermolecular interactions and folding.

Based on the MS characterization (Figure 7.4b and 7.4c), it was found that the product obtained from CMD-Q and CMD-K synthesis was primarily PAMAM G1.5-$(CMP\text{-}Q)_6$ (MW: ~20 kDa) and PAMAM G1.5-$(CMP\text{-}K)_7$ (MW: ~24 kDa), respectively. Higashi and co-workers reported previously that the conjugation of short peptides onto a generation 3 PAMAM dendrimer was incomplete and limited which they attributed to the steric bulkiness of the oligopeptides (12 amino acid long) (Higashi et al., 2000). Similarly, the peripheral carboxylic groups of PAMAM G1.5 were not fully conjugated with the collagen-mimetic peptides probably because of the large size of the peptides (CMP-Q: 2906 Da; CMP-K: 3119 Da) thus resulting in steric hindrance. The propensity of the peptides to self-assemble into triple-helical structures may also contribute to lower conjugation of peptides onto the dendrimers. Some works remain to be done to improve the conjugation of long peptides onto the densely packed peripheral functional groups of the dendrimers.

Nevertheless, both CMD-Q and CMD-K were found to exhibit enhanced triple-helical stability (see Table 7.1). The conformation of the collagen-mimetic dendrimers and peptides was characterized using CD spectroscopy. $(Pro\text{-}Hyp\text{-}Gly)_{10}$ was used as a stable prototype of a triple helix while $(Pro\text{-}Pro\text{-}Gly)_3$ and calf-skin collagen were used as a negative control and collagen model, respectively. It can be seen from Figure 7.2 that the CD spectra of both CMD-Q and CMD-K were diagnostic of a collagen-like triple-helical conformation, with a positive peak at approximately 225 nm and a large negative trough near 200 nm, similar to natural

collagen and $(Pro\text{-}Hyp\text{-}Gly)_{10}$. We have reported previously that the self-assembling open-chain $(GPO)_3GFOGER(GPO)_3$ (CMP') exhibited stable triple-helical structure at room temperature (Khew et al., 2007; Khew and Tong, 2007b). In this study, we found that both CMP-Q and CMP-K were also triple-helical as can be seen from their collagen-like CD spectra (Figure 7.2c and 7.2d). The establishment of triple-helical conformations by CD spectral band positions was also supported by comparing the CD spectra of CMD-Q and CMD-K with that of native collagen after thermal denaturation. At elevated temperature, a significant decrease in the intensity of both positive and negative peaks of calf-skin collagen was observed (Figure 7.2e), resulted in a CD spectrum similar to that of $(Pro\text{-}Pro\text{-}Gly)_3$ (Figure 7.2f), indicating a thermal transition from a higher order structure to an unfolded conformation. A similar trend was observed for the CD spectra of both CMD-Q and CMD-K at higher temperatures. Conversely, $(Pro\text{-}Pro\text{-}Gly)_3$ displayed a CD spectrum of polyproline II-like structure characterized by the shallow peak at around 200nm and the lack of the positive peak (Feng et al., 1996; Kwak et al., 2002). The patterns of these CD spectra are similar to that of the denatured collagen as given in Figure 7.2e, which is known to have no triple-helical conformation in solution.

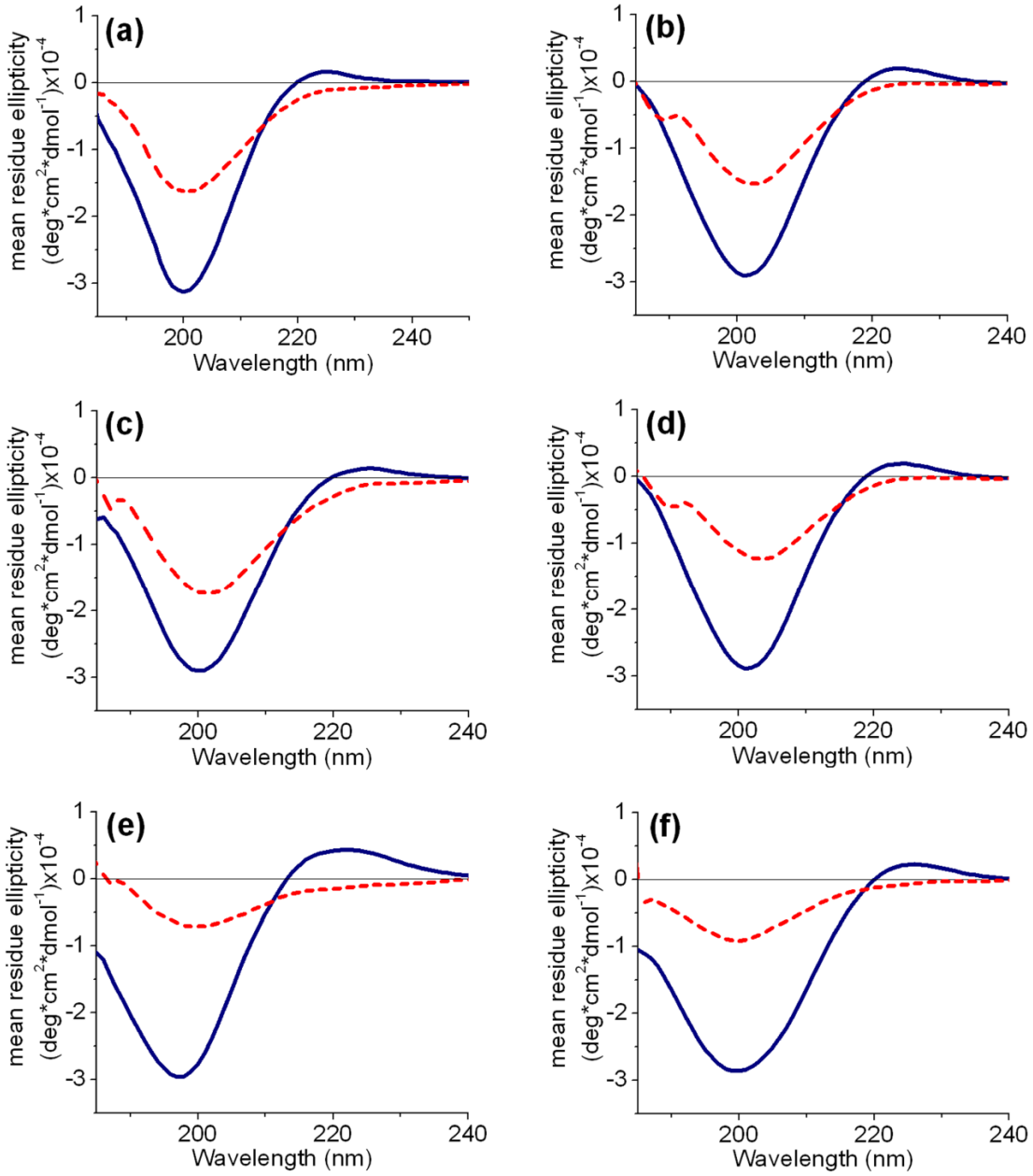

Figure 7.2. CD spectra of (a) CMD-Q, (b) CMD-K, (c) CMP-Q, (d) CMP-K, and (e) collagen obtained at room temperature (solid line) and 80 ^{o}C (segmented line); CD spectra of (f) $(Pro\text{-}Hyp\text{-}Gly)_{10}$ (solid line) and $(Pro\text{-}Pro\text{-}Gly)_3$ (segmented line) obtained at room temperature. Samples were at 0.25 mg/ml in water.

Rpn values denote the ratio of positive peak over the negative peak intensity in the CD spectra (Feng et al., 1996a and 1996b). The Rpn values of the collagen-mimetic dendrimers and peptides, ranging from 0.09 to 0.11 (see Table 7.1), were found to be comparable to that of calf-skin collagen (0.12) and $(Pro\text{-}Hyp\text{-}Gly)_{10}$ (0.10), suggesting that the molecules were in triple-helical form. Furthermore, triple helices melt in a highly cooperative manner as the structures are stabilized by both intra- and interstrand hydrogen-bonding water networks (Bella et al., 1994 and 1995; Jefferson et al., 1998) and thus can be distinguished from the polyproline II-like and nonsupercoiled structures based on the thermal melting characteristic. The melting transition curves are given in Figure 7.3. The midpoint of the transition was taken as the melting point temperature (T_m) and is presented in Table 7.1. The observation of a cooperative transition curve together with a proper CD spectrum is indicative of the presence of stable triple-helical conformation (Feng et al., 1997). All samples, except $(Pro\text{-}Pro\text{-}Gly)_3$, displayed a cooperative melting pattern thus confirming the presence of the triple-helical structures. Higashi et. al. and Goodman et. al. have also reported on the efficacy of the PAMAM dendrimers in enhancing the peptide folding into higher order structures (Higashi et al., 2000; Kinberger et al., 2006). Similarly, the use of PAMAM dendrimers to conjugate CMP-Q and CMP-K also resulted in a more stable collagen-like molecular architecture. The stabilizing effect of the PAMAM dendrimers in promoting the assembly of triple-helical structures of the short peptide sequences was evidential, based on the increase of T_m of CMD-Q and CMD-K when compared to their non-templated counterparts, CMP-Q and CMP-K.

Table 7.1. Melting point temperatures (T_m) of the collagen-mimetic dendrimers and their counterparts, open-chain collagen-mimetic peptides, as determined by temperature-dependent UV absorbance measurement at 225 nm. Cell recognition site (GFOGER) corresponding to residues 502-507 of the collagen α1 (I) is shown in bold, whereas the tissue TGase substrate peptide sequences (Q-donor or K-donor) are underlined.

Protein/Peptides	Sequence[a]	Rpn[b]	T_m (oC)
X-CMD	Cross-linked CMD-Q + CMD-K	0.09	38
CMD-Q	PAMAM G1.5-[(GPO)$_3$**GFOGER**(GPO)$_3$<u>APQQEA</u>]$_6$	0.10	34
CMD-K	PAMAM G1.5-[(GPO)$_3$**GFOGER**(GPO)$_3$<u>EDGFFKI</u>]$_7$	0.11	38
CMP-Q	(GPO)$_3$**GFOGER**(GPO)$_3$<u>APQQEA</u>	0.09	24
CMP-K	(GPO)$_3$**GFOGER**(GPO)$_3$<u>EDGFFKI</u>	0.11	27
CMP'	(GPO)$_3$**GFOGER**(GPO)$_3$	0.09	25
CMP''	**GFOGER**GGG	-	No transition
(Pro-Pro-Gly)$_3$	(PPG)$_3$	-	No transition
(Pro-Hyp-Gly)$_{10}$	(POG)$_{10}$	0.10	60
Collagen	Calfskin collagen	0.12	38

[a]Standard one letter code is used to express amino acid sequences, except where noted. O represents Hydroxyproline residue. [b]Rpn denotes the ratio of positive and negative peak intensities in the CD spectra.

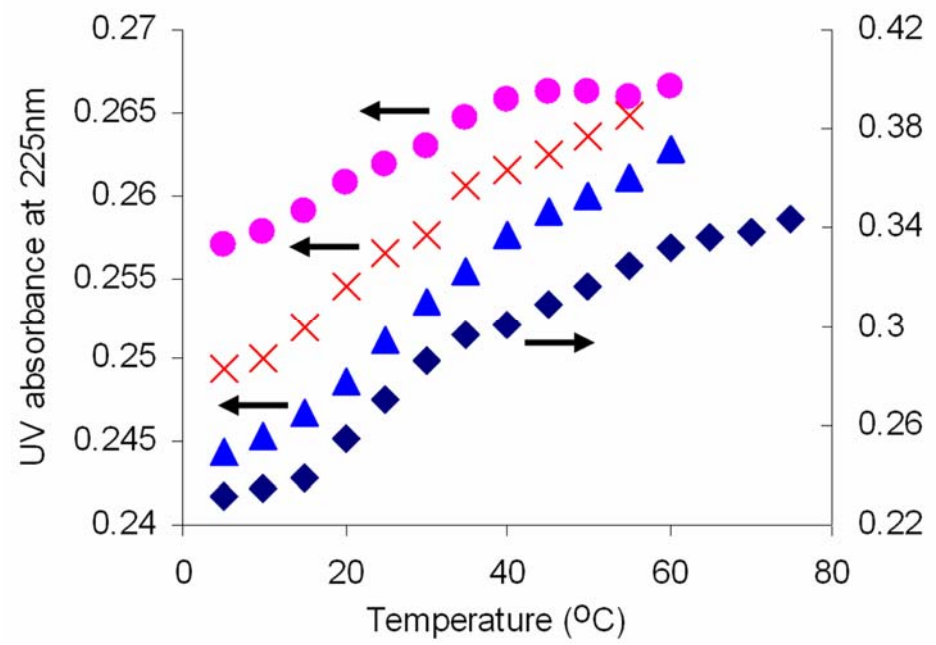

Figure 7.3. Melting transition curves of CMD-Q (▲), CMD-K (◆), CMP-Q (**X**), and CMP-K (●). Samples were at 0.25 mg/ml in water.

Tissue transglutaminase-catalyzed crosslinking of collagen-mimetic dendrimers

Several lines of evidences show that tissue TGase acts physiologically in the stabilization of the ECM by crosslinking numerous ECM proteins, such as fibronectin (Fesus et al., 1986), collagen (Bowness et al., 1987; Kleman et al., 1995), and laminin (Aeschlimann et al., 1992). The formation of crosslinks between collagen α-chains (Jelenska et al., 1980) and the crosslinking of fibronectin to specific sites in collagen types I and III (Mosher and Schad, 1979; Mosher et al., 1980) imply an important role of transglutaminase in the organization of supramolecular structure of collagen. While many different collagen mimics have been successfully synthesized and characterized (Goodman et al., 1998; Koide, 2005), none have incorporated the enzymatic crosslinking characteristic into these synthetic collagen. In this study, we have

identified a novel amine donor substrate sequence (EDGFFKI) for tissue TGase from the C-terminal of human fibrillin-1 using a previously characterized amine acceptor substrate peptide (APQQEA), derived from human osteonectin (Hohenadl et al., 1995). The specific substrate peptides for tissue TGase were integrated into the molecular design of collagen-mimetic dendrimers to tailor crosslinkable collagen-like biomaterials. It can be seen from Figure 7.4a that the collagen-mimetic dendrimers supplemented with the specific enzyme substrates, CMD-Q and CMD-K of molecular weight of approximately 20 kDa and 24 kDa (Figure 7.4b and 7.4c), respectively, were enzymatically crosslinked into macromolecules of higher molecular weight. Both CMD-Q and CMD-K remained intact in the control reaction (without tissue TGase) confirmed that the observed crosslinks were entirely a result of tissue TGase-catalyzed reaction (see inset of Figure 7.4a). The crosslinked product (hereinafter denoted as X-CMD) was found to remain in triple-helical conformation with T_m (38 ^{o}C) similar to that of natural collagen and CMD-K (Figure 7.4d and 7.4e). The melting of X-CMD at elevated temperature (80 ^{o}C), as indicated by the decrease in both positive and negative peak intensities on CD spectroscopy, further confirmed the presence of the collagen-like molecular architecture in the X-CMD solution. The preservation of the collagen-like triple-helical structure is a crucial prerequisite for X-CMD to serve as a potential cell adhesion matrix material as most natural proteins fold into a well-defined structure to implement their biological functions.

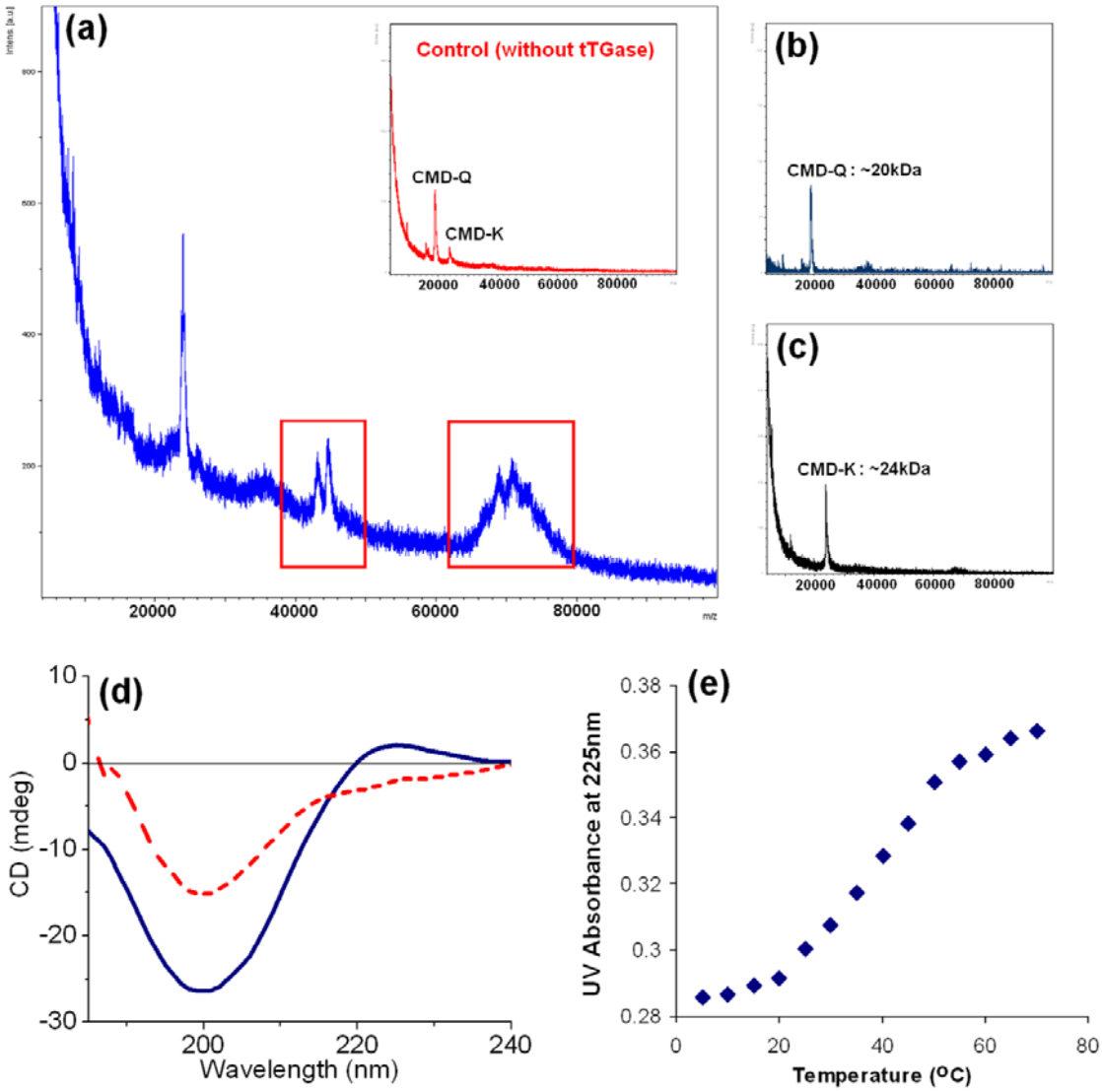

Figure 7.4. (a) Tissue transglutaminase (TGase)-catalyzed crosslinking between CMD-Q and CMD-K resulted in additional peaks, corresponding to crosslink product, on MALDI-TOF MS (boxed regions). No crosslinking was observed in the control reaction (without tissue TGase) (inset of a), confirming that the coupling between the two substrates was a tissue TGase-catalyzed reaction; (b) MADLI-TOF mass spectrum of CMD-Q; (c) MALDI-TOF mass spectrum of CMD-K; (d) the crosslink product, X-CMD, exhibited collagen-like CD spectrum (solid line) with a large negative peak at approximately 200 nm and a large positive at 225 nm. A significant decrease of CD peak intensities was observed at elevated temperature (80 ^{o}C) (segmented line); (e) the crosslinked product, X-CMD, displayed a cooperative thermal transition thus confirming the presence of triple-helical structures.

Cytotoxicity

All peptides and collagen-mimetic dendrimers were assessed for their cytotoxicity before any other assay. The viability of cells incubated in serum-free DMEM (blank) was taken as the 100% reference level. No significant changes were observed between cell viability (Figure 7.5) and cell morphology (result not shown) after 24 h and 72 h of incubation in the presence of the samples tested. The result was indicative of noncytotoxic responses.

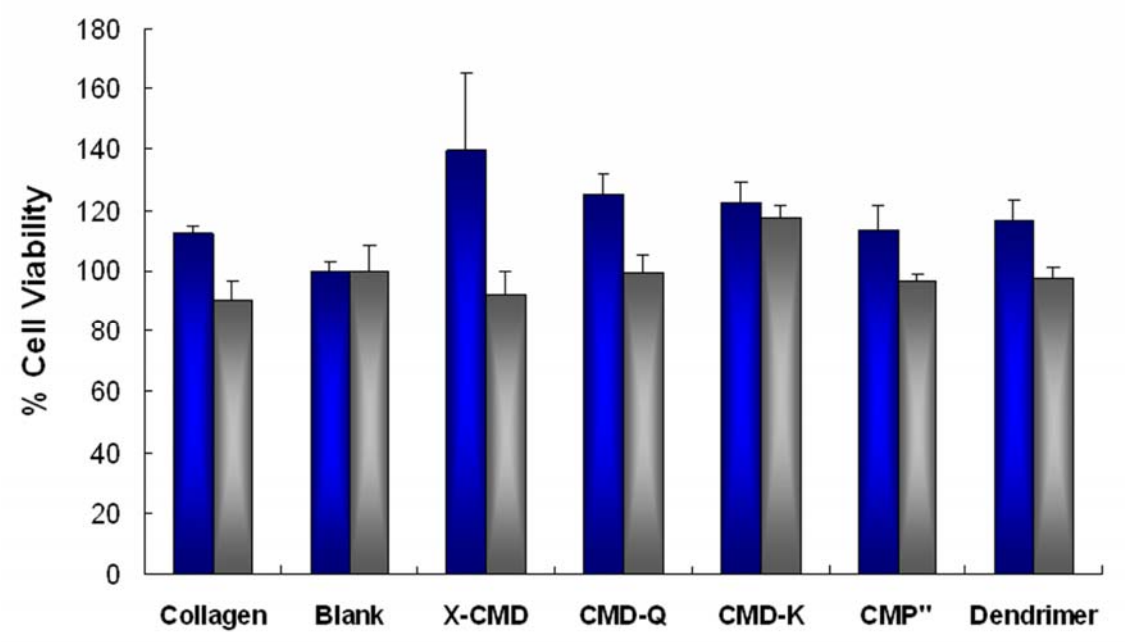

Figure 7.5. Cell viability of L929 mouse fibroblast incubated in serum-free medium containing different samples: calf-skin collagen (collagen), crosslinked collagen-mimetic dendrimers (X-CMD), PAMAM G1.5-$[(GPO)_3GFOGER(GPO)_3APQQEA]_6$ (CMD-Q), PAMAM G1.5-$[(GPO)_3GFOGER(GPO)_3EDGFFKI]_7$ (CMD-K), GFOGERGGG (CMP''), and PAMAM G1.5 (dendrimer), at 50 μg/ml was assessed by MTT assay after 24 h (dark) and 72 h (grey). Viability percentage of L929 cells incubated in serum-free medium (blank) was used as the 100% reference level.

Cell adhesion to enzymatically crosslinked collagen-mimetic dendrimers

A cell adhesion assay was performed to study the cellular recognition of tissue TGase-modified collagen-mimetic dendrimers. Calf-skin collagen and heat-denatured BSA (denoted as blank) were used as a positive and negative control in this assay, respectively. Human carcinoma Hep3B cell lines of high constitutive activity in adhesion to collagen were used as a model cell type (Masumoto et al., 1999).

It can be seen from Figure 7.6a that the maximum adhesion of Hep3B cells (~80%) occurred on the X-CMD substrate. There is no significant statistical difference between cell adhesion to calf-skin collagen and to X-CMD, suggesting that the tissue TGase-modified collagen-like supramolecules could be used as a potential bioadhesive matrix to promote cell adhesion. Cell adhesion to PAMAM G1.5 dendrimers was negligible thus indicating that the cellular recognition of the substrate may originate from the attached peripheral peptides. Cell adhesion or cellular recognition of GFOGER cell-binding sequence appeared to be conformation-dependent, as can be observed from the cell adhesion level on CMD-K, CMD-Q, and CMP" of different triple-helical stability, consistent with our previously reported observations (Khew and Tong, 2007a). The non-triple-helical CMP" suffered a significant loss of cellular recognition (<10% cell adhesion), suggesting that the triple helix structure may play an important role in preserving the GFOGER cell binding site. Nevertheless, there was a significant difference in the cell adhesion level between X-CMD and CMD-K. Although both of them exhibited similar triple-helical

stability, the cell binding activity of X-CMD was notably higher than that of CMD-K. The result hints that the tissue TGase-mediated crosslinking may play a crucial role in stabilizing and engineering protein matrix favorable to cell adhesion. Furthermore, tissue TGase-mediated protein crosslinking is a common physiological phenomenon. Many ECM proteins were found crosslinked *in vivo*. Although the relationship between the matrix protein crosslinking and the cell adhesion and spreading is still not fully understood, it is hypothesized that the supramolecular structures formed in the crosslinked X-CMD could promote integrin clustering. The enhanced cellular recognition of X-CMD by Hep3B cells represents preliminary evidence that the protein crosslinking may be important for building the basement matrix for cell adhesion. Another possible reason for the observed cell adhesion responses could be the possible differences in the adsorption amounts of each adhesive dendrimer onto the culture substrate. It has been reported previously that the differences in cell adhesion can probably also arise from the differences in the adsorbed densities (Reyes and García, 2003). Some works remain to be done before the exact role of tissue TGase-mediated protein crosslinking in cellular recognition and adhesion processes can be completely established.

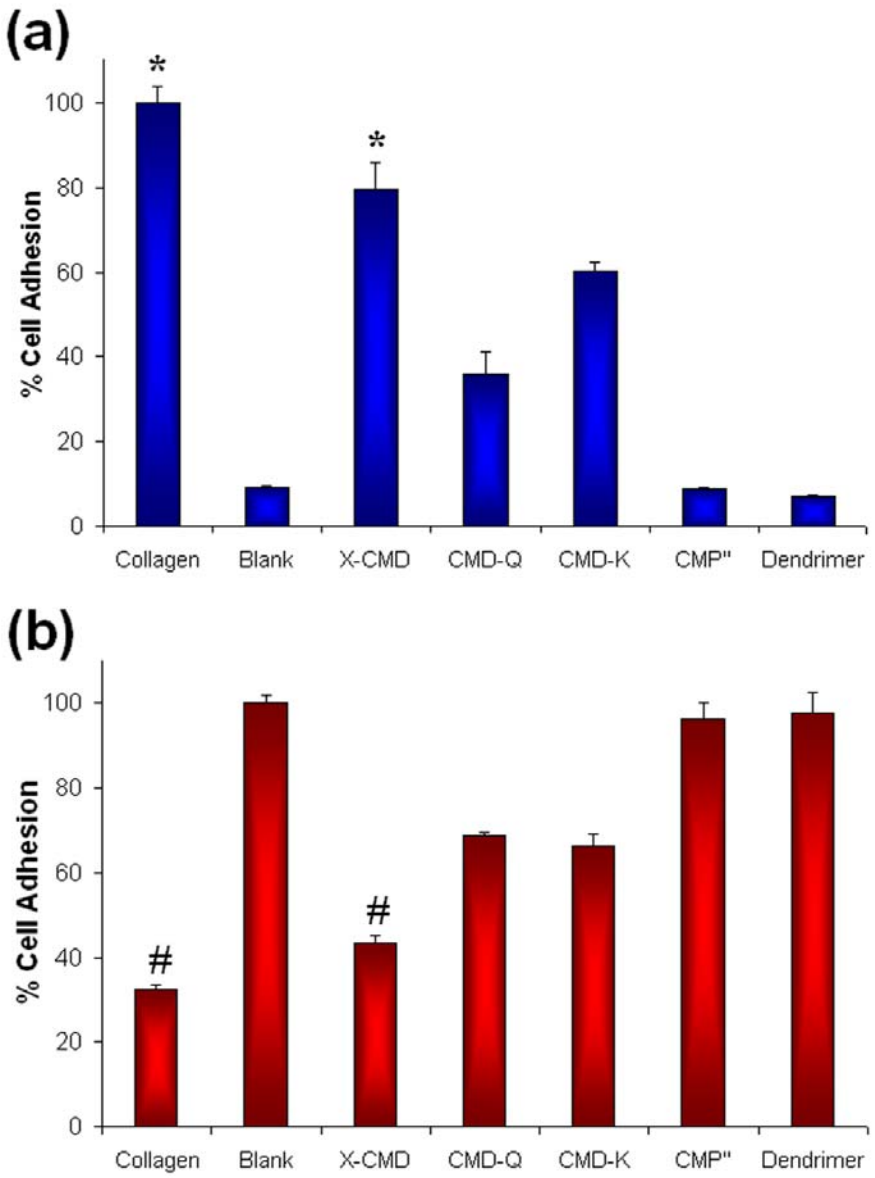

Figure 7.6. (a) Hep3B cell adhesion as a function of substrate: calf-skin collagen (collagen), heat-denatured BSA (blank), crosslinked collagen-mimetic dendrimers (X-CMD), PAMAM G1.5-$[(GPO)_3GFOGER(GPO)_3APQQEA]_6$ (CMD-Q), PAMAM G1.5-$[(GPO)_3GFOGER(GPO)_3EDGFFKI]_7$ (CMD-K), GFOGERGGG (CMP''), and PAMAM G1.5 (dendrimer). Cells in serum-free medium were allowed to adhere to different substrates for 1h at room temperature. Student's *t* test with $*p< 0.05$ are significantly different from blank, CMD-Q, CMD-K, CMP'', and dendrimer but not significantly different from each other. (b) Competition inhibition of Hep3B cell adhesion to the collagen coated surface in the presence of different molecules. Cell in serum-free medium were incubated with 25 μg/ml peptides or calf-skin collagen for 30 min before seeding. The competition adhesion was allowed to take place for 1h at room temperature. Cell adhesion in blank serum-free medium (blank) was used as a positive control. Student's *t* test with $^{\#}p< 0.05$ are significantly different from blank, CMP'', and dendrimer but not significantly different from each other.

Competitive inhibition of Hep3B cells to calf-skin collagen substrate

The competitive inhibition assay is an indirect screening assay for the cell-binding activity displayed by collagen-mimetic dendrimers or peptides. Cell adhesion to collagen is inhibited when the cell surface receptors are presaturated with the adhesive molecules prior to cell seeding. Adhesion of cells onto the collagen surface in blank serum-free medium was used as the 100% reference level. It can be seen from Figure 7.6b that the cells displayed specific interaction with the soluble calf-skin collagen thus inhibiting the binding of cell surface collagen receptors to the collagen substrate. The inhibitory activity of X-CMD was comparable to that of the calf-skin collagen. The inhibition was most probably due to the specific interactions between the GFOGER cell-binding sequence of X-CMD and the cell surface receptors, suggesting that the cell adhesion to X-CMD is an integrin-mediated process. The inhibitory activity exhibited by soluble CMD-Q and CMD-K, although lower, is still significant, confirming the participation of specific GFOGER receptors in the adhesion process. The lower inhibitory activity displayed by CMD-Q when compared to that of X-CMD of similar triple-helical stability is consistent with the cell adhesion assay, strengthening the observation that the tissue TGase-modified supramolecular structure may be crucial in promoting the integrin clustering. Similar to previous assay, loss of the triple-helical conformation resulted in collagen-mimetic peptides lacking the ability to inhibit the integrin-mediated cell adhesion, as can be observed from the markedly low inhibitory activity displayed by CMP''.

Cytoskeletal organization and focal adhesion of Hep3B cells

The adhered Hep3B cells were fixed and stained for vinculin (FITC-antivinculin; green), actin stress fibers (TRITC-phalloidin; red), and nuclei (DAPI; blue) after 3h of incubation in serum-free medium to study the cytoskeletal organization and focal adhesion of Hep3B cells as a function of substrates. Focal adhesions are sites where integrin-mediated adhesion links to the actin cytoskeleton (Wozniak et al., 2004). Multimeric ECM proteins bind to the integrins and thereby stimulate receptor clustering, namely focal adhesions, dynamic protein complexes that contain cytoplasmic structural proteins such as vinculin through which the actin cytoskeleton of a cell links to the ECM (Burridge et al., 1997). It can be seen that the Hep3B cells displayed a well-developed actin cytoskeletal structure on calf-skin collagen, X-CMD, CMD-K (Figure 7.7), and CMD-Q (result not shown) substrates. The assembled distinct actin stress fibers indicated the formation of strong actin cytoskeletal organization in the cells seeded on these substrates, which also demonstrated the ability of X-CMD, CMD-Q and CMD-K to mimic the collagen adhesion profile. Conversely, the actin cytoskeletal organization became less pronounced in the cells seeded on non-triple-helical CMP". While cells developed extensive actin stress fibers on calf-skin collagen and collagen-mimetic dendrimers, most of them remained in spherical morphology when seeded on PAMAM dendrimers (result not shown) and CMP". The substantial decrease in the cell spreading activities demonstrated that the cell development is substrate specific. The potential of the collagen-mimetic dendrimers to mimic cell binding activity of parental molecules may provide a

biomolecular strategy for optimizing cellular responses and to regulate cell behaviors. It can be seen from the vinculin staining (Figure 7.7) that the cells formed strong focal adhesion contacts on calf-skin collagen, X-CMD, and CMD-K. Most of the focal adhesions were found at the cell periphery, associated with the ends of actin stress fibers of the cells. Although the cell adhesion activities cannot be measured quantitatively by immunofluorescence staining, it can be seen from the confocal images qualitatively that the vinculin concentration exhibited by the cells adhered on X-CMD was comparable to, if not higher than, that displayed by the cells on calf-skin collagen. The clustering of vinculin, stimulated by the integrins binding, on the cell periphery with a sharp spike across the actin stress fibers indicated the formation of firm adhesion. The focal adhesion position at the convergence of integrin adhesion, signaling and the actin cytoskeleton, generally involves integral membrane protein integrins which bind to ECM proteins via specific peptide sequences, such as the RGD motif. Therefore, it appears that the cell adhesion and spreading on collagen and collagen-mimetic dendrimers are unlike the cell-synthetic polymer interaction, which merely depends on the non-specific contact between the cell membrane proteins and the functional groups of polymers (Bačáková et al., 2000a and 2000b). The extensive cell spreading could, in fact, be a result of the integrin-mediated cell adhesion (Hynes, 1992; Fields et al., 1993b). Conversely, the cells did not form strong focal adhesion contact on PAMAM dendrimer (result not shown) and CMP", as there was no obvious vinculin clustering. The organization of actin filaments and formation of strong focal adhesion in the cells seeded on X-CMD was similar to that seen in the cells

spreading on calf-skin collagen. The ability of X-CMD to support collagen-like adhesion patterns is desirable for supporting cell development, such as cell adhesion, spreading, and cytoskeletal reorganization thus controlling long term cellular behavior, including migration and differentiation.

7.4 Conclusion

This study contributes to taking us one step closer to making artificial collagen of more complete functions and cellular recognition. Enzymatic protein crosslinking is a common physiological event in extracellular environment. We showed that the integration of collagen-like structural domain and biologically relevant epitopes, such as cell binding motif and enzyme-specific crosslinking domain, into the molecular design of a biomimetic collagen could be a promising approach for making its biological function and characteristic a little, if not significant, closer to that of the natural collagen.

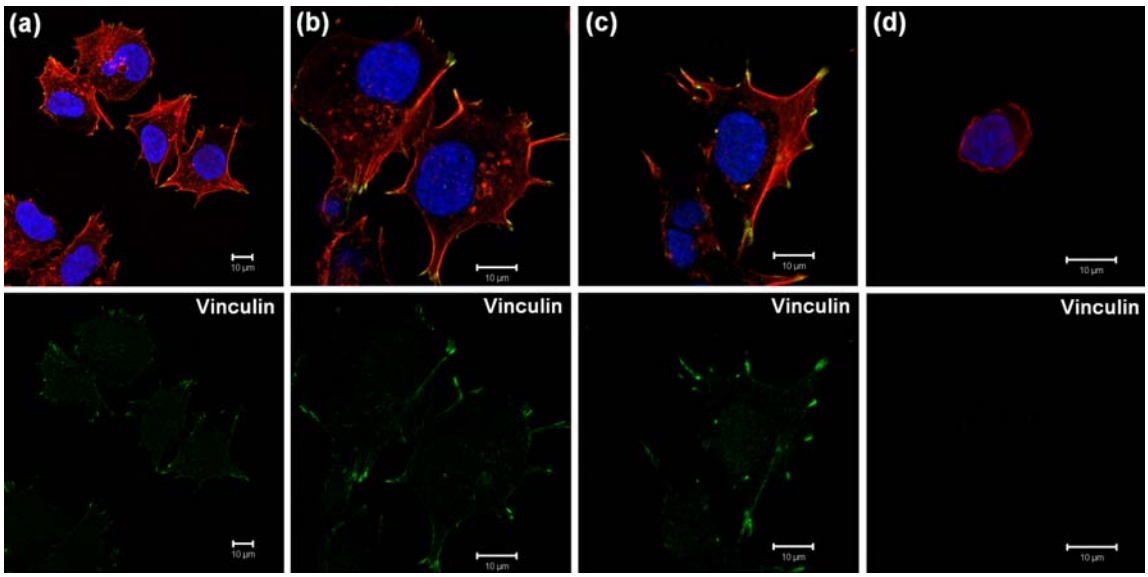

Figure 7.7. Cytoskeletal organization and focal adhesions of Hep3B cells as a function of substrates: (a) calf-skin collagen, (b) crosslinked collagen-mimetic dendrimers (X-CMD), (c) PAMAM G1.5-$[(GPO)_3GFOGER(GPO)_3EDGFFKI]_7$ (CMD-K), and (d) GFOGERGGG (CMP''). Cells were fixed and stained for vinculin (FITC-antivinculin; green), actin stress fibers (TRITC-phalloidin; red), and nuclei (DAPI; blue) after 3h of adhesion in serum-free medium and imaged using a confocal microscopy (60x magnification).

CHAPTER 8

CONCLUSIONS AND RECOMMENDATIONS

The presence of an environment conducive to cell adhesion is crucial to the success in engineering tissues. Among the extracellular matrices (ECM), collagen is the most abundant type of protein that is intimately associated with cell adhesion and growth. Many attempts have been made to create collagen-like substrate to promote integrin-specific cell adhesion and thus survival *in vitro* (Qian and Bhatnagar, 1996; Reyes and García, 2003 and 2004). The transition from understanding a natural system to creating biomimetic materials involves tremendous amount of studies and researches. The work presented in this thesis could be one important step forward for this area of research. This thesis established a molecular strategy for engineering an enzymatically crosslinkable collagen-like biomaterial, namely a biomimetic collagen that resembles the native molecular architecture and cell binding activity of collagen.

A series of open-chain collagen-mimetic peptides (CMPs) supplemented with a specific cell binding sequence spanning residues 502-507 of collagen α_1(I) (GFOGER) have been successfully synthesized and characterized. The results

demonstrate that the self-assembled CMPs adopted collagen-like triple-helical conformation. The study showed that the synthetic CMPs could be used as a tissue support matrix to promote cell adhesion as well as to optimize cell proliferation and differentiation. The cellular recognition of the CMPs was achieved mainly by "sandwiching" the naturally-derived cell binding domain (GFOGER) between the structural domains of the peptide, which are known to play an important role in the preservation of the cell binding activity of the GFOGER sequence. The results established the potential of the CMPs to create a collagen-like microenvironment for optimizing cellular responses for cell and tissue engineering.

Most proteins fold into a well-defined structure to implement their biological functions. Therefore, the creation of a protein-like molecular architecture is the fundamental prerequisite to realize a novel biologically active protein-like biomaterial. The second part of the thesis focused on developing a template-assembly system, wherein no complex strategies were used to covalently hold three CMPs in a staggered array thus promoting the assembly of the triple-helical conformation. A template characterized by its fully amino acid based constituents and collagen-like primary structure composed of GFGEEG sequence was devised and employed to covalently assemble CMPs and facilitate the folding of triple helix. The template-assembled $(Pro\text{-}Hyp\text{-}Gly)_3$ and $(Pro\text{-}Hyp\text{-}Gly)_5$ displayed significantly enhanced stability and remained almost intact even at elevated temperatures. This is probably due to the stabilizing effect of the template, which is primarily entropic thus

preventing unfolding at one end of the triple helix and shifting the folding/unfolding equilibrium. Conversely, non-templated peptides showed no evidence of assembly of triple-helical structure. This peptide template assembly strategy appears to be versatile for creating and stabilizing desired collagen-like molecular architectures. Such template-assembly system could be used to further study the protein folding and to create novel protein mimetics.

In the third part of the thesis, the specific recognition of the template-assembled CMPs supplemented with a cell binding motif of collagen (GFOGER) by various cell types, such as Hep3B and L929 cell lines, was studied. It was shown that the template-assembled CMPs promoted adhesion of both human carcinoma Hep3B liver cells and mouse L929 fibroblast cells considerably. Cell recognition of the collagen peptides supplemented with GFOGER appeared to be both conformation- and sequence-specific, the absence of which resulted in a marked loss of cell recognition. Unlike the interaction between cells and synthetic polymers, which merely depends on the non-specific contact between the cell membrane proteins and the functional groups of polymers (Bačáková et al., 2000a and 2000b), the extensive cell adhesion and spreading could, in fact, be a result of the integrin-mediated cell adhesion process (Hynes, 1992; Fields et al., 1993b). The result may have great impact for biological chemists in their biomolecular design: shorter, and hence less expensive, CMPs can be used as a stable triple-helical molecular architecture with a proper template assembly strategy to improve their cell recognition

by supplementing them with a specific cell binding sequence. However, it was also demonstrated in this study that different cell types may recognize GFOGER sequence at different levels. The integrins $\alpha_1\beta_1$, $\alpha_2\beta_1$, and $\alpha_{11}\beta_1$ have been shown to bind GFOGER and GFOGER-like motifs found in collagen (Knight et al., 2000; Xu et al., 2000; Zhang et al., 2003; Siljander et al., 2004). The difference in cell recognition is thus probably due to the difference in their expression of these specific integrins for GFOGER. Both hepatocytes and fibroblast have been shown to bind natural collagen. However, the repertoire of integrins expressed by the hepatocytes is strikingly different from that of most other fibroblast cells (Knight et al., 1998 and 2000; Siljander et al., 2004). This study may contribute to a better understanding of the specific recognition of a cell binding sequence by different cell types and the need to use specific cell binding sequences for precisely controlling adhesion of a particular cell type.

Furthermore, a specific sequence spanning residues 2800-2807 of human fibrillin-1 (EDGFFKI) was identified and characterized as an amine donor substrate for tissue TGase, using a previously characterized APQ^{3}Q^{4}EA, derived from human osteonectin as an amine acceptor probe. The peptide patterned on the C-terminal propeptide of fibrillin-1, EDGFFKI, exhibited good substrate reactivity towards the tissue transglutaminase (TGase) and it bound specifically only to Q^3 of the acceptor probe. Identification of more native amine donor as well as acceptor substrates will eventually contribute to a better understanding of the *in vivo* TGase-mediated

crosslinking in relation to their biological functions and diseases. The identification of a short peptide substrate containing a lysine donor and an easily recognizable reporter group made it possible to detect the intrinsic TGase activity in tissues as demonstrated in this thesis. Use of such biotinylated lysine donor substrate could also aid in an enzyme-directed site-specific labeling of potential amine acceptor substrates for TGase in skin tissues as well as other biological systems. The identification of short naturally derived substrate peptides could also lead to tailoring novel protein-like crosslinkable biomaterials.

Collagens are a diverse family of the extracellular matrices, found generally crosslinked *in vivo*. The study that naturally follows the identification of the tissue TGase crosslinking domain in the native protein would be the development of a molecular strategy to engineer a functional biomimetic collagen that exhibits stable collagen-like triple-helical conformation, cell binding activity, and substrate specificity for tissue TGase. CMPs supplemented with the identified EDGFFKI and APQQEA substrate sequences were conjugated onto a generation 1.5 poly(amidoamine) dendrimer, resulting in a crosslinkable collagen-mimetic dendrimer, denoted as CMD-K and CMD-Q, respectively. Tissue TGase-mediated crosslinking between CMD-K and CMD-Q resulted in supramolecular structure that exhibited stable collagen-like triple-helical conformation and improved cellular recognition. The result showed that the triple helix structure is important in preserving the GFOGER cell binding site and the tissue TGase-mediated protein crosslinking may be

also a crucial recognition mark for cell surface integrin-receptors. Enzymatic protein crosslinking is a common physiological event in the extracellular environment. We showed that the integration of collagen-like structural domain and biologically relevant epitopes, such as cell binding motif and enzyme-specific crosslinking domain, into the molecular design of a biomimetic collagen could be a promising approach for making its biological function and characteristic a little, if not significant, closer to that of the natural collagen.

In this thesis each peptide activity and biological assay were performed *in vitro*. It would be interesting to apply the enzymatically crosslinked collagen-mimetic dendrimers as a tissue support matrix for *in vivo* or animal model studies. The presence of the tissue TGase crosslinking domains may possibly allow mingling of the collagen-mimetic dendrimers with the ECM in a more natural way, probably through crosslinking mediated by intrinsic tissue TGase, and is thus worthy of more extensive researches. Additionally, *in vivo* experiments are also important to examine whether the collagen-mimetic dendrimers perform similarly in inducing cellular response *in vivo* as they were in the *in vitro* experiments and exhibit collagen-like cell adhesion activity. Wound tissue healing or repair using the crosslinked collagen-mimetic dendrimers as a tissue scaffold could be a good starting point to study the tissue response toward the biomimetic collagen *in vivo*.

The biological assays in this thesis have been performed with Hep3B liver

cells or L929 fibroblast cells as a model cell type. Knowing collagen is a ubiquitous protein in mammalians and there may be differences in the expression of integrin-receptors for collagen by different cell types, the cellular recognition of the collagen-mimetic peptides or dendrimers could be further investigated using a diversity of cell types thus contributing to a better understanding of the specific recognition of GFOGER by a variety of cell types. Additionally, a combination of peptide models of collagen integrin-binding sequences and other ECM sequences has been studied previously and found to have potential to mimic biological activities of an ECM (Malkar et al., 2003; Baronas-Lowell et al., 2004). Further examination of the activity of collagen-mimetic peptides of additional cell adhesion domains derived from natural collagen (see Table 2.2) also represents an excellent starting point for future works. Incorporation of more adhesion peptide into the design of the collagen mimics may improve the cell binding activity of the biomimetic collagen and better imitate the adhesion profile of the natural collagen. One potential cell-binding domain to be added could be P-15 (GTPGPQGIAGQRGVV), which has been reported to be 45,000 times more potent than RGD in competition with collagen for cell binding (Bhatnagar et al., 1997).

The inherent globular shape of high generation dendrimers makes them ideal candidates for making macromolecules biomimetics that resemble macromolecular architectures present in nature, such as collagen triple helix. Additionally, a variety of dendritic systems have also demonstrated promises for gene therapy (Sato et al., 2001;

Luo et al., 2002) and drug delivery (Esfand and Tomalia, 2001). It would be of interest to develop a tissue engineering and drug delivery dual system using the collagen-mimetic dendrimers. The "porous" structures or void spaces of dendrimers may be used to entrap drugs (Cloninger, 2002) and the enzymatic crosslinking could be further researched to produce densely crosslinked macromolecules or protein-like hydrogel materials as a tissue engineering scaffold thus leading to a bi-functional tissue culture and drug therapy system.

One key contribution of this thesis is the effort made in creating an "artificial collagen" which mimics certain features of natural collagen, such as molecular architecture, cell binding activity, and substrate specificity for tissue TGase-mediated crosslinking. Knowing the intrinsic problems, such as poor reproducibility, difficulties in purification, possible induction of systemic immune response and potential risk of disease transmission (Sakaguchi et al., 1999; Lynn et al., 2004), associated with the use of animal-derived collagen, the works presented in this thesis may be of significant value for biomaterial science: short, and hence cost-effective, multifunctional collagen mimics could be used as a safe, reproducible, and stable collagen-like biomaterial. This research may contribute to taking us one step forward in realizing an artificial protein biomaterial that emulates the desired characteristics of the ECM for precisely controlling integrin-specific cell adhesion and eliciting specific responses such as signaling and stimulation.

REFERENCES

Aeschlimann, D., Paulsson, M. and Mann, K. (1992) Identification of Gln^{726} in nidogen as the amine acceptor in transglutaminase-catalyzed cross-linking of laminin-nidogen complexes, *J. Biol. Chem 267*, 11316-11321.

Aeschlimann, D., Wetterwald, A., Fleisch, H. and Paulsson, M. (1993) Expression of tissue transglutaminase in skeletal tissues correlates with events of terminal differentiation of chondrocytes, *J. Cell Biol 120*, 1461-1470.

Akimov, S. S. and Belkin, A. M. (2001) Cell surface tissue transglutaminase is involved in adhesion and migration of monocytic cells on fibronectin, *Blood 98*, 1567-1576.

Akimov, S. S., Krylov, D., Fleischman, L. F. and Belkin, A. M. (2000) Tissue transglutaminase is an integrin-binding adhesion coreceptor for fibronectin, *J. Cell Biol. 148*, 825-838.

Aota, S., Nomizu, M. and Yamada, K. (1994) The short amino acid sequence Pro-His-Ser-Arg-Asn in human fibronectin enhances cell-adhesive function, *J. Biol. Chem. 269*, 24756 - 24761.

Bačáková, L., Mareš, V., Bottone, M.G., Pellicciari, C., Lisá V. and Švorčík, V. (2000a) Fluorine-ion-implanted polystyrene improves growth and viability of vascular smooth

muscle cells in culture, *J Biomed Mater Res 49*, 369-379.

Bačáková, L., Walachová, K., Švorčík, V. and Hnatowicz, V. (2000b) Molecular mechanisms of improved adhesion and growth of an endothelial cell line cultured on polystyrene implanted with fluorine ions, *Biomaterials 21*, 1173-1179.

Balklava, Z., Verderio, E., Collighan, R., Gross, S., Adams, J. and Griffin, M. (2002) Analysis of tissue transglutaminase function in the migration of Swiss 3T3 fibroblasts. The active-state conformation of the enzyme does not affect cell motility but is important for its secretion, *J. Biol. Chem 277*, 16567-16575.

Baronas-Lowell, D., Lauer-Fields, J. L. and Fields, G. B. (2004) Induction of endothelial cell activation by a triple helical $\alpha_2\beta_1$ integrin ligand derived from type I collagen α_1(I) 496-07, *J. Biol. Chem 279*, 952-962.

Bella, J., Brodsky, B. and Berman, H. M. (1995) Hydration structure of a collagen peptide, *Structure 3*, 893-906.

Bella, J., Eaton, M., Brodsky, B. and Berman, H. M. (1994) Crystal and molecular structure of a collagen-like peptide at 1.9 Å resolution, *Science 266*, 75-81.

Benedetti, L., Grignani, F., Scicchitano, B., Jetten, A., Diverio, D., Coco, F. L., Avvisati, G., Gambacorti-Passerini, C., Adamo, S., Levin, A., Pelicci, P. and Nervi, C. (1996) Retinoid-induced differentiation of acute promyelocytic leukemia involves PML-RARα-mediated increase of type II transglutaminase, *Blood 87*, 1939-1950.

Berbers, G. A. M., Feenstra, R. W., Bos, R. V. D., Hoekman, W. A., Bloemendal, H. and de Jong, W.W. (1984) Lens transglutaminase selects specific β-crystallin sequences as substrate, *PNAS 81*, 7017-7020.

Bhandari, R., Riccalton, L., Lewis, A., Fry, J., Hammond, A., Tendler, S. and Shakesheff, K. (2001) Liver tissue engineering: A role for co-culture systems in modifying hepatocyte function and viability, *Tissue Eng. 7*, 345-357.

Bhatnagar, R. S., Qian, J. J. and Gough, C. A. (1997) The role in cell binding of a beta-bend within the triple helical region in collagen α_1(I)chain: structural and biological evidence for conformational tautomerism on fiber surface, *J. Biomol. Struct. Dyn. 14*, 547.

Biery, N. J., Eldadah, Z. A., Moore, C. S., Stetten, G., Spencer, F. and Dietz, H. C. (1999) Revised genomic organization of FBN1 and significance for regulated gene expression, *Genomics 56*, 70-77.

Boateng, S. Y., Lateef, S. S., Mosley, W., Hartman, T. J., Hanley, L. and Russell, B. (2005) RGD and YIGSR synthetic peptides facilitate cellular adhesion identical to that of laminin and fibronectin but alter the physiology of neonatal cardiac myocytes, *Am J Physiol Cell Physiol 288*, 30-38.

Boot-Handford, R. P., Tuckwell, D. S., Plumb, D. A., Rock, C. F. and Poulsom, R. (2003) A novel and highly conserved collagen (pro1(XXVII)) with a unique expression pattern and unusual molecular characteristics establishes a new clade within the vertebrate fibrillar collagen family, *J. Biol. Chem 278*, 31067-31077.

Bowness, J., Folk, J. and Timpl, R. (1987) Identification of a substrate site for liver transglutaminase on the aminopropeptide of type III collagen, *J. Biol. Chem 262*, 1022-1024.

Brieva, T. A. and Moghe, P. V. (2004) Engineering the hepatocyte differentiation-

proliferation balance by acellular cadherin micropresentation, *Tissue Eng. 10*, 553-564.

Brodsky, B., Li, M.-H., Long, C. G., Apigo, J. and Baum, J. (1992) NMR and CD studies of triple-helical peptides, *Biopolymers 32*, 447-451.

Brodsky, B. and Ramshaw, J. A. M. (1997) The Collagen Triple-Helix Structure, *Matrix Biol 15*, 545-554.

Brown, F. R., Corato, A. D., Lorenzi, G. P. and Blout, E. R. (1972) Synthesis and structural studies of two collagen analogues Poly (-prolyl-seryl-glycyl) and poly (-prolyl-alanyl-glycyl), *J. Mol. Biol. 63*, 85-99.

Burridge, K., Chrzanowska-Wodnicka, M. and Zhong, C. (1997) Focal adhesion assembly, *Trends Cell Biol 7*, 342-347.

Calderwood, D. A., Tuckwell, D. S., Eble, J., Kühn, K. and Humphries, M. J. (1997) The integrin alpha1 A-domain is a ligand binding site for collagens and laminin, *J. Biol. Chem 272*, 12311-12317.

Camper, L., Hellman, U. and Lundgren-Åkerlund, E. (1998) Isolation, cloning, and sequence analysis of the integrin subunit α_{10}, a β_1-associated collagen binding integrin expressed on chondrocytes, *J. Biol. Chem. 273*, 20383-20389.

Chan, B. M. C., Kassner, P. D., Schiro, J. A., Byers, H. R., Kupper, T. S. and Hemler, M. E. (1992) Distinct cellular functions mediated by different VLA integrin α subunit cytoplasmic domains, *Cell 68*, 1051-1060.

Chelberg, M. K., McCarthy, J. B., Skubitz, A. P. N., Furcht, L. T. and Tsilibary, E. C. (1990) Characterization of a synthetic peptide from Type IV collagen that promotes

melanoma cell adhesion, spreading, and motility, *J. Cell Biol 111*, 261-270.

Clarke, A. W., Wise, S. G., Cain, S. A., Kielty, C. M. and Weiss, A. S. (2005) Coacervation is promoted by molecular interactions between the PF2 segment of fibrillin-1 and the domain 4 region of tropoelastin, *Biochemistry 44*, 10271-10281.

Cloninger, M. J. (2002) Biological applications of dendrimers, *Curr Opin Chem Biol 6*, 742-748.

Coussons, P. J., Price, N. C., Kelly, S. M., Smith, B. and Sawyer, L. (1992) Factors that govern the specificity of transglutaminase-catalysed modification of proteins and peptides, *Biochem. J. 282*, 929-930.

Danen, E. H. J., Aota, S.-i., Kraats, A. A. v., Yamada, K. M., Ruiter, D. J. and Muijen, G. N. P. v. (1995) Requirement for the Synergy Site for Cell Adhesion to Fibronectin Depends on the Activation State of Integrin $\alpha_5\beta_1$, *J. Biol. Chem 270*, 21612 - 21618.

Davis, G. E. (1992) Affinity of integrins for damaged extracellular matrix: $\alpha_v\beta_3$ binds to denatured collagen type I through RGD sites, *Biochem Bioph Res Co 182*, 1025-1031.

Dhoot, N. O., Tobias, C. A., Fischer, I. and Wheatley, M. A. (2004) Peptide-modified alginate surfaces as a growth permissive substrate for neurite outgrowth, *J. Biomed Mater Res 71A*, 191-200.

Eble, J. A., Golbik, R., Mann, K. and Kühn, K. (1993) The alpha 1 beta 1 integrin recognition site of the basement membrane collagen molecule [alpha 1(IV)]2 alpha 2(IV), *EMBO J. 12*, 4795-4802.

Eitan, S., Solomon, A., Lavie, V., Yoles, E., Hirschberg, D. L., Belkin, M. and

Schwartz, M. (1994) Recovery of visual response of injured adult rat optic nerves treated with transglutaminase, *Science 264*, 1764-1768.

Elices, M. J. and Hemler, M. E. (1989) The human integrin VLA-2 is a collagen receptor on some cells and a collagen/laminin receptor on others, *PNAS 86*, 9906-9910.

Emsley, J., Knight, C. G., Farndale, R. W., Barnes, M. J. and Liddington, R. C. (2000) Structural basis of collagen recognition by integrin $\alpha_2\beta_1$, *Cell 101*, 47-56.

Engel, J., Chen, H.-T., Prockop, D. J. and Klump, H. (1977) The triple helix=coil conversion of collagen-like polytripeptides in aqueous and nonaqueous solvents. Comparison of the thermodynamic parameters and the binding of water to (L-Pro-L-Pro-Gly)n and (L-Pro-L-Hyp-Gly)n, *Biopolymers 16*, 601.

Engel, J. and Prockop, D. J. (1991) The zipper-like folding of collagen triple helices and the effects of mutations that disrupt the zipper, *Annu Rev Bioph and Bioph Chem 20*, 137-152.

Esfand, R. and Tomalia, D. A. (2001) Poly(amidoamine) (PAMAM) dendrimers: from biomimicry to drug delivery and biomedical applications, *Drug Discov Today 6*, 427-436.

Esposito, C. and Caputo, I. (2004) Mammalian transglutaminases. Identification of substrates as a key to physiological function and physiopathological, *FEBS J. 58*, 63-68.

Ezzell, R. M., Goldmann, W. H., Wang, N., Parasharama, N. and Ingber, D. E. (1997) Vinculin promotes cell spreading by mechanically coupling integrins to the

cytoskeleton, *Exp. Cell Res. 231*, 14-26.

Faassen, A. E., Schrager, J. A., Klein, D., Oegema, T. R., Couchman, J. and McCarthy, J. B. (1992) A Cell Surface Chondroitin Sulfate Proteoglycan, Immunologically Related to CD44, Is Involved in Type I Collagen-mediated Melanoma Cell Motility and Invasion, *J. Cell Biol 116*, 521-531.

Feng, Y., Melacini, G. and Goodman, M. (1997) Collagen-based structures containing the peptoid residue N-Isobutylglycine (Nleu)-synthesis and biophysial studies of Gly-Nleu-Pro sequences by CD and optical rotation, *Biochemistry 36*, 8716-8724.

Feng, Y., Melacini, G., Taulane, J. P. and Goodman, M. (1996a) Acetyl-terminated and template-assembled collagen-based polypeptides composed of Gly-Pro-Hyp sequences. 2. Synthesis and conformational analysis by CD, UV absorbance and optical rotation, *J. Am. Chem. Soc. 118*, 10351-10358.

Feng, Y., Melacini, G., Taulane, J. P. and Goodman, M. (1996b) Collagen-based structures containing the peptoid residue Nleu- synthesis and biophysical studies of Gly-Pro-Nleu sequences by CD, UV absorbance and optical rotation, *Biopolymers 39*, 859-872.

Fesus, L., Metsis, M. L., Muszbek, L. and Koteliansky, V. E. (1986) Transglutaminase-sensitive glutamine residues of human plasma fibronectin reveled by studying its proteolytic fragments, *Eur. J. Biochem. 154*, 371-374.

Fesus, L., Thomazy, V. and Falus, A. (1987) Induction and activation of tissue transglutaminase during programmed cell death, *FEBS Letters 224*, 104-108.

Fields, C. G., Grab, B., Lauer, J. L. and Fields, G. (1995) Purification and analysis of

synthetic, triple-helical "minicollagens" by reversed-phase high-performance liquid chromatography, *Anal. Biochem. 231*, 57-64.

Fields, C. G., Lovdahl, C. M., Miles, A. J., Hageini, V. L. M. and Fields, G. B. (1993a) Solid-Phase synthesis and stability of triple-helical peptides incorporating native collagen sequences, *Biopolymers 33*, 1695-1707.

Fields, C. G., Mickelson, D. J., Drake, S. L., McCarthy, J. B. and Fields, G. B. (1993b) Melanoma cell adhesion and spreading activities of a synthetic 124-residue triple-helical "mini-collagen", *J. Biol. Chem 268*, 14153-14160.

Fields, G. B. (1991) A model for interstitial collagen catabolism by mammalian collagenases, *J. Theor. Biol. 153*, 585-602.

Fields, G. B. (1995) The collagen triple-helix: correlation of conformation with biological activities, *Connect. Tissue Res 31*, 235-243.

Fields, G. B., Lauer, J. L., Dori, Y., Forns, P., Yu, Y.-C. and Tirrell, M. (1998) Proteinlike molecular architecture: biomaterial applications for inducing cellular receptor binding and signal transduction, *Biopolymers 47*, 143-151.

Forsberg, E., Paulsson, M., Timpl, R. and Johansson, S. (1990) Characterization of a laminin receptor on rat hepatocytes, *J. Biol. Chem. 265*, 6376-6381.

García, A. J., Vega, M. D. and Boettiger, D. (1999) Modulation of cell proliferation and differentiation through substrate-dependent changes in fibronectin conformation, *Mol Biol Cell 10*, 785-798.

Gardner, H., Broberg, A., Pozzi, A., Laato, M. and Heino, J. (1999) Absence of integrin alpha1beta1 in the mouse causes loss of feedback regulation of collagen

synthesis in normal and wounded dermis, *J. Cell Sci. 112*, 263-272.

Gaudry, C. A., Verderio, E., Jones, R. A., Smith, C. and Griffin, M. (1999) Tissue transglutaminase is an important player at the surface of human endothelial cells: evidence for its externalization and its colocalization with the β_1 integrin, *Exp. Cell Res. 252*, 104-113.

Gentile, V., Thomazy, V., Piacentini, M., Fesus, L. and Davies, P. J. A. (1992) Expression of tissue transglutaminase in Balb-C 3T3 fibroblasts: effects on cellular morphology and adhesion, *J. Cell Sci. 119*, 463-474.

Germann, H. P. and Heidemann, E. (1988) A synthetic model of collagen: An experimental investigation of the triple-helix stability, *Biopolymers 27*, 157-163.

Gilmartin, B. P., McLaughlin, R. L. and Williams, M. E. (2005) Artificial tripeptide scaffolds for self-assembly of heteromultimetallic structures with tunable electronic and magnetic properties, *Chem. Mater. 17*, 5446-5454.

Glicklis, R., Shapiro, L., Agbaria, R., Merchuk, J. and Cohen, S. (2000) Hepatocyte behavior within three-dimensional porous alginate scaffolds, *Biotechnol Bioeng 67*, 344-353.

Goodman, M., Bhumralkar, M., Jefferson, E. A., Kwak, J. and Locardi, E. (1998) Collagen mimetics, *Pept Sci 47*, 127-142.

Goodman, M., Cai, W. and Kinberger, G. A. (2003) The new science of protein mimetics, *Macromol Symp 201*, 223-236.

Goodman, M., Feng, Y., Melacini, G. and Taulane, J. P. (1996) A template-induced incipient collagen-like triple-helical structure, *J. Am. Chem. Soc. 118*, 5156-5157.

Grab, B., Miles, A. J., Furcht, L. T. and Fields, G. B. (1996) Promotion of fibroblast adhesion by triple-helical peptide models of type I collagen-derived sequences, *J. Biol. Chem. 271*, 12234-12240.

Graf, J., Iwamoto, Y., Sasaki, M., Martin, G. R., Kleinman, H. K., Robey, F. A. and Yamada, Y. (1987a) Identification of an amino acid sequence in laminin mediating cell attachment, chemotaxis, and receptor binding, *Cell 48*, 989-996.

Graf, J., Ogle, R. C., Robey, F. A., Sasaki, M., Martin, G. R., Yamada, Y. and Kleinman, H. K. (1987b) A pentapeptide from the laminin β1 chain mediates cell adhesion and binds to 67000 laminin receptor, *Biochemistry 26*, 6896-6900.

Greenberg, C., Birckbichler, P. and Rice, R. (1991) Transglutaminases: multifunctional cross-linking enzymes that stabilize tissues, FASEB J. 5, 3071-3077.

Greiche, Y. and Heidemann, E. (1979) Collagen model peptides with antiparallel structure, *Biopolymers 18*, 2359-2361.

Griffin, M., Casadio, R. and Bergamini, C. M. (2002) Transglutaminases: Nature's biological glues, *Biochem. J. 368*, 377-396.

Groenen, P. J., Grootjans, J. J., Lubsen, N. H., Bloemendal, H. and de Jong, W.W. (1994) Lys-17 is the amine-donor substrate site for transglutaminase in beta βA3-crystallin, *J. Biol. Chem. 269*, 831-833.

Groenen, P. J. T. A., Bloemendal, H. and de Jong, W.W. (1992) The carboxy-terminal lysine of αβ-crystallin is an amine-donor substrate for tissue transglutaminase, *Eur. J. Biochem. 205*, 671-674.

Groenen, P. J. T. A., Smulders, R. H. P. H., Peters, R. F. R., Grootjans, J. J., Ijssel, P. R.

L. A. V. d., Bloemendal, H. and de Jong, W.W. (1994) The amine-donor substrate specificity of tissue-type transglutaminase. Influence of amino acid residues flanking the amine-donor lysine residue, *Eur. J. Biochem. 220*, 795-799.

Grootjans, J. J., Groenen, P. J. T. A. and de Jong, W.W. (1995) Substrate requirements for Transglutaminases. Influence of the amino acid residue preceding the amine donor lysine in a native protein, *J. Biol. Chem 270*, 22855-22858.

Groth, T., Altankov, G., Kostadinova, A., Krasteva, N., Albrecht, W. and Paul, D. (1999) Altered vitronectin receptor (α_v integrin) function in fibroblasts adhering on hydrophobic glass, *J Biomed Mater Res 44*, 341-351.

Grzesiak, J. J., Davis, G. E., Kirchhofer, D. and Pierschbacher, M. D. (1992) Regulation of $\alpha_2\beta_1$-mediated fibroblast migration on type I collagen by shifts in the concentrations of extracellular Mg^{2+} and Ca^{2+}, *J. Cell Biol 117*, 1109-1117.

Guler, M. O., Hsu, L., Soukasene, S., Harrington, D. A., Hulvat, J. F. and Stupp, S. I. (2006) Presentation of RGDS epitopes on self-assembled nanofibers of branched peptide amphiphiles, *Biomacromolecules 7*, 1855-1863.

Gullberg, D., Gehlsen, K.R., Turner, D.C., Åhlén, K., Zijenah, L.S., Barnes, M.J. and Rubin, K. (1992) Analysis of $\alpha_1\beta_1$, $\alpha_2\beta_1$ and $\alpha_3\beta_1$ integrins in cell-collagen interactions: identification of conformation dependent $\alpha_1\beta_1$ binding sites in collagen type I, *EMBO J. 11*, 3865-3873.

Gullberg, D., Terracio, L., Borg, T. and Rubin, K. (1989) Identification of integrin-like matrix receptors with affinity for interstitial collagens, *J. Biol. Chem. 264*, 12686-12694.

Gumbiner, B. M. (1996) Cell adhesion: the molecular basis of tissue architecture and morphogenesis, *Cell 84*, 345-357.

Hanks, T. and Atkinson, B. L. (2004) Comparison of cell viability on anorganic bone matrix with or without P-15 cell binding peptide, *Biomaterials 25*, 4831-4836.

Hersel, U., Dahmen, C. and Kessler, H. (2003) RGD modified polymers: biomaterials for stimulated cell adhesion and beyond, *Biomaterials 24*, 4385-4415.

Higashi, N., Koga, T. and Niwa, M. (2000) Dendrimers with attached helical peptides, *Adv. Mater. 12*, 1373-1375.

Hohenadl, C., Mann, K., Mayer, U., Timpl, R., Paulsson, M. and Aeschlimann, D. (1995) Two adjacent N-terminal glutamines of BM-40 (Osteonectin, SPARC) act as amine acceptor sites in transglutaminase-catalyzed modification, *J. Biol. Chem 270*, 23415-23420.

Hojo, H., Akamatsu, Y., Yamauchi, K. and Kinoshita, M. (1997) Synthesis and structural characterization of triple-helical peptides which mimic the ligand binding site of the human macrophage scavenger receptor, *Tetrahedron 53*, 14263.

Holmgren, S. K., Bretscher, L. E., Taylor, K. M. and Raines, R. T. (1999) A hyperstable collagen mimic, *Chem Biol 6*, 63-70.

Holmgren, S. K., Taylor, K. M., Bretscher, L. E. and Raines, R. T. (1998) Code for collagen's stability deciphered, *Nature 392*, 666-667.

Huang, S., Chen, C. S. and Ingber, D. E. (1998) Control of cyclin D1, p27(Kip1), and cell cycle progression in human capillary endothelial cells by cell shape and cytoskeletal tension, *Mol Biol Cell 9*, 3179-3193.

Huber, M., Rettler, I., Bernasconi, K., Frenk, E., Lavrijsen, S. P. M., Ponec, M., Bon, A., Lautenschlager, S., Schorderet, D. F. and Hohl, D. (1995) Mutations of keratinocyte transglutaminase in lamellar ichthyosis, *Science 267*, 525-528.

Huebsch, J. C., McCarthy, J. B., Diglio, C. A. and Mooradian, D. L. (1995) Endothelial cell interactions with synthetic peptides from the carboxyl-terminal heparin-binding domains of fibronectin, *Circ. Res. 77*, 43-53.

Humphries, M., Akiyama, S., Komoriya, A., Olden, K. and Yamada, K. (1986) Identification of an alternatively spliced site in human plasma fibronectin that mediates cell type-specific adhesion, *J. Cell Biol 103*, 2637-2647.

Hynes, R. O. (1992) Integrins: Versatility, modulation, and signaling in cell adhesion, *Cell 69*, 11-25.

Ikura, K., Nasu, T., Yokota, H., Tsuchiya, Y., Sasaki, R. and Chiba, H. (1988) Amino acid sequence of guinea pig liver transglutaminase from its cDNA sequence, *Biochemistry 27*, 2898-2905.

Ikura, K., Takahata, K. and Sasaki, R. (1993) Cross-linking of a synthetic partial-length (1-8) peptide of the Alzheimer βA4 amyloid protein by transglutaminase, *FEBS Letters 326*, 109-111.

Inouye, K., Kobayashi, Y., Kyogoku, Y., Kishida, Y., Sakakibara, S. and Prockop, D. J. (1982) Synthesis and physical properties of (hydroxyproline-proline-glycine)$_{10}$: Hydroxyproline in the X-position decreases the melting temperature of the collagen triple helix, *Arch. Biochem. Biophys. 219*, 198-203.

Jefferson, E. A., Locardi, E. and Goodman, M. (1998) Incorporation of achiral

peptoid-based trimeric sequences into collagen mimetics, *J. Am. Chem. Soc. 120*, 7420-7428.

Jeitner, T. M., Fuchsbauer, H.-L., Blass, J. P. and Cooper, A. J. L. (2001) A sensitive fluorometric assay for tissue transglutaminase, *Anal Biochem 292*, 198-206.

Jelenska, M. M., Fesus, L. and Kopec, M. (1980) The comparative ability of plasma and tissue transglutaminases to use collagen as a substrate, *Biochim. Biophys. Acta 616*, 167-178.

Johnson, G., Jenkins, M., McLean, K. M., Griesser, H. J., Kwak, J., Goodman, M. and Steele, J. G. (2000) Peptoid-containing collagen mimetics with cell binding activity, *J. Biomed Mater Res 51*, 612-624.

Jokinen, J., Dadu, E., Nykvist, P., Kapyla, J., White, D. J., Ivaska, J., Vehvilainen, P., Reunanen, H., Larjava, H., Hakkinen, L. and Heino, J. (2004) Integrin-mediated cell adhesion to type I collagen fibrils, *J. Biol. Chem. 279*, 31956-31963.

Kahlem, P., Terré, C., Green, H. and Djian, P. (1996) Peptides containing glutamine repeats as substrates for transglutaminase-catalyzed cross-linking: relevance to diseases of the nervous system, *PNAS 93*, 14580-14585.

Kajiyama, K., Tomiyama, T., Uchiyama, S. and Kobayashi, Y. (1995) Phase transitions of sequenced polytripeptides observed by microcalorimetry, *Chem Phys Lett 247*, 299-303.

Khew, S. T. and Tong, Y. W. (2007a) The specific recognition of a cell binding sequence derived from type I collagen by Hep3B and L929 cells, *Biomacromolecules 8*, 3153-3161.

Khew, S. T. and Tong, Y. W. (2007b) Template-assembled triple-helical peptide molecules: mimicry of collagen by molecular architecture and integrin-specific cell adhesion, *Biochemistry 47*, In press.

Khew, S. T., Zhu, X. H. and Tong, Y. W. (2007) An integrin-specific collagen-mimetic peptide approach for optimizing Hep3B liver cell adhesion, proliferation, and cellular functions, *Tissue Eng. 13*, 2451-2463.

Kim, J. K., Xu, Y., Xu, X., Keene, D. R., Gurusiddappa, S., Liang, X., Wary, K. K. and Höök, M. (2005) A novel binding site in collagen type III for integrins $\alpha_1\beta_1$ and $\alpha_2\beta_1$, *J. Biol. Chem 280*, 32512-32520.

Kinberger, G. A., Cai, W. and Goodman, M. (2002) Collagen mimetic dendrimers, *J Am Chem Soc 124*, 15162-15163.

Kinberger, G. A., Taulane, J. P. and Goodman, M. (2006) The design, synthesis, and characterization of a PAMAM-based triple helical collagen mimetic dendrimer, *Tetrahedron 62*, 5280-5286.

Kleinman, H. K., McGoodwin, E. B., Martin, G. R., Klebe, R. J., Fietzek, P. P. and Woolley, D. E. (1978) Localization of the binding site for cell attachment in the α_1(I) chain of collagen, *J. Biol. Chem 253*, 5642-5646.

Kleman, J.-P., Aeschlimann, D., Paulsson, M. and van der Rest, M. (1995) Transglutaminase-catalyzed cross-linking of fibrils of collagen V/XI in A204 rhabdomyosarcoma cells, *Biochemistry 34*, 13768-13775.

Knight, C. G., Morton, L. F., Onley, D. J., Peachey, A. R., Messent, A. J., Smethurst, P. A., Tuckwell, D. S., Farndale, R. W. and Barnes, M. J. (1998) Identification in

collagen type I of an integrin $\alpha_2\beta_1$-binding site containing an essential GER sequence, *J. Biol. Chem. 273*, 33287-33294.

Knight, C. G., Morton, L. F., Peachey, A. R., Tuckwell, D. S., Farndale, R. W. and Barnes, M. J. (2000) The collagen-binding A-domains of integrins $\alpha_1\beta_1$ and $\alpha_2\beta_1$ recognize the same specific amino acid sequence, GFOGER, in native (triple-helical) collagens, *J. Biol. Chem. 275*, 35 - 40.

Kobayashi, Y., Sakai, R., Kakiuchi, K. and Isemura, T. (1970) Physicochemical analysis of $(Pro\text{-}Pro\text{-}Gly)_n$ with defined molecular weight-temperature dependence of molecular weight in aqueous solution, *Biopolymers 9*, 415-25.

Koide, T. (2005) Triple helical collagen-like peptides: engineering and applications in matrix biology, *Connect. Tissue Res 46*, 131-141.

Kramer, R. and Marks, N. (1989) Identification of integrin collagen receptors on human melanoma cells, J. Biol. Chem. 264, 4684-4688.

Kühn, K. and Eble, J. (1994) The structural bases of integrin-ligand interactions, *Trends Cell Biol 4*, 231-270.

Kwak, J., Capua, A. D., Locardi, E. and Goodman, M. (2002) TREN (Tris(2-aminoethyl)amine)- an effective scaffold for the assembly of triple helical collagen mimetic structures, *J. Am. Chem. Soc 124*, 14085-14091.

Kwak, J., Jefferson, E. A., Bhumralkar, M. and Goodman, M. (1999) Triple helical stabilities of guest-host collagen mimetic structures, *Bioorg Med Chem 7*, 153-160.

LeBaron, R. G., Esko, J. D., Woods, A., Johansson, S. and Höök, M. (1988) Adhesion of glycosaminoglycan-deficient chinese hamster ovary cell mutants to fibronectin

substrata, *J. Cell Biol 10*, 945-952.

LeCluyse, E., Bullock, P. and Parkinson, A. (1996) Strategies for restoration and maintenance of normal hepatic structure and function in long-term cultures of rat hepatocytes, *Adv. Drug. Deliv. Rev. 22*, 133-86.

Lee, C. H., Singla, A. and Lee, Y. (2001) Biomedical applications of collagen, *Int. J. Pharm. 221*, 1-22.

Legrand, Y. J., Karniguian, A., Francier, P. L., Fauvel, F. and Caen, J. P. (1980) Evidence that a collagen-derived nonapeptide is a specific inhibitor of platelet-collagen interaction, *Biochem. Biophys. Res. Commun. 96*, 1579-1585.

Li, M., Fan, P., Brodsky, B. and Baum, J. (1993) Two-dimensional NMR assignments and conformation of $(Pro\text{-}Hyp\text{-}Gly)_{10}$ and a designed collagen triple-helical peptide, *Biochemistry 32*, 7377-7387.

Long, C. G., Braswell, E., Zhu, D., Apigo, J., Baum, J. and Brodsky, B. (1993) Characterization of collagen-like peptides containing interruptions in the repeating Gly-X-Y sequence, *Biochemistry 32*, 11688-11695.

Longhurst, C. M. and Jennings, L. K. (1998) Integrin-mediated signal transduction, *Cell. Mol. Life Sci. 54*, 514-526.

Lorand, L. and Campbell, L. K. (1971) Transamidating enzymes: I. rapid chromatographic assays, *Anal Biochem 44*, 207-220.

Lorand, L. and Graham, R. M. (2003) Transglutaminases: crosslinking enzymes with pleiotropic functions, *Nat Rev Mol Cell Biol 4*, 140-156.

Lorand, L., Siefring, G. E., Tong, Y. S., Bruner-Lorand, J. and Gray, A. J. (1979)

Dansylcadaverine specific staining for transamidating enzymes, *Anal Biochem 93*, 453-458.

Lorand, L., Valasco, P. T., Murthy, S. N. P., Wilson, J. and Parameswaran, K. N. (1992) Isolation of transglutaminase-reactive sequences from complex biological systems: a prominent lysine donor sequence in bovine lens, *PNAS 89*, 11161-11163.

Lullo, G. A. D., Sweeney, S. M., Körkkö, J., Ala-Kokko, L. and Antonio, J. D. S. (2002) Mapping the ligand-binding sites and disease-associated mutations on the most abundant protein in the human-type I collagen, *J. Biol. Chem 277*, 4223-4231.

Luo, D., Haverstick, K., Belcheva, N., Han, E. and Saltzman, W. M. (2002) Poly(ethyleneglycol)-conjugated PAMAM dendrimer for biocompatible, high-efficiency DNA delivery, *Macromolecules 35*, 3456-3462.

Lynn, A. K., Yannas, I. V. and Bonfield, W. (2004) Antigenicity and immunogenicity of collagen, *J. Biomed Mater Res 71B*, 343-354.

Majoros, I. J., Thomas, T. P., Mehta, C. B. and Jr.Baker, J. R. (2005) Poly(amidoamine) dendrimer-based multifunctional engineered nanodevice for cancer therapy, *J. Med. Chem. 48*, 5892-5899.

Malkar, N. B., Lauer-Fields, J. L., Juska, D. and Fields, G. B. (2003) Characterization of peptide-amphiphiles possessing cellular activation sequences, *Biomacromolecules 4*, 518-528.

Mann, B. K. and West, J. L. (2002) Cell adhesion peptides alter smooth muscle cell adhesion, proliferation, migration, and matrix protein synthesis on modified surfaces and in polymer scaffolds, *J. Biomed Mater Res 60*, 86-93.

Mardilovich, A., Craig, J. A., McCammon, M. Q., Garg, A. and Kokkoli, E. (2006) Design of a novel fibronectin-mimetic peptide-amphiphile for functionalized biomaterials, *Langmuir 22*, 3259-3264.

Mariniello, L., Esposito, C., Pierro, P. D., Cozzolino, A., Pucci, P. and Porta, R. (1993) Human-immunodeficiency-virus transmembrane glycoprotein gp41 is an amino acceptor and donor substrate for transglutaminase in vitro, *Eur. J. Biochem. 215*, 99-104.

Massia, S. and Hubbell, J. (1991) An RGD spacing of 440 nm is sufficient for integrin $\alpha_v\beta_3$-mediated fibroblast spreading and 140 nm for focal contact and stress fiber formation, *J. Cell Biol 114*, 1089-1100.

Massia, S., Rao, S. and Hubbell, J. (1993) Covalently immobilized laminin peptide Tyr-Ile-Gly-Ser-Arg (YIGSR) supports cell spreading and co-localization of the 67-kilodalton laminin receptor with α-actinin and vinculin, *J. Biol. Chem. 268*, 8053-8059.

Massia, S. P. and Stark, J. (2001) Immobilized RGD peptides on surface-grafted dextran promote biospecific cell attachment, *J Biomed Mater Res* 56, 390-399.

McCarthy, J. B., Vachhani, B. and Iida, J. (1996) Cell adhesion to collagenous matrices, *Pept Sci 40*, 371-381.

Masumoto, A., Arao, S. and Otsuki, M. (1999) Role of β_1 integrins in adhesion and invasion of hepatocellular carcinoma cells, *Hepatology 29*, 68-74.

Melacini, G., Feng, Y. and Goodman, M. (1996) Acetyl-terminated and template-assembled collagen-based polypeptides composed of Gly-Pro-Hyp

sequences. 3. conformational analysis by H-NMR and molecular modeling studies, *J. Am. Chem. Soc. 118*, 10359-10364.

Merck, K. B., Groenen, P. J., Voorter, C. E., Haard-Hoekman, W. A. d., J Horwitz, H. B. and de Jong, W.W. (1993) Structural and functional similarities of bovine α-crystallin and mouse small heat-shock protein. A family of chaperones, *J. Biol. Chem 268*, 1046-1052.

Miles, A. J., Skubitz, A. P. N., Furcht, L. T. and Fields, G. B. (1994) Promotion of cell adhesion by single-stranded and triple-helical peptide models of basement membrane collagen α_1(IV) 531-543, *J. Biol. Chem 269*, 30939-30945.

Moiseeva, E. P. (2001) Adhesion receptors of vascular smooth muscle cells and their functions, *Cardiovasc Res* 52, 372-386.

Mosher, D., Schad, P. and Vann, J. (1980) Cross-linking of collagen and fibronectin by factor XIIIa. Localization of participating glutaminyl residues to a tryptic fragment of fibronectin, *J. Biol. Chem 255*, 1181-1188.

Mosher, D. F. and Schad, P. E. (1979) Cross-linking of fibronectin to collagen by blood coagulation Factor XIIIa, *J . Clin. Invest. 64*, 781-787.

Mulders, J. W. M., Hoekman, W. A., Bloemendal, H. and de Jong, W.W. (1987) βB1 crystallin is an amine-donor substrate for tissue transglutaminase, *Exp. Cell Res. 171*, 296-305.

Murthy, S. N. P., Wilson, J. H., Lukas, T. J., Kuret, J. and Lorand, L. (1998) Cross-linking sites of the human tau protein, probed by reactions with human transglutaminase, *J. Neurochem. 71*, 2607-2614.

Mutter, M., Tuchscherer, G. G., Miller, C., Altmann, K. H., Carey, R. I., Wyss, D. F., Labhardt, A. M. and Rivier, J. E. (1992) Template-assembled synthetic proteins with four-helix-bundle topology. Total chemical synthesis and conformational studies, *J. Am. Chem. Soc. 114*, 1463-1470.

Nakaoka, H., Perez, D. M., Baek, K. J., Das, T., Husain, A., Misono, K., Im, M.-J. and Graham, R. M. (1994) Gh: A GTP-Binding Protein with Transglutaminase Activity and Receptor Signaling Function, *Science 264*, 1593-1596.

Nejjari, M., Hafdi, Z., Dumortier, J., Bringuier, A.-F., Feldmann, G. and Scoazec, J.-Y. (1999) $\alpha_6\beta_1$ integrin expression in hepatocarcinoma cells: Regulation and role in cell adhesion and migration, *Int. J. Cancer 83*, 518-525.

Nomizu, M., Kim, W. H., Yamamura, K., Utani, A., Song, S.-Y., Otaka, A., Roller, P. P., Kleinman, H. K. and Yamada, Y. (1995) Identification of cell binding sites in the Laminin α1 chain carboxyl-terminal globular domain by systematic screening of synthetic peptides, *J. Biol. Chem 270*, 20583-20590.

Ottl, J., Battistuta, R., Pieper, M., Tschesche, H., Bode, W., Kuhn, K. and Moroder, L. (1996) Design and synthesis of heterotrimeric collagen peptides with a built-in cystine knot Models for collagen catabolism by matrix-metalloproteases, *FEBS Letters 398*, 31-36.

Ottl, J. and Moroder, L. (1999) Disulfide-bridged heterotrimeric collagen peptides containing the collagenase cleavage site of collagen type I. synthesis and conformational properties, *J. Am. Chem. Soc. 121*, 653-661.

Parameswaran, K. N., Velasco, P. T., Wilson, J. and Lorand, L. (1990) Labeling of

ε-lysine crosslinking sites in proteins with peptide substrates of factor XIIIa and transglutaminase, *PNAS 87*, 8472-8475.

Perets, A., Baruch, Y., Weisbuch, F., Shoshany, G., Neufeld, G. and Cohen, S. (2003) Enhancing the vascularization of three-dimentional porous alginate scaffolds by incorporation controlled release basic fibroblast growth factor microspheres, *J Biomed Mater Res 65A*, 489-497.

Perris, R., Syfrig, J., Paulsson, M. and Bronner-Fraser, M. (1993) Molecular mechanisms of neural crest cell attachment and migration on types I and IV collagen, *J Cell Sci 106*, 1357-1368.

Pfaff, M., Aumailley, M., Specks, U., Knolle, J., Zerwes, H. G. and Timpl, R. (1993) Integrin and Arg-Gly-Asp dependence of cell adhesion to the native and unfolded triple helix of collagen type VI, *Exp. Cell Res. 206*, 167-176.

Pierschbacher, M., Hayman, E. G. and Ruoslahti, E. (1983) Synthetic peptide with cell attachment activity of fibronectin, *PNAS 80*, 1224-1227.

Pierschbacher, M. D. and Ruoslahti, E. (1984) Cell attachment activity of fibronectin can be duplicated by small synthetic fragments of the molecule, *Nature 309*, 30-34.

Porta, R., Esposito, C., Metafora, S., Malorni, A., Pucci, P., Siciliano, R. and Marino, G. (1991) Mass spectrometric identification of the amino donor and acceptor sites in a transglutaminase protein substrate secreted from rat seminal vesicles, *Biochemistry 30*, 3114-3120.

Pucci, P., Malorni, A., Marino, G., Metafora, S., Esposito, C. and Porta, R. (1988) β-Endorphin modification by transglutaminase in vitro: Identification by FAB/MS of

glutamine-11 and lysine-29 as acyl donor and acceptor sites, *Biochem. Biophys. Res. Commun. 154*, 735-740.

Qian, J. J. and Bhatnagar, R. S. (1996) Enhanced cell attachment to anorganic bone mineral in the presence of a synthetic peptide related to collagen, *J. Biomed. Mater. Res. 31*, 545-554.

Qian, R. and Glanville, R. (1997) Alignment of fibrillin molecules in elastic microfibrils is defined by transglutaminase-derived cross-links, *Biochemistry 36*, 15841-15847.

Raghunath, M., Hennies, H. C., Velten, F., Wiebe, V., Steinert, P. M., Reis, A. and Traupe, H. (1998) A novel in situ method for the detection of deficient transglutaminase activity in the skin, *Arch. Dermatol. Res. 290*, 621-627.

Raghunath, M., Putnam, E. A., Ritty, T., Hamstra, D., Park, E. S., Tschodrich-Rotter, M., Rehemtulla, R. P. A. and Milewicz, D. M. (1999) Carboxy-terminal conversion of profibrillin to fibrillin at a basic site by PACE/furin-like activity required for incorporation in the matrix, *J. Cell Sci. 112*, 1093-1100.

Renner, C., Sacca, B. and Moroder, L. (2004) Synthetic heterotrimeric collagen peptides as mimics of cell adhesion sites of the basement membrane, *Biopolymers 76*, 34-47.

Reyes, C. D. and García, A. J. (2003) Engineering integrin-specific surfaces with a triple-helical collagen-mimetic peptide, *J. Biomed Mater Res 65A*, 511-523.

Reyes, C. D. and García, A. J. (2004) $\alpha_2\beta_1$ integrin-specific collagen-mimetic surfaces supporting osteoblastic differentiation, *J. Biomed Mater Res 69A*, 591-600.

Rippon, W. B. and Walton, A. G. (1971) Optical properties of the polyglycine II helix, *Biopolymers 10*, 1207-1212.

Ritty, T. M., Broekelmann, T. J., Werneck, C. C. and Mecham, R. P. (2003) Fibrillin-1 and -2 contain heparin-binding sites important for matrix deposition and that support cell attachment, *Biochem. J. 375*, 425-432.

Rock, M. J., Cain, S. A., Freeman, L. J., Morgan, A., Mellody, K., Marson, A., Shuttleworth, C. A., Weiss, A. S. and Kielty, C. M. (2004) Molecular basis of elastic fiber formation: critical interactions and a tropoelastin fibrillin-1 cross-link, *J. Biol. Chem 279*, 23748-23758.

Roth, W. and Heidemann, E. (1976) Triple helix-coil transition of covalently bridged collagenlike peptides, *Biopolymers 19*, 1909-1917.

Rubin, K., Höök, M., Öbrink, B. and Timpl, R. (1981) Substrate adhesion of rat hepatocytes: mechanism of attachment to collagen substrates, *Cell 24*, 463-470.

Rump, E. T., Rijkers, D. T. S., Hilbers, H. W., Groot, P. G. d. and Liskamp, R. M. J. (2002) Cyclotriveratrylene (CTV) as a new chiral triacid scaffold capable of inducing triple helix formation of collagen peptides containing either a native sequence or Pro-Hyp-Gly repeats, *Chemistry - Eur J 8*, 4613-4621.

Ruoslahti, E. and Pierschbacher, M. D. (1987) New perspectives in cell adhesion: RGD and integrins, *Science 238*, 491-497.

Ruoslahti, E. and Reed, J. C. (1994) Anchorage dependence, integrins, and apoptosis, *Cell 77*, 477-478.

Sánchez, A., Álvarez, A.M., Pagan, R., Roncero, C., Vilaró, S., Benito, X. and

Fabregat, I. (2000) Fibronectin regulates morphology: Cell organization and gene expression of rat fetal hepatocytes in primary culture, *J. Hepatol, 32*, 242-250.

Sakaguchi, M., Hori, H., Hattori, S., Irie, S., Imai, A., Yanagida, M., Miyazawa, H., Toda, M. and Inouye, S. (1999) IgE reactivity to α1 and α2 chains of bovine type 1 collagen in children with bovine gelatin allergy, *J. Allergy Clin. Immunol. 104*, 695-699.

Sakakibara, S., Inouye, K., Shudo, K., Kishida, Y., Kobayashi, Y. and Prockop, D. J. (1973) Synthesis of $(Pro\text{-}Hyp\text{-}Gly)_n$ of defined molecular weights evidence for the stabilization of collagen triple helix by hydroxypyroline, *BBA-Protein Struct 303*, 198-202.

Sakakibara, S., Kishida, Y., Kikuchi, Y., Sakai, R. and Kakiuchi, K. (1968) Synthesis of poly-(L-prolyl-L-prolylglycyl) of defined molecular weight, *Bull. Chem. Soc. Jpn. 41*, 1273.

Sakakibara, S., Kishida, Y., Okuyama, K., Tanaka, N., Ashida, T. and Kakudo, M. (1972) Single crystals of $(Pro\text{-}Pro\text{-}Gly)_{10}$, a synthetic polypeptide model of collagen, *J. Mol. Biol. 65*, 371-372.

Santoro, S. A. (1986) Identification of a 160,000 dalton platelet membrane protein that mediates the initial divalent cation-dependent adhesion of platelets to collagen, *Cell 46*, 913-920.

Sato, N., Kobayashi, H., Saga, T., Nakamoto, Y., Ishimori, T., Togashi, K., Fujibayashi, Y., Konishi, J. and Brechbiel, M. W. (2001) Tumor targeting and imaging of intraperitoneal tumors by use of antisense oligo-DNA complexed with dendrimers

and/or avidin in mice, *Clin. Cancer Res. 7*, 3606-3612.

Scharffetter-Kochanek, K., Klein, C. E., Heinen, G., Mauch, C., Schaefer, T., Adelmann-Grill, B. C., Goerz, G., Fusenig, N. E., Krieg, T. M. and Plewig, G. (1992) Migration of a human keratinocyte cell line (HACAT) to interstitial collagen type I is mediated by the $\alpha_2\beta_1$-integrin receptor, *J Invest Dermatol 98*, 3-11.

Schittny, J. C., Paulsson, M., Vallan, C., Burri, P. H., Kedei, N. and Aeschlimann, D. (1997) Protein cross-linking mediated by tissue transglutaminase correlates with the maturation of extracellular matrices during lung development, *Am. J. Respir. Cell Mol. Biol. 17*, 334-343.

Schmidt, G., Selzer, J., Lerm, M. and Aktories, K. (1998) The Rho-deamidating cytotoxic necrotizing factor 1 from Escherichia coli possesses transglutaminase activity. Cysteine 866 and Histidine 881 are essential for enzyme activity, *J. Biol. Chem 273*, 13669-13674.

Shin, H., Jo, S. and Mikos, A. G. (2003) Biomimetic materials for tissue engineering, *Biomaterials 24*, 4353-4364.

Siljander, P. R.-M., Hamaia, S., Peachey, A. R., Slatter, D. A., Smethurst, P. A., Ouwehand, W. H., Knight, C. G. and Farndale, R. W. (2004) Integrin activation state determines selectivity for novel recognition sites in fibrillar collagens, *J. Biol. Chem 279*, 47763-47772.

Simon, M. and Green, H. (1988) The glutamine residues reactive in transglutaminase-catalyzed cross-linking of involucrin, *J. Biol. Chem 263*, 18093-18098.

Sorensen, E. S., Rasmussen, L. K., Moller, L., Jensen, P. H., Hojrup, P. and Petersen, T. E. (1994) Localization of transglutaminase-reactive glutamine residues in bovine osteopontin, *Biochem. J 304*, 13-16.

Staatz, W., Fok, K., Zutter, M., Adams, S., Rodriguez, B. and Santoro, S. (1991) Identification of a tetrapeptide recognition sequence for the $\alpha_2\beta_1$ integrin in collagen, *J. Biol. Chem 266*, 7363-7367.

Staatz, W., Walsh, J., Pexton, T. and Santoro, S. (1990) The $\alpha_2\beta_1$ integrin cell surface collagen receptor binds to the α_1(I)-CB3 peptide of collagen, *J. Biol. Chem. 265*, 4778-4781.

Tanaka, T., Wada, Y., Nakamura, H., Doi, T., Imanishi, T. and Kodama, T. (1993) A synthetic model of collagen structure taken from bovine macrophage scavenger receptor, *FEBS Letters 334*, 272-276.

Tanaka, Y., Suzuki, K. and Tanaka, T. (1998) Synthesis and stabilization of amino and carboxy terminal constrained collagenous peptides, *J. Pept. Res. 51*, 413-419.

Thakur, S., Vadolas, D., Germann, H. P. and Heidemann, E. (1986) Influence of different tripeptides on the stability of the collagen triple helix. II. An experimental approach with appropriate variations of a trimer model oligotripeptide, *Biopolymers 25*, 1081-1086.

Thorwarth, M., Schultze-Mosgau, S., Wehrhan, F., Kessler, P., Srour, S., Wiltfang, J. r. and Schlegel, K. A. (2005) Bioactivation of an anorganic bone matrix by P-15 peptide for the promotion of early bone formation, *Biomaterials 26*, 5648-5657.

Thurmond, F. A. and Trotter, J. A. (1996) Morphology and biomechanics of the

microfibrillar network of sea cucumber dermis, *J. Exp. Biol. 199*, 1817-1828.

Tuckwell, D., Ayad, S., Grant, M., Takigawa, M. and Humphries, M. (1994) Conformation dependence of integrin-type II collagen binding. Inability of collagen peptides to support $\alpha_2\beta_1$ binding, and mediation of adhesion to denatured collagen by a novel $\alpha_5\beta_1$-fibronectin bridge, *J. Cell Sci. 107*, 993-1005.

Tulla, M., Pentikainen, O. T., Viitasalo, T., Kapyla, J., Impola, U., Nykvist, P., Nissinen, L., Johnson, M. S. and Heino, J. (2001) Selective Binding of Collagen Subtypes by Integrin α1I, α2I, and α10I Domains, *J. Biol. Chem 276*, 48206-48212.

Vandenberg, P., Kern, A., Ries, A., Luckenbill-Edds, L., Mann, K. and Kühn, K. (1991) Characterization of a type IV collagen major cell binding site with affinity to the $\alpha_1\beta_1$ and the $\alpha_2\beta_1$ integrins, *J. Cell Biol 113*, 1475-1483.

Velling, T., Kusche-Gullberg, M., Sejersen, T. and Gullberg, D. (1999) cDNA cloning and chromosomal localization of human α_{11} integrin. A collagen-binding, I domain-containing, β_1-associated integrin α-chain present in muscle tissues, *J. Biol. Chem. 274*, 25735-25742.

Verderio, E., Nicholas, B., Gross, S. and Griffin, M. (1998) Regulated expression of tissue transglutaminase in Swiss 3T3 fibroblasts: effects on the processing of fibronectin, cell attachment, and cell death, *Exp. Cell Res. 239*, 119-138.

White, D. J., Puranen, S., Johnson, M. S. and Heino, J. (2004) The collagen receptor subfamily of the integrins, *Int. J. Biochem. Cell. Biol. 36*, 1405-1410.

Wilke, M. S. and Furcht, L. T. (1990) Human keratinocytes adhere to a unique heparin-binding peptide sequence within the triple helical region of type IV collagen,

J. Invest. Dermatol. 95, 264-270.

Wood, G. C. (1963) Spectral changes accompanying the thermal denaturation of collagen, *Biochem. Biophys. Res. Commun. 13*, 95-99.

Woods, A. and Couchman, J. R. (1992) Protein kinase C involvement in focal adhesion formation, *J. Cell Sci. 101*, 277-290.

Wozniak, M. A., Modzelewska, K., Kwong, L. and Keely, P. J. (2004) Focal adhesion regulation of cell behavior, *Biochim. Biophys. Acta 1692*, 103-119.

Xu, Y., Gurusiddappa, S., Rich, R.L., Owens, R.T., Keene, D.R., Mayne, R., Höök, A., and Höök, M. (2000) Multiple binding sites in collagen type I for the integrins $\alpha_1\beta_1$ and $\alpha_2\beta_1$, *J. Biol. Chem 275*, 38981-38989.

Yamamoto, K. and Yamamoto, M. (1994) Cell adhesion receptors for native and denatured type I collagens and fibronectin in rabbit arterial smooth muscle cells in culture, *Exp. Cell. Res. 214*, 258-263.

Yamazaki, S., Sakamoto, M., Suzuri, M., Doi, M., Nakazawac, T. and Kobayashi, T. (2001) Synthesis of novel all-cis-functionalized cyclopropane template assembled collagen models, *J. Chem. Soc., Perkin Trans. 1*, 1870-1875.

Yang, X. B., Bhatnagar, R. S., Li, S. and Oreffo, R. O. C. (2004) Biomimetic collagen scaffolds for human bone cell growth and differentiation, *Tissue Eng. 10*, 1148-1159.

Yang, Y., Chia, H. and Chung, T. (2000) Effect of preparation temperature on the characteristics and release profiles of PLGA microspheres containing protein fabricated by double-emulsion solvent extraction/evaporation method, *J Cont Rel 69*, 81-96.

Yin, C., Ying, L., Zhang, P.-C., Zhuo, R.-X., Kang, E.-T., Leong, K. W. and Mao, H.-Q. (2002) High density of immobilized galactose ligand enhances hepatocyte attachment and function, *J Biomed Mater Res 67*, 1093-1104.

Zhang, W.-M., Käpylä, J., Puranen, J.S., Knight, C.G., Tiger, C.-F., Pentikäinen, O.T., Johnson, M.S., Farndale, R.W., Heino, J., and Gullberg, D. (2003) $\alpha_{11}\beta_1$ integrin recognizes the GFOGER sequence in interstitial collagens, *J. Biol. Chem 278*, 7270-7277.

Zhang, Z.-Y., Shum, P., Yates, M., Messersmith, P. B. and Thompson, D. H. (2002) Formation of fibrinogen-based hydrogels using phototriggerable diplasmalogen liposomes, *Bioconjugate Chem. 13*, 640-646.

Zhu, X. H., Wang, C.-H. and Tong, Y. W. (2006) Growing tissue-like constructs with Hep3B/HepG2 liver cells on PHBV microspheres of different sizes, *J. Biomed Mater Res 82b*, 7-16.

Zijenah, L. S. and Barnes, M. J. (1990) Platelet-reactive sites in human collagens I and III: Evidence for cell-recognition sites in collagen unrelated to RGD and like sequences, *Thrombosis Res. 59*, 553-566.

APPENDIX A

LIST OF AMINO ACIDS

Table A.1. Letter codes of naturally occurring and non-natural (marked with *) amino acids.

Amino acids	3 letter code	1 letter code
Alanine	Ala	A
Arginine	Arg	R
Asparagine	Asn	N
Aspartic acid/ Aspartate	Asp	D
Cysteine	Cys	C
Glutamine	Gln	Q
Glutamic Acid/ Glutamate	Glu	E
Glycine	Gly	G
Histidine	His	H
Hydroxyproline*	Hyp*	O*
Isoleucine	Ile	I
Leucine	Leu	L
Lysine	Lys	K
Methionine	Met	M

Phenylalanine	Phe	F
Proline	Pro	P
Serine	Ser	S
Threonine	Thr	T
Tryptophane	Trp	W
Tyrosine	Tyr	Y
Valine	Val	V

APPENDIX B

LIST OF PUBLICATIONS

Journal papers:

1. **Khew, S.T.**, Tong, Y.W. (2007) Characterization of triple-helical conformations and melting analyses of synthetic collagen-like peptides by reverse phase HPLC, *J. Chromatogr. 858B*, 79-90.
2. **Khew, S.T.**, Zhu, X.H., Tong, T.W. (2007) An integrin-specific collagen-mimetic peptide approach for optimizing Hep3B liver cell adhesion, proliferation, and cellular functions, *Tissue Eng. 13*, 2451-2463.
3. **Khew, S.T.** , Tong, Y.W. (2007) The specific recognition of a cell binding sequence derived from type I collagen by Hep3B and L929 cells, *Biomacromolecules 8*, 3153-3161.
4. **Khew, S.T.**, Tong Y.W. (2008) Template-assembled triple-helical peptide molecules: mimicry of collagen by molecular architecture and integrin-specific cell adhesion, *Biochemistry* 47, 585-596.

5. **Khew, S.T.,** Panengad, P. P., Raghunath, M., Tong, Y. W. (2007) Identification of a specific sequence of human fibrillin-1 as an amine donor substrate for tissue transglutaminase, *Chem. Biol.*, submitted.
6. **Khew, S.T.**, Panengad, P. P., Raghunath, M., Tong, Y. W. (2007) Characterization of amine donor and acceptor sites for tissue type transglutaminase using a sequence from the C-terminus of human fibrillin-1 and the N-terminus of osteonectin, *J. Biol. Chem.*, submitted.
7. **Khew, S.T**., Yang, Q.J., Tong, Y.W. (2008) Enzymatically crosslinked collagen-mimetic dendrimers that promote integrin-specific cell adhesion, *Biomaterials*, In press.
8. Nie, H.M., **Khew, S.T.**, Tong, Y.W., Wang, C.H. (2007) Functionalized PLGA foam for controlled gene delivery, *Langmuir*, submitted.
9. Zeugolis, D.I., **Khew, S.T.**, Yew Y.S.E., Ekaputra, A.K., Tong, Y.W., Yung, L.L.Y Hutmacher, D. W., Sheppard, C., Raghunath, M. (2007) Electro-spinning of pure collagen nano-fibres – just an expensive way to make gelatin? *Biomaterials* 29, 2293-2305 (Leading Opinion Paper).

International conference papers:

10. **Khew, S.T.**, Tong, Y.W. (2006) Biophysical studies of collagen-like triple helical peptides using reverse-phase high performance liquid chromatography, *American Institute of Chemical Engineers (AIChE) Annual Meeting*, San Francisco, USA.

11. **Khew, S.T.**, Zhu, X.H., Tong, T.W. (2006) Collagen-mimetic peptides (CMPs) for integrin-specific cellular recognition and tissue engineering, *AIChE Annual Meeting*, San Francisco, USA.
12. **Khew, S.T.**, Tong, Y.W. (2007) Template-assembly of collagen-mimetic peptides (CMPs) incorporating collagen α_1(I) 502-507 cell binding site, *Society for Biomaterials (SFB) Annual Meeting*, Chicago, USA.
13. Zeugolis, D.I., **Khew, S.T.**, Yew Y.S.E., Ekaputra, A.K., Tong, Y.W., Yung, L.L.Y Hutmacher, D. W., Sheppard, C., Raghunath, M. (2007) Electro-spinning of collagen-What collagen? *Tissue Engineering & Regenerative Medicine International Society (TERMIS) North America Meeting*, Toronto, Ontario, Canada.
14. **Khew, S.T.**, Tong, Y.W. (2007) An artificial collagen: from amino acids to collagen-like triple-helical peptides, *International Conference on Materials and Advanced Technologies (ICMAT)*, Singapore.
15. **Khew, S.T.**, Tong, Y.W. (2007) The specific recognition of a collagen mimetic cell-binding peptide sequence derived from type I collagen for different cell types, *AIChE Annual Meeting*, Salt Lake City, USA.
16. **Khew, S.T.**, Yang, Q.J., Tong, Y.W. (2008) Development of an enzymatically crosslinkable biomimetic collagen that exhibits collagen-like molecular architecture with improved cellular recognition, *AIChE Annual Meeting*, USA.